95

JAERI-TECH-99-009

FERMILAB
MAY 17 1999
LIBRARY

Fermilab Library
0 1160 0062400 1

JAERI-Tech
99-009

DESIGN AND DEVELOPMENT OF IN-VESSEL VIEWING PERISCOPE FOR ITER

(INTERNATIONAL THERMONUCLEAR EXPERIMENTAL REACTOR)

February 1999

Kenjiro OBARA, Satoshi KAKUDATE, Akira ITO,
Kiyoshi SHIBANUMA and Eisuke TADA

日本原子力研究所
Japan Atomic Energy Research Institute

本レポートは、日本原子力研究所が不定期に公刊している研究報告書です。
入手の問合わせは、日本原子力研究所研究情報部研究情報課（〒319-1195　茨城県那珂郡東海村）あて、お申し越しください。なお、このほかに財団法人原子力弘済会資料センター（〒319-1195　茨城県那珂郡東海村日本原子力研究所内）で複写による実費頒布をおこなっております。

This report is issued irregularly.
Inquiries about availability of the reports should be addressed to Research Information Division, Department of Intellectual Resources, Japan Atomic Energy Research Institute, Tokai-mura, Naka-gun, Ibaraki-ken 319-1195, Japan.

© Japan Atomic Energy Research Institute, 1999

編集兼発行　日本原子力研究所

Design and Development of In-Vessel Viewing Periscope for ITER (International Thermonuclear Experimental Reactor)

Kenjiro OBARA, Satoshi KAKUDATE, Akira ITO※
Kiyoshi SHIBANUMA and Eisuke TADA

Department of Fusion Engineering Research
Naka Fusion Research Establishment
Japan Atomic Energy Research Institute
Naka-machi, Naka-gun, Ibaraki-ken

(Received January 25, 1999)

An in-vessel viewing system is essential not only to detect and locate damage of components exposed to plasma, but also to monitor and assist in-vessel maintenance operation. In ITER, the in-vessel viewing system must be capable of operating at high temperature (200℃), under intense gamma radiation (30kGy/h) and high vacuum or 1 bar inert gas. A periscope-type in-vessel viewing system has been chosen as a reference of the ITER in-vessel viewing system due to its wide viewing capability and durability for severe environments. According to the ITER research and development program, a full-scale radiation hard periscope with a length of 15m has been successfully developed by the Japan Home Team. The performance tests have shown sufficient capability at high temperature up to 250℃ and radiation resistance over 100MGy.

This report describes the design and R&D results of the ITER in-vessel viewing periscope based on the development of 15-m-long radiation hard periscope.

Keywords : In-vessel Viewing, Periscope, Remote Maintenance, Radiation Hardness, ITER, Fusion

---

These activities are credited as an ITER Technology R&D and this report describes the design and test results in a part of 1998 ITER Design Task (D311) and 1998 ITER R&D Task (T328), respectively.
※ Visiting Researcher : Ishikawajima Harima Heavy Industries Inc.

ITER（国際熱核融合実験炉）用ペリスコープ型炉内観察装置の開発

日本原子力研究所那珂研究所核融合工学部
小原建治郎・角舘　聡・伊藤　彰※
柴沼　清・多田　栄介

（１９９９年１月２５日受理）

ITER（国際熱核融合実験炉）の炉内観察装置は、ブランケットやダイバータなどの損耗、破損の検査および炉内保守作業時の支援を主な目的とし、高温（最大：200℃）、高放射線（ガンマ線：30kGy/h）、真空あるいは1気圧の不活性ガス環境下で使用される。従って、観察装置には強度の耐久性と高精度の観察性能が求められる。

ペリスコープ型炉内観察装置は、イメージファイバ方式に比べ獲得視野が大きく、耐環境性に対処しやすいなどの観点からITERの炉内観察装置の主案に選定され、日本ホームチームによって開発が進められた。その結果、耐放射線性レンズによる実機サイズ（15m）の耐放射線性ペリスコープが試作され、高温下（250℃）での観察性能を確認できた。

本レポートでは、15m長さの耐放射線性ペリスコープをベースとしたITER用ペリスコープ型炉内観察装置の設計検討とR&Dの結果について述べる。

本報告は、ITER工学R&Dの一環として実施したものであり、報告内容はR&Dタスク番号D311の一部およびT328の結果についてまとめたものである。
那珂研究所：〒311-0193　茨城県那珂郡那珂町向山801-1
※　外来研究員：石川島播磨重工業（株）

Contents

1. Introduction 1
2. Design Requirements 1
3. Deliverables 2
4. Design Studies for In-vessel Viewing Periscope 2
4.1 Structure of In-vessel Viewing Periscope 2
4.2 Outline of Major Components 3
4.3 Estimated Viewing Resolution 9
4.4 Kinematics Study 10
4.5 Assessment on Environmental Conditions 11
4.6 Control System 15
5. Status of Technology Development 42
5.1 Background and Scope 42
5.2 Refracting Type Optical Periscope 42
5.3 Mirror Driving Mechanism 44
5.4 CCD Camera 46
5.5 Cooling System for CCD Camera 49
6. Remaining Issues 82
7. Conclusion 82
Acknowledgments 82
References 82

目　　次

1．はじめに …… 1
2．設計要求 …… 1
3．提出書類 …… 2
4．ペリスコープ型炉内観察装置の設計検討 …… 2
　4．1　構　　造 …… 2
　4．2　構成機器概要 …… 3
　4．3　観察性能 …… 9
　4．4　基本動作 …… 10
　4．5　耐環境性 …… 11
　4．6　制御システム …… 15
5．ペリスコープ型炉内観察装置のR&D …… 42
　5．1　背　　景 …… 42
　5．2　屈折式光学ペリスコープ …… 42
　5．3　ミラー駆動機構 …… 44
　5．4　CCDカメラ …… 46
　5．5　CCDカメラ用冷却システム …… 49
6．検討課題 …… 82
7．ま と め …… 82
謝　　辞 …… 82
参考文献 …… 82

TABLES AND FIGURES

I. DESIGN STUDIES FOR IN-VESSEL VIEWING PERISCOPE

Table 1 Comparison of optical performances of 11m-long and 15m-long periscopes. 22
Table 2 Calculation results of temperature rise of CFRP periscope body. 38
Table 3 Calculation results of temperature rise of Al alloy periscope body. 38
Fig. 1 Overall assembly of in-vessel viewing periscope for ITER. 16
Fig. 2 Design concept of 11m-long in-vessel viewing periscope. 17
Fig. 3 Design concept of 11m-long in-vessel viewing periscope body. 18
Fig 4 Optical arrangement of 11m-long in-vessel viewing periscope. 19
Fig. 5 Comparison of achromatic aberation in the longitudinal direction of 11m-long and 15m-long periscopes. 20
Fig. 6 Modulation transfer function (MTF) changes of 11m-long and 15m-long periscopes. 21
Fig. 7 Overall layout of 11m-long periscope for ITER in-vessel viewing. 23
Fig. 8 Optical lenses composition of 11m-long in-vessel viewing periscope. 24
Fig. 9 A part of eyepiece of 11m-long in-vessel viewing periscope. 25
Fig. 10 Visible range of movable mirror attached to tip of the periscope body. 26
Fig. 11 Schemtic diagrams of mirror driving mechanism. 27
Fig. 12 Design concept of lighting device attached to tip of the periscope body. 28
Fig. 13 Illuminance distribution of halogen lamp used the lighting device. 29
Fig. 14 Schematic diagram of off-centered driving mechanism for the lighting device. 30
Fig. 15 Design concept of tilting mechanism for the lighting device. 31
Fig. 16 Outline of winch for insertion/lifting equipment. 32
Fig. 17 Concept of upper port interface. 33
Fig. 18 Concept of movable container for maintenance of the periscope. 34
Fig. 19 Design concept of shielding plug. 35
Fig. 20 Installation position and viewing range of in-vessel viewing periscope. 36
Fig. 21 Visible range of periscope in the toroidal direction. 37
Fig. 22 Temperature rise of CFRP and Al alloy periscope bodies by thermal radiation heat from in-vessel wall. 39
Fig. 23 Tensile strength change of CFRP and Al alloy as a function of temperature. 40
Fig. 24 Schematic diagram of control system for in-vessel viewing periscope system. 41

TABLES AND FIGURES (cont'd)

II. R&D STUDIES FOR IN-VESSEL VIEWING PERISCOPE

Fig. 25 Layout of rad-hard type 6m-long periscope with a zooming mechanism in gamma irradiation cell. 50
Fig. 26 Appearance of rad-hard type 6m-long periscope in gamma irradiation cell. 51
Fig. 27. 1 Measured images by rad-hard type 6m-long periscope as a function of doses. . 52
Fig. 27. 2 Measured images by rad-hard type 6m-long periscope as a function of doses. . 53
Fig. 27. 3 Measured images by rad-hard type 6m-long periscope as a function of doses. . 54
Fig. 28 Appearance of relay lenses for 6m-long periscope after irradiation of 26.5 MGy. 55
Fig. 29 Transmittance changes of relay lenses for 6m-long periscope after irradiation of 26.5 MGy (horozontal line : wavelength (400-800nm), vertical line : transmittance (%)). 56
Fig. 30 Appearance of reflecting mirrors for 6m-long periscope after irradiation of 26.5 MGy (specification of the mirror : aluminum coating on synthetic quartz)). 57
Fig. 31 Reflectance changes of mirror for 6m-long periscope after irradiation of 26.5 MGy (horozontal line : wavelength (400-800nm), vertical line : reflectance (%)). 58
Fig. 32 Outline of full-scale rad-hard type 15m-long periscope for ITER iv-vessel viewing. 59
Fig. 33 Appearance of full-scale rad-hard type 15m-long periscope for ITER. 60
Fig. 34 Thermal expansion test results of 15m-long periscope (original length and diameter are 14,835 mm and 100 mm, respectively). 61
Fig. 35 Measured images taked by 15m-long periscope as a function of baking temperature (distance from the objective lens to the bar chart : 5 m, width of black lines on the bar chart : 32, 25, 16, 12, 8, 6 mm from right side, illuminance : 3,500 lx). 62
Fig. 36 Fabricated mirror driving mechanism for 15m-long periscope. 63
Fig. 37 Mirror driving mechanism installed in a vacuum chamber for irradiation test. 64
Fig. 38 Kinematics of mirror tilting/rotating mechanism for 15m-long periscope. 65
Fig. 39 Experimental setup of standard type CCD cameras for irradiation test in gamma irradiation cell. 66
Fig. 40 Measured images taken by No. 1 CCD camera as a function of doses under dose rate of 1 kGy (the brownish lens was replaced a new one after irradaition of 1 kGy). 67
Fig. 41 Dark current changes of std. CCD cameras as a function of doses (* to make an allowance for deterioration of amplifier). 68

Fig. 42 Change of S/N and white pattern noise of std. CCD cameras as a function of doses (* the S/N seems good in appearance caused by increasing the white pattern noise). 69
Fig. 43 Transmittance changes of objective lenses for No. 1, 2, 3 CCD cameras irradiated under 1.01E04, 1.09E03 and 1.02E02 R/h, respectively. 70
Fig. 44 External view of modified CCD camera, new correction circuits (left) was equipped to the standard CCU (right). 71
Fig. 45 Block diagram of modified CCU. 72
Fig. 46 Experimental setup of the radiation hard CCD camera systems in gamma irradiation cell. 73
Fig. 47 Changes of video output signals measured by the video tape recorder (VTR) as a functin of accumulation doses. 74
Fig. 48 Effect of sensitivity correction circuit on the video output signals of the C41 camera irradiated under 1.15 kR/h. 75
Fig. 49 Total effect of a combination of the correction circuits for sensitivity, OB level and shading on the gray-scale and color-bar charts of the C41 camera irradiated after 3 kGy. 77
Fig. 50 Transmittance changes of the objective lenses equipped to each CCD camera at a wave length of 540 nm. 79
Fig. 51 Cooling chamber including a CCD camera and an focal adjusting mechanism attached to the eyepiece of 15m-long periscope. 80
Fig. 52 Measured temperature profile of CCD camera in the cooling chamber heated up to 100 °C. 81

図表目次

1．ペリスコープ型炉内観察装置の設計検討

表　1　11m と 15m 長さのペリスコープの光学性能の比較 22
表　2　CFRP 製鏡筒の温度上昇に関する評価.....38
表　3　アルミニウム合金製鏡筒の温度上昇に関する評価 38
図　1　ITER 用炉内観察ペリスコープの全体概念図 16
図　2　11m 長炉内観察ペリスコープの全体概念図.....17
図　3　11m 長ペリスコープ本体 18
図　4　11m 長ペリスコープの光学系全体構成図 19
図　5　11m 及び 15m 長ペリスコープの縦色収差の比較 20
図　6　11m 長及び 15m 長ペリスコープの
　　コントラスト伝達関数の評価比較 21
図　7　ITER 用 11m 長炉内観察ペリスコープ全体図 23
図　8　11m 長ペリスコープの光学レンズ構成図 24
図　9　11m 長ペリスコープ接眼部 25
図　10　ペリスコープ先端部可動ミラーの可視範囲 26
図　11　可動ミラーの駆動機構 27
図　12　ペリスコープ先端部光源装置 28
図　13　光源用ハロゲンランプの照度分布図 29
図　14　ペリスコープ先端部光源装置の駆動模式図 30
図　15　光源装置の傾斜駆動機構 31
図　16　ペリスコープ昇降用ウインチ概念図 32
図　17　ペリスコープ挿入用上部ポート概念図の照度分布図 33
図　18　ペリスコープ保守用キャスク概念図 34
図　19　遮蔽プラグ概念図 35
図　20　ペリスコープの炉内挿入位置と観察範囲 36
図　21　トロイダル方向の観察範囲 37
図　22　鏡筒を CFRP 及びアルミ合金にしたときの温度上昇の比較.....39
図　23　CFRP 及びアルミ合金の温度を関数としたときの
　　引張強度の変化 40
図　24　炉内観察ペリスコープの制御システム概念図 41

2．ペリスコープ型炉内観察装置のＲ＆Ｄ

図　25　6m 長ペリスコープの照射セル内配置図 50
図　26　照射セル内の 6m 長ペリスコープ 51
図　27　6m 長ペリスコープの観察画像の照射量による変化（１） 52

図表目次（続き）

図 27 6m 長ペリスコープの観察画像の照射量による変化（2） 53
図 27 6m 長ペリスコープの観察画像の照射量による変化（3）.....54
図 28 26.5MGy 照射後の 6m 長ペリスコープのリレーレンズ 55
図 29 6m 長ペリスコープ用リレーレンズの照射前後の透過量変化.....56
図 30 26.5MGy 照射後の 6m 長ペリスコープの反射鏡 57
図 31 6m 長ペリスコープ用反射鏡の照射前後の反射率変化 58
図 32 ITER 用実機サイズ 15m 長ペリスコープ全体図 59
図 33 製作された ITER 用実機サイズ 15m 長ペリスコープ 60
図 34 15m 長ペリスコープの熱伸び試験 61
図 35 15m 長ペリスコープの高温加熱試験時の観察画像 62
図 36 15m 長ペリスコープのミラー駆動装置概念図 63
図 37 試験用真空容器に収納されたミラー駆動装置 64
図 38 ミラー駆動装置の駆動機構模式図 65
図 39 CCD カメラのガンマ線照射試験配置図 66
図 40 CCD カメラの観察画像の照射量による変化 67
図 41 CCD カメラの暗電流の照射量による変化 68
図 42 CCD カメラの S/N とホワイトパターンノイズの
照射量による変化 69
図 43 CCD カメラ用対物レンズの照射量による透過量変化 70
図 44 補正回路を取り付けた CCD カメラの外観写真 71
図 45 補正回路ブロック図 72
図 46 耐放射線性 CCD カメラの照射試験配置図 73
図 47 耐放性 CCD カメラのビデオ出力信号の照射量による変化 74
図 48 補正回路による感度補正効果 75
図 49 補正回路によるカラーチャート上に見る総合補正効果 77
図 50 標準及び耐放性対物レンズの透過率の照射量による変化 79
図 51 接眼部 CCD カメラ用冷却チャンバ ...80
図 52 CCD カメラ用冷却チャンバの性能試験 81

1. Introduction

Development of in-vessel viewing system for ITER has been conducted on three home teams (EU, JA, US). In the Japan Home Team, the development is categorized into three development stages. On the first stage, selection of the most suitable in-vessel viewing system was investigated based on the in-vessel viewing systems experienced, which were fabricated for the JT-60 and JT-60U tokamak machines. As a result, periscope and image fiber methods were selected as a candidate for ITER in-vessel viewing system. Based on this, application of the periscope and image fiber methods for the ITER was assessed in the second stage and a periscope method which is inserted from top port has been chosen as a reference in-vessel viewing system due to its relatively clear and wide viewing capability [1]. On the third stage, the conceptual design and R&D of the in-vessel viewing periscope have been conducted in accordance with the design requirements. And these studies has been carried out based on a policy, which has to be realized with the existing technology or the technology which can be developed within the EDA. As a result, a full-scale radiation hard periscope with a length of 15 m was fabricated and tested. And it has been verified that the developed 15m-long periscope has sufficient viewing capability under high temperature operation up to 250 ℃ [2]. Based on this, in the fourth stage, further examination of the in-vessel viewing periscope has been conducted in accordance with the latest Revised In-Vessel Viewing System Requirements which was presented July 30, 1997.

This report mainly summarizes the fourth stage's results ('97 Design Task (D311)) concerning conceptual study and design of the in-vessel viewing periscope, together with the status of the technology development of the R&D Task (T328).

2. DESIGN REQUIREMENTS

The in-vesel viewing periscope is to be designed according to the following conditions.

(1) Frequency of deployment
- BPP : apporoximately once per week during operational campaigns
- EPP : apporoximately once per week during operational campaigns

(2) Environmental conditions during viewing/inspection

(2)-1 Just after plasma operations
- Atmosphere : none
- Pressure : ultra-high vacuum
- Temperature : max. 200 ℃
- Radiation : max. 3×10^6 R/hr (24 hours after shutdown; 10-30 times higher immediately after shut down. Deployment may be required before 24 hours)
- Contamination : tritium, activated dust, beryllium
- Magnetic field : TF magnetic field energized, CS and PF magnets de-energized. Intensity of the magnetic field is estimated about 5.7 tesla at R = 8.14 m)

(2)-2 For maintenance periods
- Atmosphere : inert gas
- Pressure : atmospheric (about 0.1 MPa)
- Temperature : ambient
- Radiation : max. 3×10^6 R/hr
- Contamination : tritium, activated dust, beryllium
- Magnetic field : TF magnetic field energized, CS and PF magnets de-energized. Intensity of the magnetic field is estimated about 5.7 tesla at R = 8.14 m)

(3) Deployment
- Installation port : top port (the assumed radial position is 7450 mm)
- Available number of ports : 10

(4) Dimensions and structure
- Diameter of viewing probe : under 150 mm
- Length of viewing equipment : below the bioshield during storage and operation
- Viewing equipment must be of a diameter sufficient to provide clear viewing information and sufficient stiffness to minimize the deflection and vibration
- Lighting : the in-vessel viewing probe shall be completely self contained with lighting equipment
- Viewing equipment must be compatible with the top port design
- Viewng equipment must be located behind a shield plug during plasma operations to minimize neutron streaming and heat loads from the plasma
- The shield plug must allow for prompt insertion of the probe into the vacuum vessel in preparation for viewing operations after plasma operations have been temporarily halted

(5) Viewing resolution
- Required resolution : 1 mm at all points on the blanket module and divertor surfaces
- Angle : between 90 and 5 degrees from the tangent to the surface
- Distance : no more than 3000 mm and no less than 500 mm from the surface
- Optical zoom capabilities : x 6

(6) Removal and replacement
- Utilizing a double seal door arrangement and a contamination control container

(7) Control system
- The operaton and remote viewing of the in-vessel viewing are controlled from the ITER control room
- All routine controls shall be from the control room locations and no control or intervention will be required at the bioshield

3. DELIVERABLE

The following deliverables are to be included in the final design report.

(1) Kinematics study with the latest ITER geometry so as to verify the number of probes needed, viewing angles, probe position
(2) Sketch level drawings of in-vessel viewing periscope
(3) Assessment of probe diameter for clear viewing and mechanical stiffness
(4) Preliminary thermal calculation to assess cooling requirements
(5) Preliminary assessment of lighting requirements such as number of lighting probes, position and illuminance

4. DESIGN STUDIES FOR IN-VESSEL VIEWING PERISCOPE

4. 1 Structure of in-vessel viewing periscope

Figures 1 and 2 show an overall layout of the in-vessel viewing periscope designed, respectively. Fig. 3 represents a periscope body, which is inserted into the ITER vacuum vessel through a vertical port. The in-vessel viewing periscope is basically composed of a long-size refracting periscope body, a lighting equipment, a mirror driving mechanism attached to the tip

of the periscope body, a CCD camera attached to the eyepiece, a winch inside a cask placed at a vertical port for containment, support structures, a shielding plug. The periscope body is 11 m in length and the total length of the in-vessel viewing periscope with associated equipment/tools is about 12 m. The design outline of the main components for the in-vessel viewing periscope are described below.

4. 2 Outline of major components

(1) 11m-long refracting periscope body

Figure 4 shows an general arrangement of optical elements which are radiation hard type developed for the in-vessel viewing periscope. An objective lens and six relay lenses are assembled into a 11m-long periscope body with a diameter of 70 mm. Viewing information is taken through these lenses to the image sensors in the CCD camera head located at the eyepiece. Figure 5 shows a difference of achromatic aberation in the longitudinal direction between 15m-long (fabricated periscope) and 11m-long (improved periscope) periscopes when the wave length of 580 nm was adjusted at the focusing point. Figure 6 represents a comparison of characteristic change of the modulation transfer function (MTF) on the both periscopes. The MTF means an optical resolution capability of the periscope. The horizontal line shows an input signal equivalent to number of line per width of 1 mm and the vertical line means an intensity of output signal. The aberration, brightness (Fno.) and MTF of the 11m-long periscope were improved drastically compared with the 15m-long periscope which was fabricated before the 11m-long periscope design studies (refer Table 1).

According to the design requirements, the in-vessel viewing periscope should be capable of operating under high temperature (150 ~ 200°C) and intense gamma radiation (3 x 10^6 R/h) conditions in high vacuum (10^{-5} Pa) or 1 bar inert gas. From this viewpoint, radiation hard lenses composed of a lead glass containing CeO_2 and an OH doped synthetic quartz, which show a good radiation hardness over 200 MGy at a dose rate of 1 x 10^6 R/h, have been integrated into the design. In addition, a focus adjustment mechanism and a lens support system have to be reflected into the design so as to accommodate thermal expansion of the periscope body due to high temperature operation. The main parameters of the periscope body is as follows.

- Dimensions	: 70 mm in outer diameter, 11 m in length
- Weight	: 36 kg
- Material of periscope body	: aluminum alloy (5052)
- Number of optical lenses	: objective lens x 1, Relay lenses x 6
- Lens material	: lead glass containing CeO2 and OH doped synthetic quartz
- Angle of visual field	: 30° (horizontal)
	: 22.7° (vertical)
	: 37.1° (opposite angle)
- Focal length of objective lens	: 50 mm
- Maximum temperature	: 250°C (max.)

Figures 7, 8 and 9 show the design concept related to the overall layout, optical lenses composition and eyepiece of the 11m-long periscope, respectively.

(2) Mirror and mirror driving mechanism

A mirror and mirror driving mechanism to rotate and tilt are attached to the periscope body so as to allow viewing and inspection of the whole in-vessel area. Figure 10 shows a relationship between the movable mirror and visible range. Since the mirror driving mechanism is designed to provide two degree of freedoms (tilting & rotating), all of mechanical and electric components such as AC servo motor and clutch are attached to the tip of periscope body. The tilting and rotating workings to the mirror are transmitted by change of the clutch through the AC servo motor. Figure 11 shows typical kinematics of the mirror tilting/rotating mechanisms. Accordingly, these mechanical and electric components in the mirror driving mechanism have to meet the same operating requirements as those of the periscope body, as mentioned above. The main parameters of the mirror driving mechanism designed are as follows.

- Overall dimensions	: 150 mm in diameter, 12 m in length (including periscope, lighting device)
- Major materials	: aluminum allot and stainless steel
- Mirror	
Dimensions	: 140 mm in length x 60 mm in width, 16 mm in thickness
Material	: aluminum alloy polished by diamond
- Movable range of mirror	: tilting (ϕ) 30 - 105°, rotating (θ) ± 180°
- Motor and reduction gear:	
Motor	: AC servo-motor with ceramic insulator
	: rated power ~62W
	: rated number of rotation 1000 rpm
	: rated torque 6 kg-cm
Operational speed	: rotating (θ) 36° / sec (6 rpm)
	: tilting (ϕ) 9° / sec (1.5 rpm)
Reduction gear	: Harmonic-drive or planet gear
Lubricants	: radiation hard grease or solid lubricants

The in-vessel viewing periscope provides three degrees of freedom for insertion/lift of the periscope body and for tilting and rotating of the mirror. The main parameters of each axis has been specified so as to keep a maximum observation speed of 100 mm/sec which is experimentally defined.

The followings are rough estimates of loading torque for the rotating (θ) and tilting (ϕ) axes.

a) Necessary loading torque for rotating axis

Loading torque for rotating axis (T_θ) is given as follow:

$$T_\theta = T_{a\theta} + T_{L\theta} \tag{4.1}$$

where, $T_{a\theta}$: instantaneous maximum torque for θ axis

$T_{L\theta}$: loading torque on bearing-θ which is applied the total weight of the periscope and the mirror driving mechanism

$T_{a\theta}$ and $T_{L\theta}$ can be estimated from the equations (4.2) and (4.3).

$$T_{a\theta} = (GD_\theta^2 \cdot N) / (375 \cdot t) \quad (4.2)$$

where,
- GD_θ^2 : loading moment in motor axis ($kg \cdot m^2$)
- N : rated rotational number of motor (1000 rpm)
- t : acceleration time of motor (0.3 sec)

$$T_{L\theta} = \mu 1 \cdot (W_P + W_M) \cdot (D_{B\theta} / 2) \cdot (1 / n) \quad (4.3)$$

where,
- $\mu 1$: friction coefficient of bearing-θ (0.02)
- W_P : weight of the periscope (~ 40 kgf)
- W_M : weight of the mirror driving mechanism (~ 50 kgf)
- $D_{B\theta}$: center radial of bearing-θ (100 mm)
- n : reduction number of reduction gear box (20)

in addition, GD_θ^2 and both loading moments of the periscope (GD_P^2) and the mirror driving mechanism (GD_M^2) can be calculated as follows:

$$GD_\theta^2 = (GD_P^2 + GD_M^2) i^2 \quad (4.4)$$

$$GD_P^2 = (W_P / 2) D^2 \quad (4.5)$$

$$GD_M^2 = (W_M / 2) \cdot (D_1^2 - d^2) \quad (4.6)$$

where,
- i : reduction gear ratio (1 / 20)
- D : outter diameter of the periscope (~ 70 mm)
- D_1 : outter diameter of the mirror driving mechanism (~ 140 mm)
- d_1 : inner diameter of the mirror driving mechanism (~ 70 mm)

As a result, the necessary loading torque of the rotating axis is calculated as follows and this value is small enough compared with the rated power of the motor for θ axis.

$$T_\theta = T_{a\theta} + T_{L\theta} = 1.04 + 0.45 = 1.49 \text{ kgf} \cdot \text{cm}$$

b) Necessary loading torque for tilting axis

Loading torque for tilting axis (T_ϕ) is given as follow:

$$T_\phi = T_{a\phi} + T_{L\phi 1} + T_{L\phi 2} \quad (4.7)$$

where,
- $T_{a\phi 1}$: instantaneous maximum torque for ϕ axis
- $T_{L\phi 1}$: loading torque on bearing-ϕ which is applied the total weight of the driving cylinders 1 and 2
- $T_{L\phi 2}$: loading torque on screw in the ball/screw driving mechanism

$T_{a\phi 1}$, $T_{L\phi 1}$ and $T_{L\phi 2}$ can be estimated from the equations (4.8), (4.9) and (4.10).

$$T_{a\phi} = (GD_{\phi}^2 \cdot N) / (375 \cdot t) \tag{4.8}$$

where, GD_{ϕ}^2 : loading moment in motor axis ($kg \cdot m^2$)
N : rated rotational number of motor (1000 rpm)
t : acceleration time of motor (0.3 sec)

$$T_{L\phi 1} = \mu 2 \cdot (W_{C1} + W_{C2}) \cdot (D_{B\phi} / 2) \cdot (1 / n) \tag{4.9}$$

where, $\mu 2$: friction coefficient of bearing-ϕ (0.02)
W_{C1} : weight of drivung cylinder-1 (~ 43 kgf)
W_{C2} : weight of driving cylinder-2 (~ 10 kgf)
$D_{B\phi}$: center radial of bearing (90 mm)
n : reduction number of reduction gear box (20)

$$T_{L\phi 2} = (\mu 3 \cdot W_{C2}) \cdot (D_{B\phi} / 2) \cdot (1 / n) \tag{4.10}$$

where, $\mu 3$: friction coefficient of screw in ball/screw driving mechanism (0.3)

in addition, GD_{ϕ}^2 and both loading moments of the driving cylinder-1 (GD_{C1}^2) and the driving cylinder-2 (GD_{C2}^2) can be calculated as follows:

$$GD_{\phi}^2 = GD_{C1}^2 + GD_{C2}^2 \tag{4.11}$$

$$GD_{C1}^2 = (W_{C1} / 2) \cdot (D_{C1}^2 - d_{C1}^2) \cdot i^2 \tag{4.12}$$

$$GD_{C2}^2 = 365 \cdot W_{C2} \cdot (v_f / n_i)^2 \tag{4.13}$$

where, i : reduction gear ratio (1 / 20)
D_{C1} : outter diameter of the driving cylinde-1 (~ 116 mm)
d_{C1} : inner diameter of the driving cylinder-1 (~ 108 mm)
v_f : velocity of the ball/screw in linear motion (0.2 m / min)
n_i : rotational number of input axis (1000 rpm)

As a result, the necessary loading torque of the tiltting axis is calculated as follows and this value is small enough compared with the rated power of the motor for ϕ axis.

$$T_{\phi} = T_{a\phi} + T_{L\phi 1} + T_{L\phi 2} = 0.215 + 0.239 + 0.675 = 1.129 \text{ kgf} \cdot \text{cm}$$

(3) Lighting device

In the current design, a lighting device, which is composed of five halogen lamps with reflectors, is attached to the tip of the periscope body as an unit (see Fig. 12). The main parameters of the lighting device listed below are defined to provide an illuminance of 6000 lx on the object located at 3-m far from the object lens. Figure 13 shows the two-dimensional illuminance distribution of the halogen lamp. The lighting device is aligned the center of the periscope at original position and it is rotated off-centered by pneumatic lifting mechanism. Figure 14 represents the off-centered rotation mechanism of the lighting device. In this concept,

additional port openings for inserting the lighting device is not necessary. In addition, lighting efficiency is good because of the lighting direction is followed the mirror movements (see Fig. 15). However, the heat loads from the lighting device is the remaining issue to be assessed. Instead of this concept, a separated type lighting equipment from the mirror driving mechanism is another possible concept although additional port openings are required. Further study including these assessment are needed.

- Lighting source	: halogen lamp
	: rated power 12 V / 50 W per lamp
	: beam width 11°
	: rated lifetime 4,000 hr
- Reflector	: aluminum treated oxidation resistant
- Driving mechanisms	: off-centered rotation / extension and contraction of welding bellows
	: tilting / follow the tilting axis of the mirror driving mech.
	: rotation / follow the rotating axis of the mirror driving mech.

Rotation and tilting motion of the lighting device follow the θ and ϕ axes of the mirror driving mechanism, respectively. The followings are basic specifications and rough estimates of the off-centered rotation mechanism in the lighting device.

a) Specifications of off-centered rotation mechanism

- Rotational range	: 180°
- Driving method	: extension & contraction of welding bellows by pressurized air
- Pressure of air	: 5 kgf / cm^2
- Welding bellows	: stroke / 16 mm
	: outter diameter / 23.8 mm
	: inner diameter / 11.1 mm
	: effective surface area / 2.4 cm^2
	: number of element / 80

b) Necessary bellows stroke

The stroke (S) is given as follow:

$$S = \pi D \cdot (\theta / 360°) \cdot (A / B) \tag{4.14}$$

where, D : ouuter diameter of rotation drum (20 mm)
θ : rotational range (180°)
A / B : gear ratio between main gear and sub-gear of the rotation drum (0.5)

therefore, S = 15.7 mm

c) Tension of returning spring

The tension (F) is given as follow:

$$F = (RW) / r \tag{4.15}$$

where, R : radius of lamp unit (61 mm)
W : weight of lamp unit (2.5 kgf)
r : radius of the rotation drum (10 mm)

therefore, F = 15.25 kgf

d) Necessary number of bellows

The number (N) is given as follow:

$$N = F / (PAe) \tag{4.16}$$

where, P : pressure of air (5 kgf / cm^2)
Ae : effective surface area per bellows (2.4 cm^2)

therefore, N = 1.27 = 2

(4) CCD camera

A CCD camera is attached to the eyepiece of the periscope body for visual information. Generally, a CCD camera is composed of image sensors based on semiconductors which is low resistance in durability against high temperature and gamma radiation. The 1st phase gamma irradiation experiments of standard type (non rad-hard) CCD cameras commercially available show that the maximum accepetance doses is about 1.5 kGy at the dose rates ranging from 1 ~ 100 Gy/h. On the 2nd phase, newly developed rad-hard CCD cameras with modified camera control units and a rad-hard objective lens were tested under the dose rates of 10 and 100 Gy/h. As the results, radiation hardness of the newly developed CCD cameras showed the accepetance doses above 3 kGy. The gamma ray irradiation results are described in the section five in this report.

Based on this dose limits of the CCD camera, the position of the eyepiece is specified to be 8 m from the plasma center. In this case, the gamma dose rate near the CCD camera region is estimated to be approximately 10 ~ 100 Gy/h which corresponds to reduction ranging from 2 ~ 3 order of magnitude comparing with the central position inside the vacuum vessel. The followings are main specifications of the newly developed rad-hard CCD camera selected for the eyepiece.

- Power and voltage : 5.2W/DC 12V
- Type of image sensor : 1/2 inch CCD area image sensor
- Number of effective pixel : 768 (Horizontal) x 494 (Vertical)
- Area of the sensor : 6.54 mm (Horizontal) x 4.89 mm (Vertical)
- Observation capability : 460 TV (Horizontal) x 350 TV (Vertical)
- Camera control unit (CCU) : modified rad-hard type CCU
- Objective lens : composed of rad-hard type lenses
- Illuminance (Std.) : more than 200 lx (F1.6, 300K)
- Illuminance (Min.) : 15 lx (F1.6, 300K)
- Allowable temperature : -10°C ~ +40°C

- Camera head cooling system	: air cooling chamber
- Allowable humidity	: 30% ~ 90%
- Weight	: camera head (without lens) 75g camera control unit 620g
- Monitor	: 21 inch CRT

(5) Insertion/Lifting equipment

A winch type system is designed for insertion and lifting of the periscope body with mirror driving mechanism and CCD camera. In this design, the total weight of the winch including wire ropes and lifting length are about 100 kg and 15m, respectively. During the insertion/lifting operation, tensions applied to the rope can be kept constant using a pulley equipped to the tip of the rope. Since the winch and AC servo-motors for driving the winch have to be installed in vacuum environment, feasibility study on heat-resistant and lubricant of these components are fundamental. In addition, a flexible guide pipe with bellows is required to allow the vertical and horizontal movements of the periscope and reliability of the bellows is to be also assessed. Figure 16 shows an outline of the winch and further studies including cable management are required.

(6) Movable container

The in-vessel viewing periscope is installed under the biological shield and is inserted through a port opening for viewing so as to enable rapid inspection just after off-normal events such as plasma disruptions. Therefore, the maintenance working is a very important for saving the reliability of in-vessel viewing periscope. Figure 17 shows an interface around the top port which is installed the in-vessel viewing periscope. The port is separated two structures of upper and lower parts for avoiding thermal deflection, in addition, the in-vessel viewing periscope is accommodated in a duoble sealed container for protection of contamination. Figure 18 shows a layout of movable container with double seal door. The in-vessel viewing periscope is accommodated with the winch when the maintenance and removing workings. This concept is a basic idea, so further studies are needed in the future.

(7) Shielding plug

A shielding plug for filling the port opening in case of stand-by mode is necessary to protect the in-vessel viewing periscope from radiation and thermal loads through the port opening. Figure 19 shows a design outline of the shielding plug. The shielding plug made of heavy concrete is composed of upper and lower plugs with a hole for inserting the periscope. When the periscope is inserted into the vacuum vessel, these two plugs are rotated so as to align two holes into a single penetration. Concerning the nuclear shield and streaming, it is necessary that the shield plug is designed to reduce dose rate by three order of magnitude. The main parameters of the shield plug is as follows.

- Dimensions	: (460 mm in dia., 1,000 mm in height) x 2 : insertion hole with a diameter of 170 mm
- Materials	: stainless steel and heavy concrete
- Drives for rotation	: radiation hard type induction motor (1 kW)
- Dead weight	: 1,850 kg

4. 3 Estimated viewing resolution

The viewing capability of the designed in-vessel viewing periscope can be estimated using the defined specifications such as periscope magnification, size of area image sensor and observation capability of a 21-inch monitor, mentioned in the previous section .

As an initial condition to estimate the viewing capability, the location of a periscope is assumed to be 6 m far from an object with a total height of 1 mm. When a magnification of relay lens is a total of 1/4, magnification (m) of the objective lens can be roughly estimated from the equation (4.17).

$$m = (f / S_1) \cdot (1 / 4) \qquad (4.17)$$

where, S_1 : distance from objective lens to object (6 m)
f : focal length of objective lens (50 mm)

Therefore, the magnification (m) can be obtained to be about 1/500. This means that the 1-mm object at a 6-m distance from the objective lens can be viewed to be $2x10^{-3}$ mm height on the area image sensor. On the other hand, the resolution capability in the x and y directions of the 21-inch monitor can be calculated as follows:

$$x = Xeff / X = 407 / 460 = 0.88 \text{ mm}$$
$$y = Yeff / Y = 305 / 350 = 0.87 \text{ mm}$$

where, X : Number of TV lines in the horizontal direction (460)
Xeff : Effective height in the horizontal direction (407 mm)
Y : Number of TV lines in the vertical direction (350)
Yeff : Effective length in the vertical direction (305 mm)

In the current technology, an electronic magnification of the 21-inch monitor to the area image sensor is about 62 and therefore the size of object on the monitor is calculated as follows:

$$2x10^{-3} \times 62 = 0.12 \text{ mm}$$

As a result, the viewing resolution using the periscope, CCD camera and 21-inch monitor is around a few mm as minimum when the periscope is located at 6 m far from the object.

4. 4 Kinematics study

(1) Visible range in the poloidal section

According to the design requirements, it is required to view all of the first wall and divertor plate inside the vacuum vessel by inserting the periscope with the mirror driving mechanism. A kinematics study has been carried out in order to define the optimum location of the periscope and the main parameters of the optical elements. Figures 10 and 20 represent typical visible range obtained from the kinematics study. As a result, it has been concluded that all of first wall and divertor plate can be inspected using the periscope with the following conditions.

- Radial position for insertion : 7,450 mm (from the machine center)
- Viewing angle of objective lens : 30°
- Vertical moveable range (Insertion) : 3700 mm below the plasma center

(Lifting) : 5945 mm above the plasma center
(Total stroke) : 9645 mm
- Tilting angle of mirror(ϕ) : 30° ~ 60°
- Rotating angle of mirror(θ) : 90° (CW, CCW)
- Dimensions of mirror : 140 mm in length, 60 mm in width

(2) Number of the periscopes

The vacuum vessel is a torus structure assembled with twenty sectors, so that the number of periscope installed has to be defined by a visible range of the periscope in the toroidal direction. Fig. 21 shows the toroidal visible range when five periscopes are installed at five upper ports equally spaced in the toroidal direction. It is found that a combination of five periscopes and five laser metrology sensors located separately from the periscope will be sufficient to inspect all of first wall. Further study based on 3-D analysis is essential to define the exact minimum number of periscope.

4. 5 Assessment on environmental conditions

(1) Temperature rise due to thermal radiation

Thermal loads applied to the periscope are the radiation heat inside the vacuum vessel and the heat input by lighting device. In this assessment, however, the effect of the radiation heat on temperature rise of periscope body made of aluminum alloy and CFRP (carbon fiber reinforced plastic) has been roughly calculated, respectively. Because the radiation heat plays major roles and the heat input from the lighting equipment can be negligible. The assumptions in this calculation are as follows:

- Shape of the periscope body is a rod.
- Surface temperature of the periscope body is estimated from a temperature of the rod center.
- Temperature of the rod center is found from the Hythier's charts.

Surface temperature of the periscope body is given as follows:

$$Tn = Tf - C \cdot Yo\,(Tf - Ti) \qquad (4.18)$$

where,
Tn : surface temperature of periscope body
Tf : environmental temperature (300°C)
C : correction factor for position
Yo : this value is obtained from the Hythier's chart
Ti : initial temperature of periscope body (20°C)

Correction factor for position, C is found by m, n and the Hythier's chart.

$$m = k / (\alpha \cdot L) \qquad (4.19)$$

where,
m : relative boundary value
k : thermal conductivity
: (CFRP (polyimide) : 197 W/m·K)
: (Al alloy (A5052) : 138.4 W/m·K)
α : temperature conductivity

: (CFRP (polyimide) : 0.425 m^2/h)
: (Al alloy (A5052) : 0.205 m^2/h)
L : radius of rod (0.05 m)

and, $n = x / L$ (4. 20)

where, n : relative position
x : calculated position of radius direction from rod center (0.05 m)

Value of horizontal line in the Hythier's chart for finding Yo can be calculated as follow:

$$X = (\alpha \cdot t) / L^2 \quad (4.21)$$

where, X : value of horizontal line in the Hythier's chart for finding Yo
t : progressing time (h)

Tables 2, 3 and Fig. 22 are calculation results and temperature change of the periscope body, respectively. As a result, the surface temperature each periscope body made of CFRP and Al alloy is reached to 300°C after 1.7 and 3 hour operation under the in-vessel surface temperature of 300°C. The temperature rising of the CFRP periscope body is higher than the Al alloy periscope body, but the thermal expansion coeficient of CFRP is small in double figures, in addition, CFRP is light weight and its mechanical strength under high temperature operation is far better than Al alloy, as shown in Fig. 23. This temperature rise causes thermal expansion of the periscope body, resulting in a possibility of the optical axis misalignment. From this viewpoint, CFRP is suitable material as a periscope body material.

(2) Gamma radiation

During the in-vessel inspection, the periscope body with lenses and mirror driving mechanism are to be operated for sufficient length of time under a high intense gamma radiation. When the observation time is assumed 50 hr per one operation, the accumulation doses of these components are reached to 1.5 MGy. However, the radiation hardness of conventional radiation hard components are quite low compared with the required doses, as listed below. Therefore, extensive development of radiation hard components to meet this requirement is essential. In this section, radiation hardness of critical components for periscope is summarized.

- Motor : 0.01 MGy	- Laser : 4-10 MGy	- Sensors : 0.1 MGy
- Optical compo. : 0.01 MGy	- Organic adhesive : 0.1 MGy	- Resistor : 10 MGy
- Semiconductor : 0.01 MGy	- Electric connector : 1 MGy	- Insulator : 1 MGy

a) Optical lenses

Generally, there are 200 kinds of glass materials available for optical lens but most of these glasses are colored by gamma irradiation. For example, a standard type periscope made of borate glass lenses degrades after 1 hr gamma irradiation and becomes invisible after 2 hr gamma irradiation [3]. Accordingly, realization of the in-vessel viewing periscope depends on selection of radiation hard glasses and optical performance of lenses made of the selected radiation hard glasses.

In order to develop a radiation hard periscope, a number of glass materials have been irradiated using a gamma ray irradiation facility with a maximum dose rate of 15 kGy/h. As a result, three types of radiation hard glasses, which are alkaline barium glass and lead glass containing CeO2, and OH doped synthetic quartz, have been chosen. Using these radiation hard

glasses, a 6-m long prototype radiation hard periscope has been fabricated and the gamma irradiation test is being conducted at a dose rate of 10 kGy/h. Up to now, the radiation hard periscope shows no degradation in viewing performance up to an accumulated dose of 50 MGy [4]. As a conclusion, the newly developed radiation hard glasses can satisfy the ITER requirements and further experiments are to be continued to define its dose limits.

b) Mirror driving mechanism

The mirror driving mechanism including the lighting device is also exposed under intense gamma radiation as well as the periscope body. The durability of the mirror driving mechanism depends on radiation hardness of mechanical and electric parts such as lubricants, motors, cables, connectors and lamps. According to the ITER R&D Task (T252), a number of radiation hard components such as AC servo-motor with ceramic insulation wire, grease lubricant, lamp, solid lubricant, microswitch with ceramic housing, polyimide and ceramic coated insulation cables have been well developed and radiation hardness of most of these components is over 10 MGy.

A design concept of the mirror driving mechanism has been developed on the basis of these developed radiation hard components. In order to verify the total performance and durability of the mirror driving mechanism, a prototypical model composed of the developed radiation hard components is under preparation for gamma irradiation tests.

c) CCD camera

Small-sized and light weight CCD image sensors are widely used in many industrial fields. The image sensor is mainly divided into three elements, which are sensing part, horizontal CCD and output circuit. These elements are assembled with many electric devices such as photodiode and semiconductor. Therefore, radiation hardness of the CCD image sensors depends on durability of the electric devices under gamma radiation.

According to the gamma ray irradiation tests of the commercial base CCD cameras, the dose limits are about 1.5 kGy at the dose rates from 1 to 100 Gy/h. Due to its nature of the electrical devices in CCD camera, improvement of radiation hardness will be limited. Some possible improvements, which is under investigation, are to separate CCU (camera control unit) from the camera head and to locate CCU outside the bioshield, electric modification of the CCU and equipment of rad-hard objective lens.

(3) Compatibility under both inert gas and vacuum environments

Due to the ITER operational requirements, the in-vessel viewing periscope has to be operated under the both conditions of a high vacuum (10^{-5}Pa) and 1 bar inert gas. According to a scoping study concerning the both environmental conditions, temperature rise and compatibility of lubricants are fundamental issues to be solved. As for temperature rise, efforts have to be made to adopt a new material with low thermal conductivity for the periscope body as well as to develop effective cooling methods. With regard to lubricants, development of solid lubricants compatible for both operations under vacuum and inert gas is essential.

(4) Magnetic field

a) Magnetic loads acting on the periscope

Magnetic loads can be generally calculated from the equation (7) and the maximum loads (Fm) acting on the periscope is estimated to be 3600 N under the assumption of a magnetic field of 6 T in the all axes directions when the periscope is inserted into the vacuum vessel just after plasma operation (rapid inspection). Although the estimated magnetic load of 3600 N is large, it

will be possible to support the periscope if a sufficient installation space and rigid supporting structures are prepared near the upper port region.

$$Fm = \{(\mu_s - 1) \cdot B^2 \cdot A\} / (2 \cdot \mu_s \cdot \mu_0) \quad (7)$$

where, μ_s : Specific magnetic permeability (1.5)
μ_0 : Magnetic permeability in vacuum ($4\pi x10^{-7}$ T·m/A)
B : Magnetic field (6T)
A : Surface area of periscope ($4.5x10^{-3}m^2$)

b) Effect of magnetic field on performance of components

The magnetic field of 6 T gives big impact on functional performance of various components for the periscope as well as the effect of magnetic loads. In particular, the mirror driving mechanism, CCD camera and winch will be malfunctioning and further assessment is needed. This section summarizes typical experimental results concerning the effect of magnetic fields on commercial base electrical devices, which have been carried out by the Superconducting Magnet Laboratory in JAERI [5].

(1) Display (cathode ray tube)

Two types of CRTs, which are a Brun tube type CRT and a plasma type CRT have been tested. As a result, in case of the Brun tube type CRT, the images on the CRT is changed at 0.3 G and distorted at 20 G. On the other hand, the images on the CRT is not changed up to 120 G but disappeared at over 120 G.

(2) High voltage amplifiers

High voltage amplifiers to measure coil voltages indicate incorrect signals at 65 G. When the amplifiers is covered with a magnetic shield made of steel plate cover, the signal output is not changed up to 110 G.

(3) Solenoid valves

Performance solenoid valves depends on direction of the magnet field but it is impossible to use over 60 G.

(4) Oscillator and amplifiers

Two types of oscillators, a multiple semiconductor sensor type and a strain gauge type have been tested. These oscillators are used for pressure gauge and flow meter. As a result, both oscillators and strain gauge type amplifiers are possible to use up to 180 G and 57 G, respectively.

(5) Video camera

An area image sensor type CCD camera has been tested and no particular change is measured up to 100 G.

(6) Lamp

Two types of lamps, a halogen lamp (100V/500W) and a silica lamp (100V/200W) have been tested. Vibration of filaments is occurred at 200 G in case of halogen lamp and at 400 G in case of silica lamp, although illuminance of both lamps is not change. The vibration will reduce the lifetime of the lamps.

4. 6 Control system

Figure 24 shows a concept of the control system for the in-vessel viewing periscope. The control system is mainly composed of two control systems, site control system and main control system, and three auxiliary systems, power supply, vacuum evacuation and CCD camera cooling systems. These site control system including the auxiliary systems and the main control system are installed in the torus hall and the central control room, respectively. All of the signals between the site control system and the main control system are transmitted by optical fiber and position data of the in-vessel viewing periscope and image data, which are taken by the rad-hard CCD camera are combined on the three dimentional graphic display. The details of the control system will be disigned after a making of the viewing scenario.

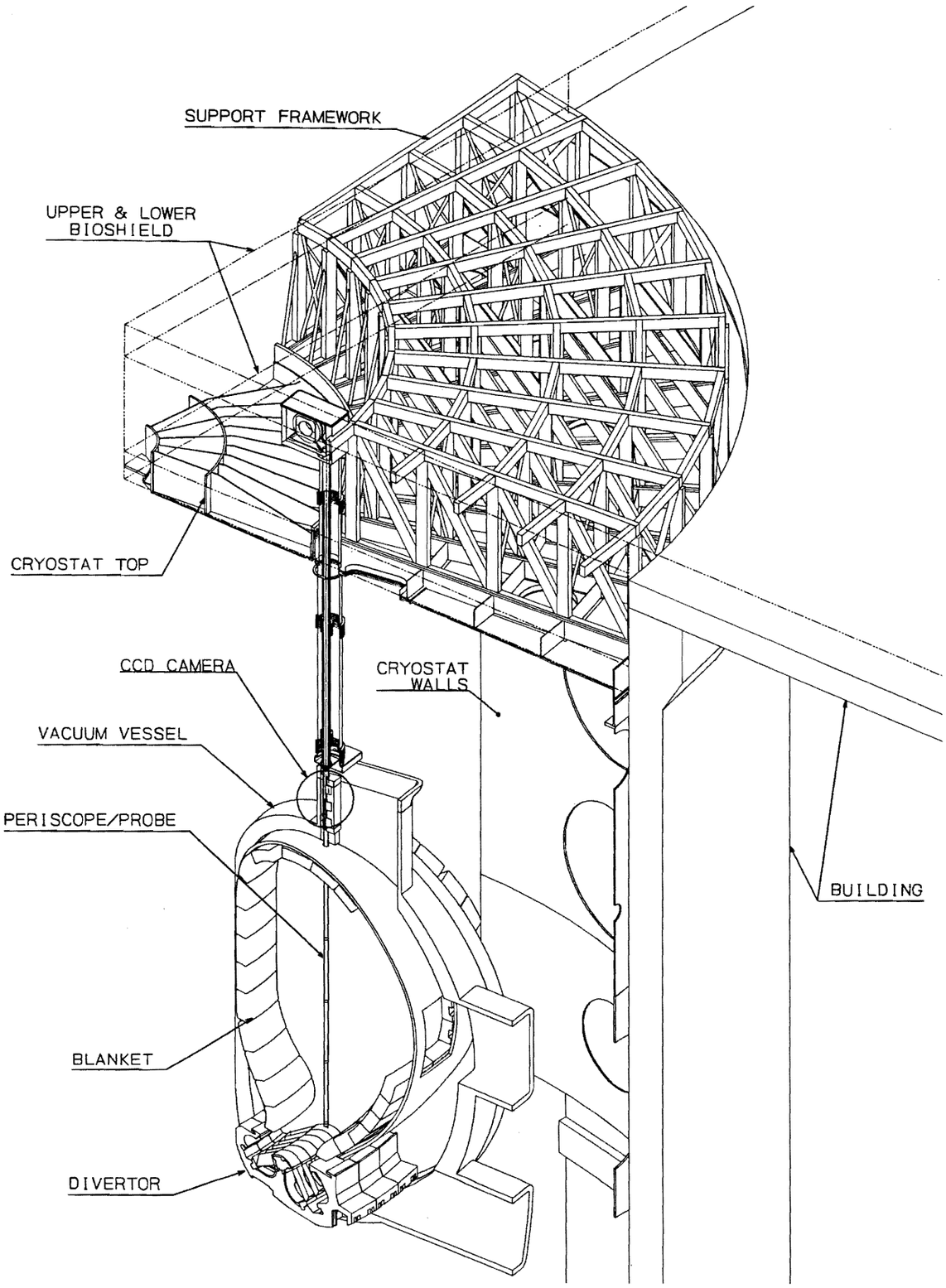

Fig. 1 Overall assembly of in-vessel viewing periscope for ITER.

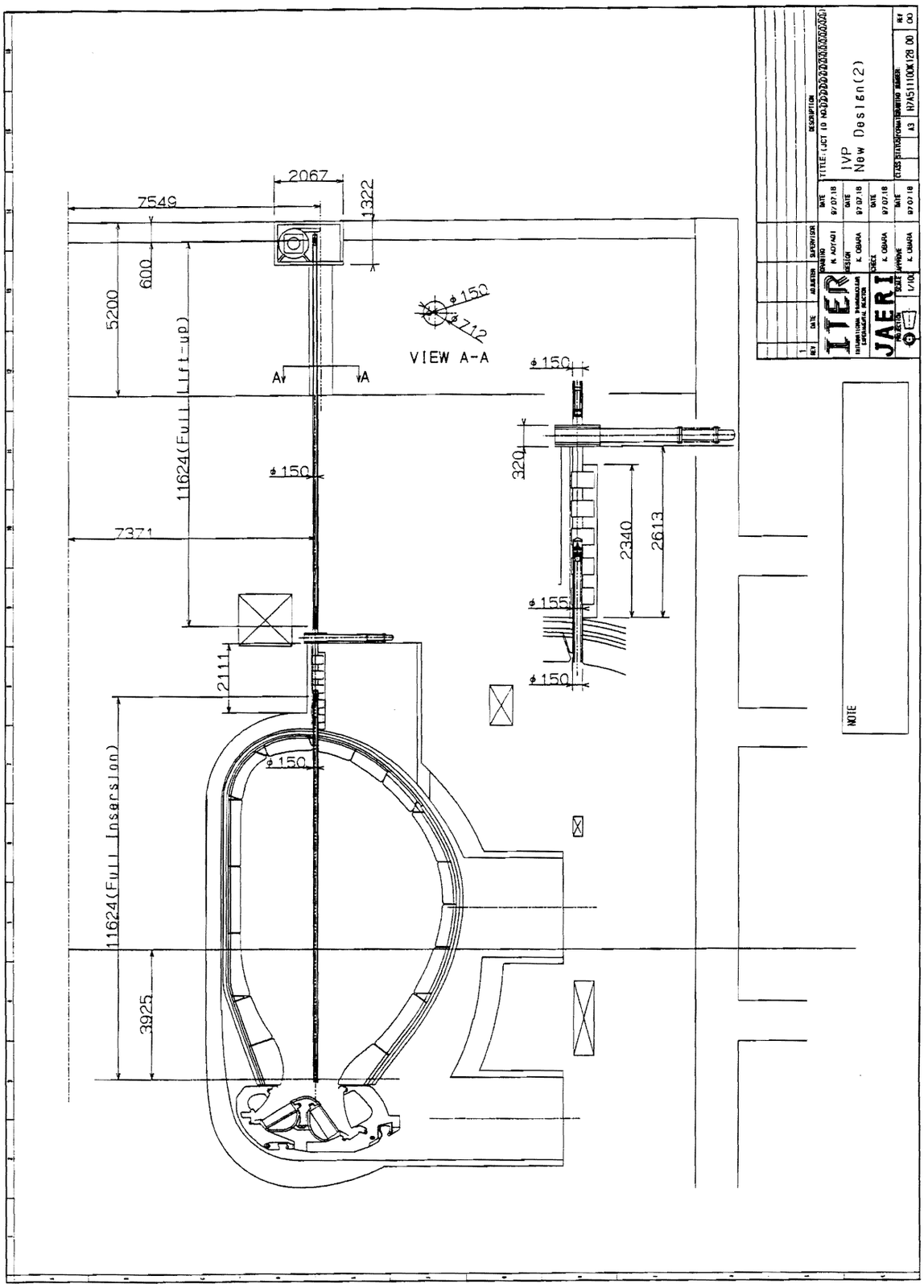

Fig. 2 Design concept of 11m-long in-vessel viewing periscope.

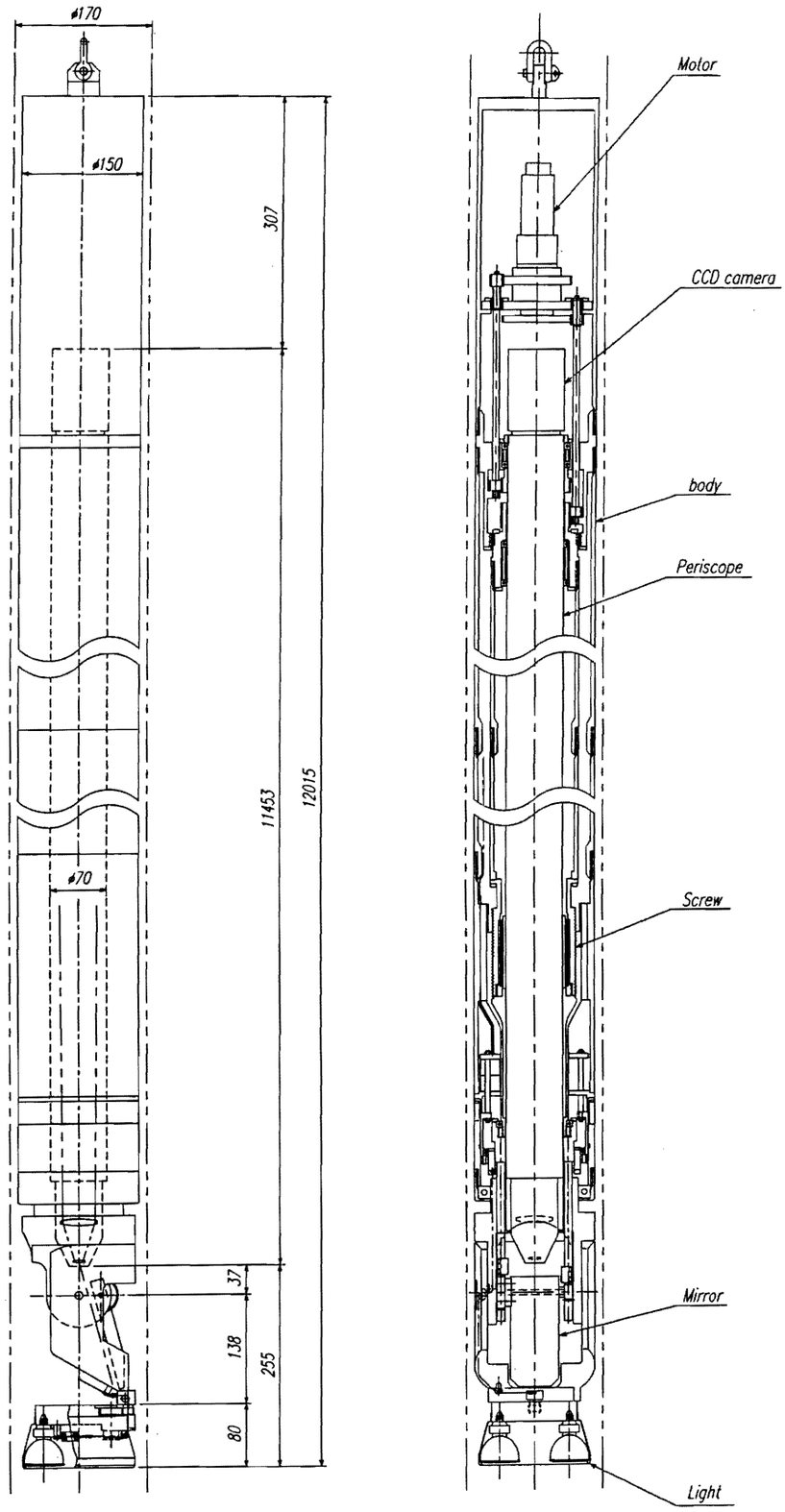

Fig. 3 Design concept of 11m-long in-vessel viewing periscope body.

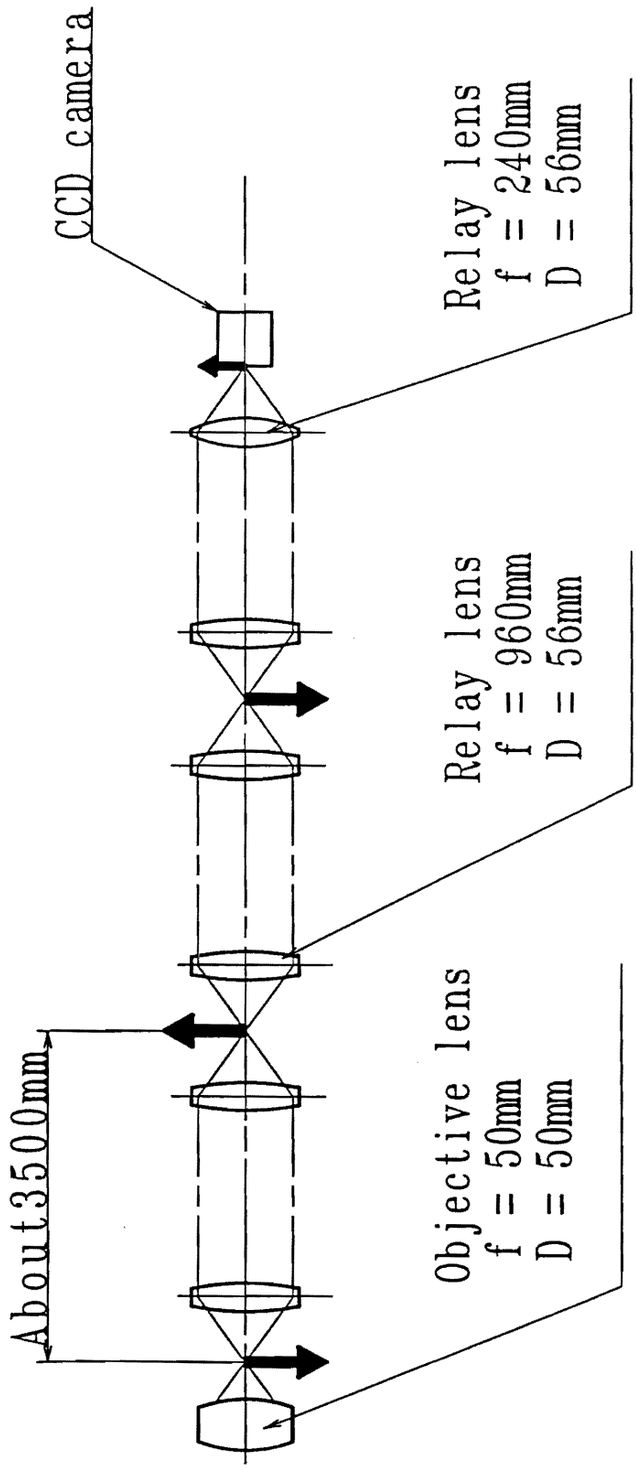

Fig. 4 Optical arrangement of 11m-long in-vessel viewing periscope.

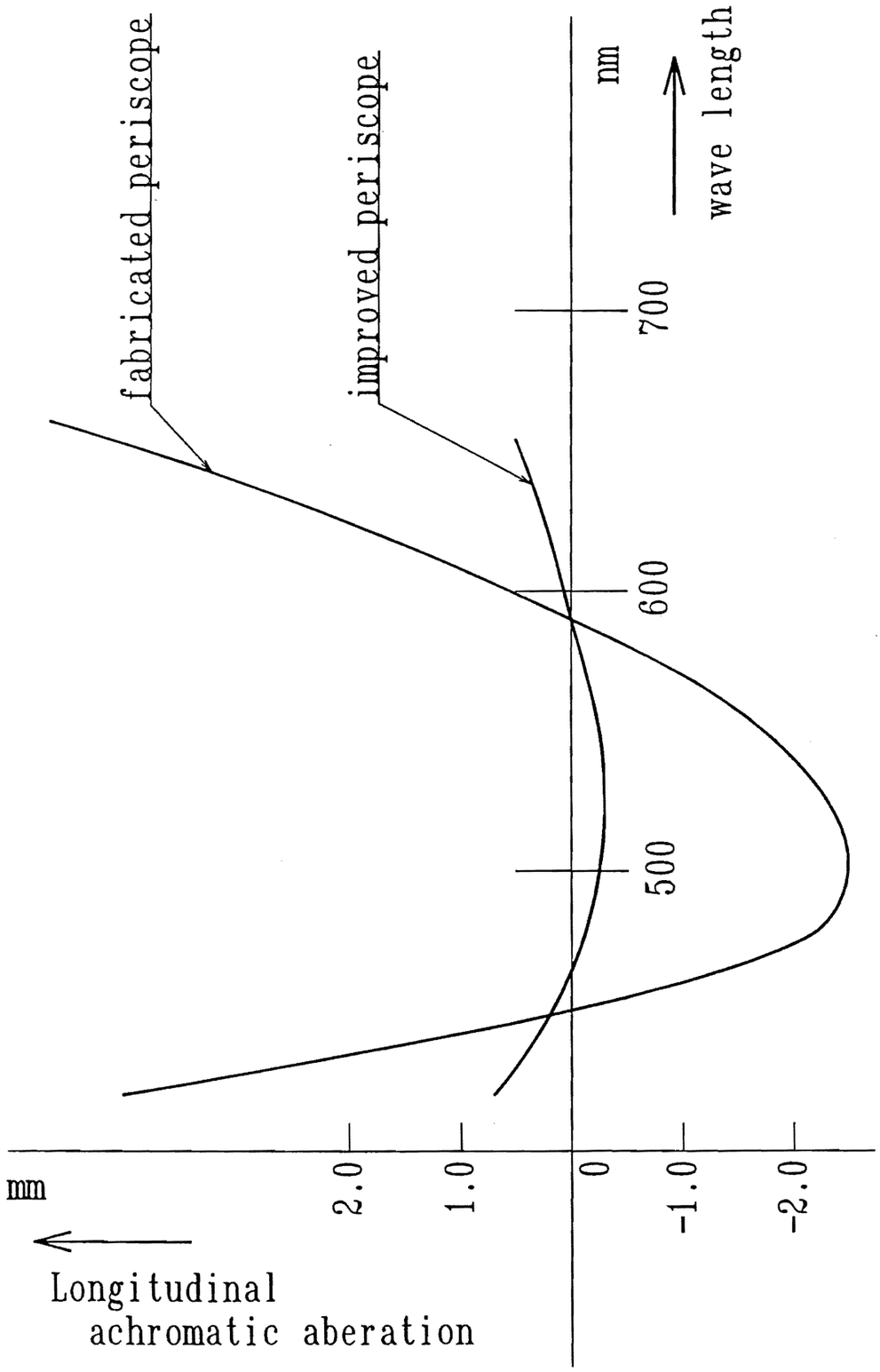

Fig. 5 Comparison of achromatic aberation in the longitudinal direction of 11m-long and 15m-long periscopes.

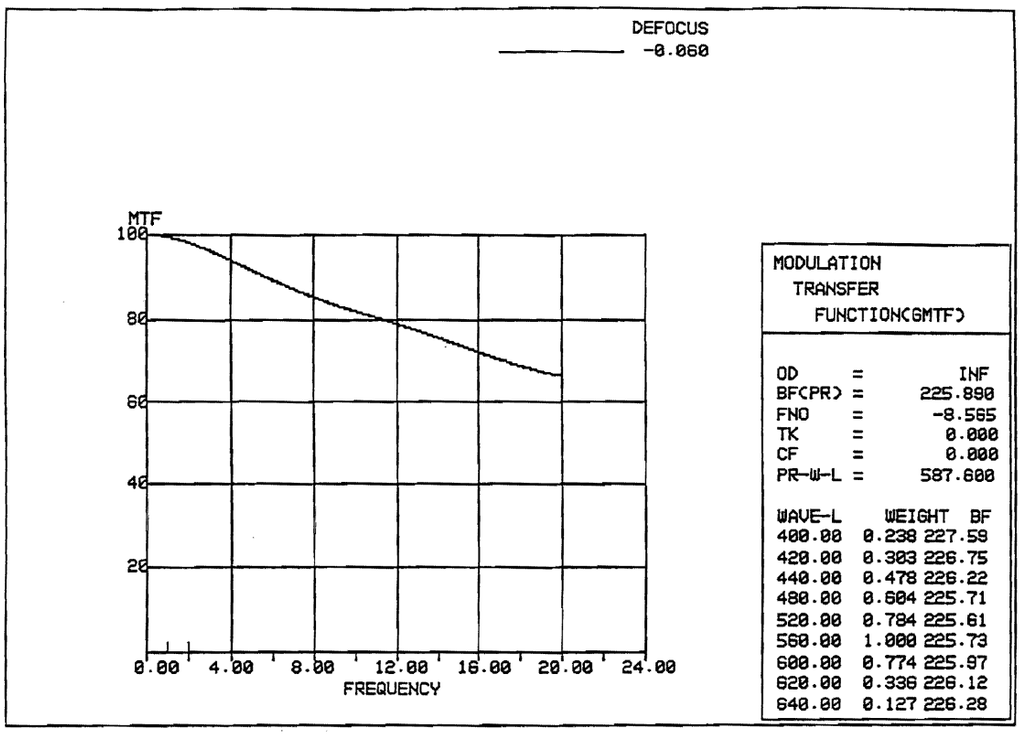

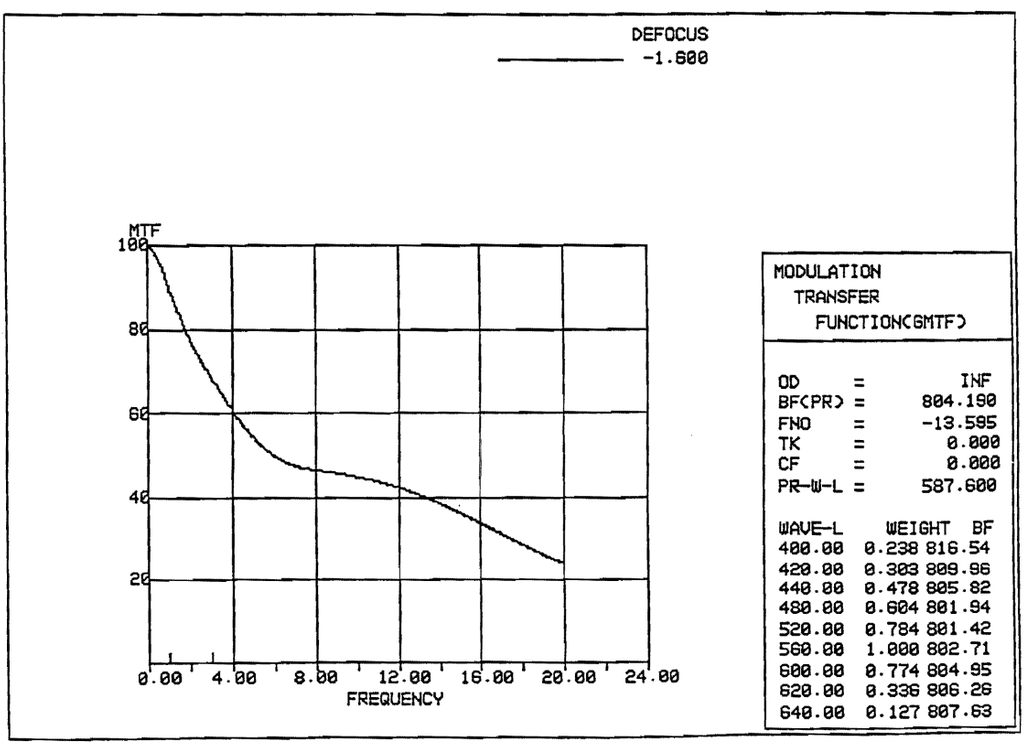

Fig. 6 Modulation transfer function (MTF) changes of 11m-long and 15m-long periscopes, upper : 11m-long periscope, bottom : 15m-long periscope.

Table 1 Comparison of optical performances of 11m-long and 15m-long periscopes.

Item	15m-long periscope	11m-long periscope
- Diameter (mm)		
Periscope body	100	70
Objective lens	20	10 and 40
Relay lens	80	56
- Length of periscope (m)	15	11.66
- Focal length (mm)		
Whole of periscope	12.5	12.5
Objective lens	12.5	50.0
Relay lens	816	1028 and 257
- Brightness (Fno.)		
Whole of periscope	13.6	8.5
Objective lens	13.6	34
Relay lens	13.6	34 and 8.5
- Number of lens		
Whole of periscope	19	18
Objective lens	7	5
Relay lens	2	2 and 3
- Lens materials	· Synthetic quartz · CeO2 contained lead glass	· Synthetic quartz · CeO2 contained lead glass
- Angle of visual field		
Opposite angle	37 °	37 °
Horizontal	30 °	30 °
Vertical	23 °	23 °
- MTF value (%)		
10 lines / width of 1 mm	44	82
20 lines / width of 1 mm	24	65

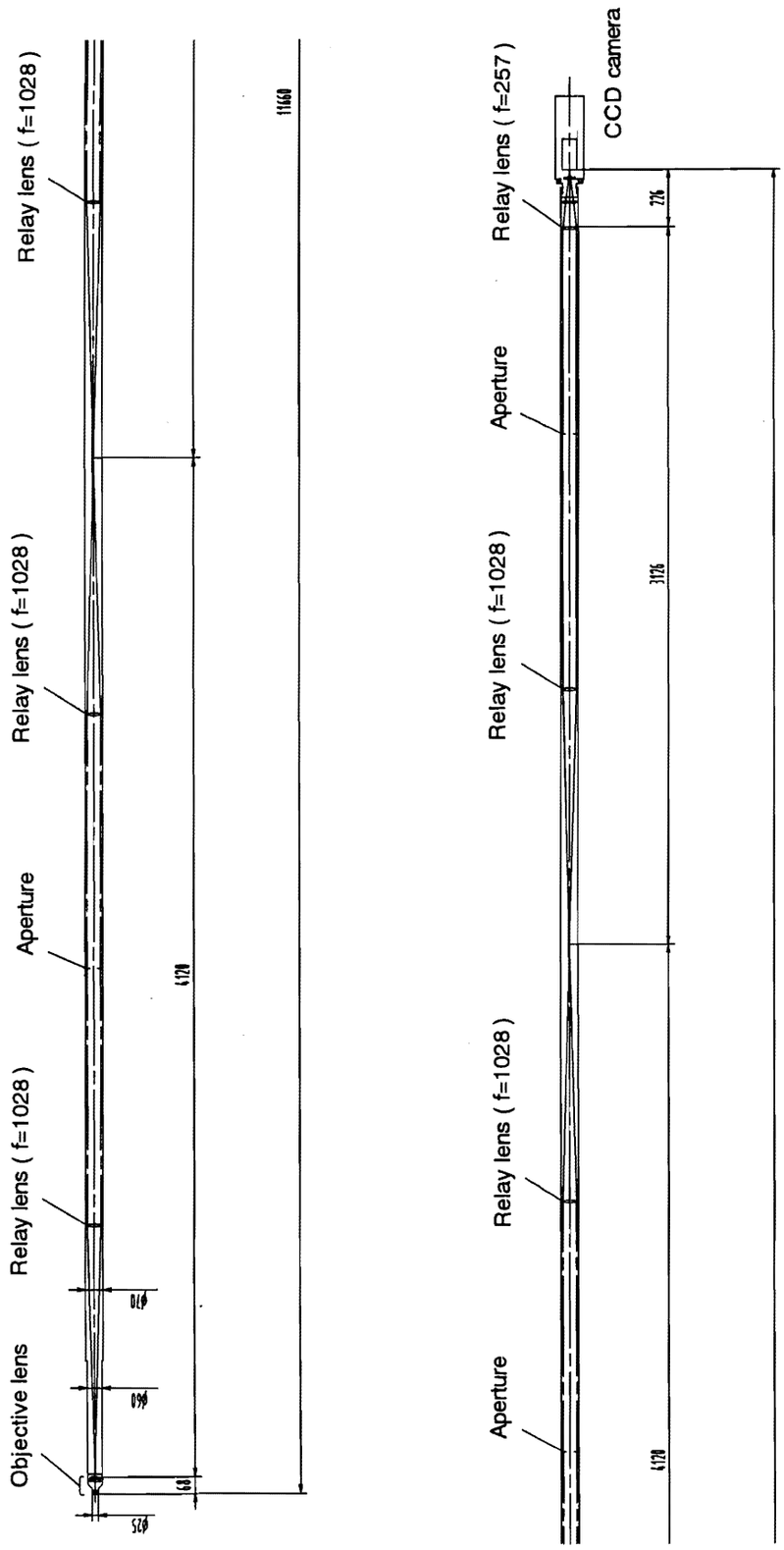

Fig. 7 Overall layout of 11m-long periscope for ITER in-vessel viewing.

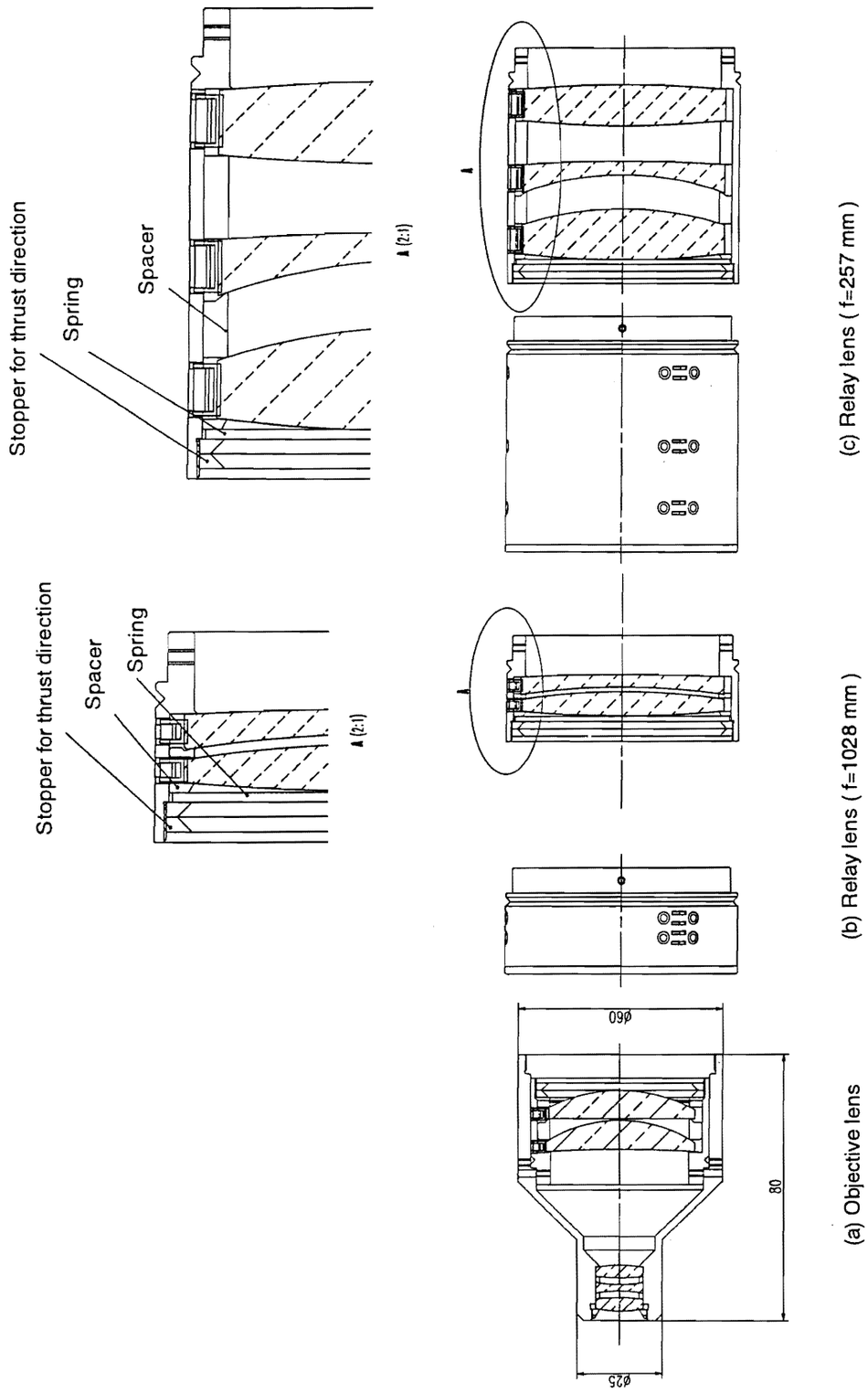

Fig. 8 Optical lenses composition of 11m-long in-vessel viewing periscope.

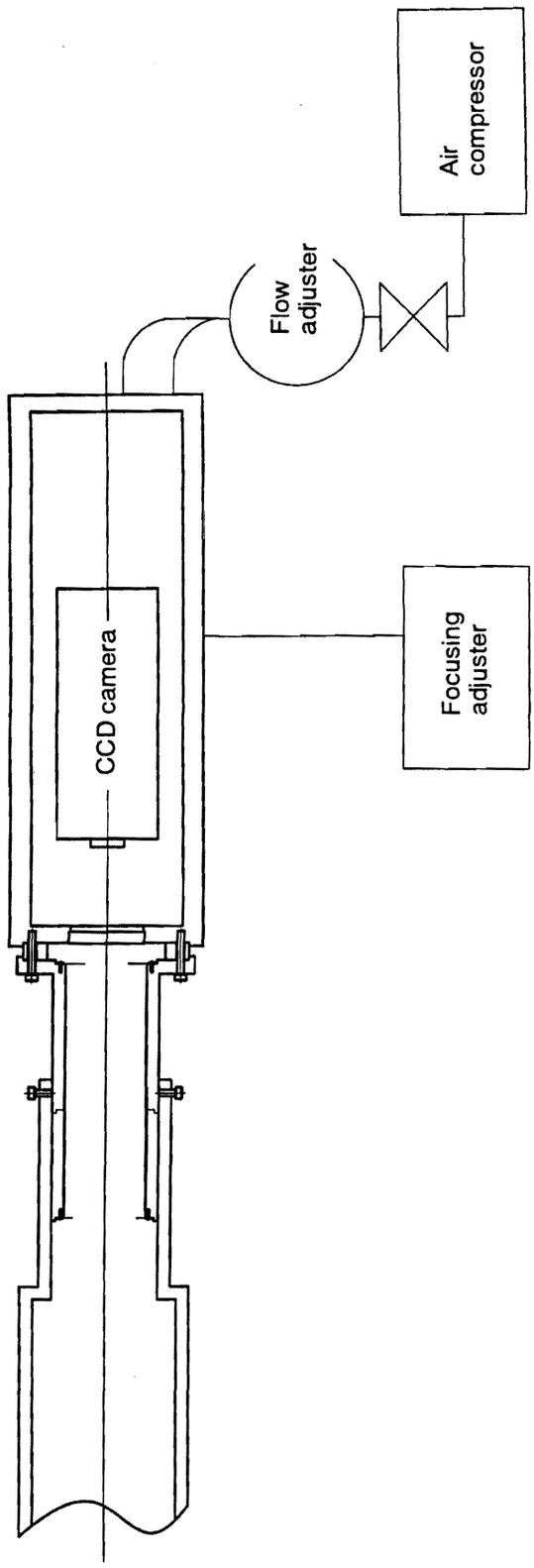

Fig. 9 A part of eyepiece of 11m-long in-vessel viewing periscope.

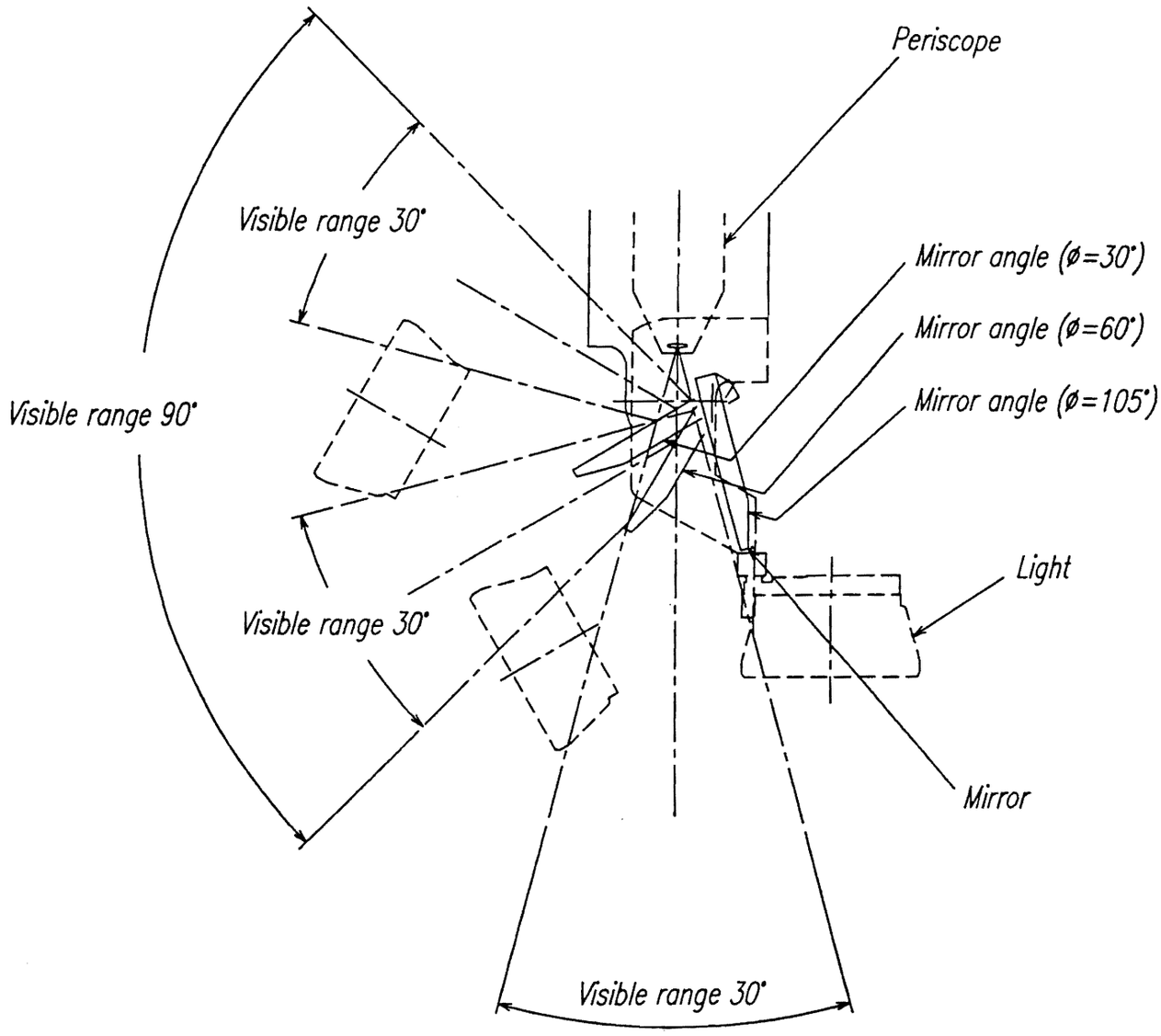

Fig. 10 Visible range of movable mirror attached to tip of the periscope body.

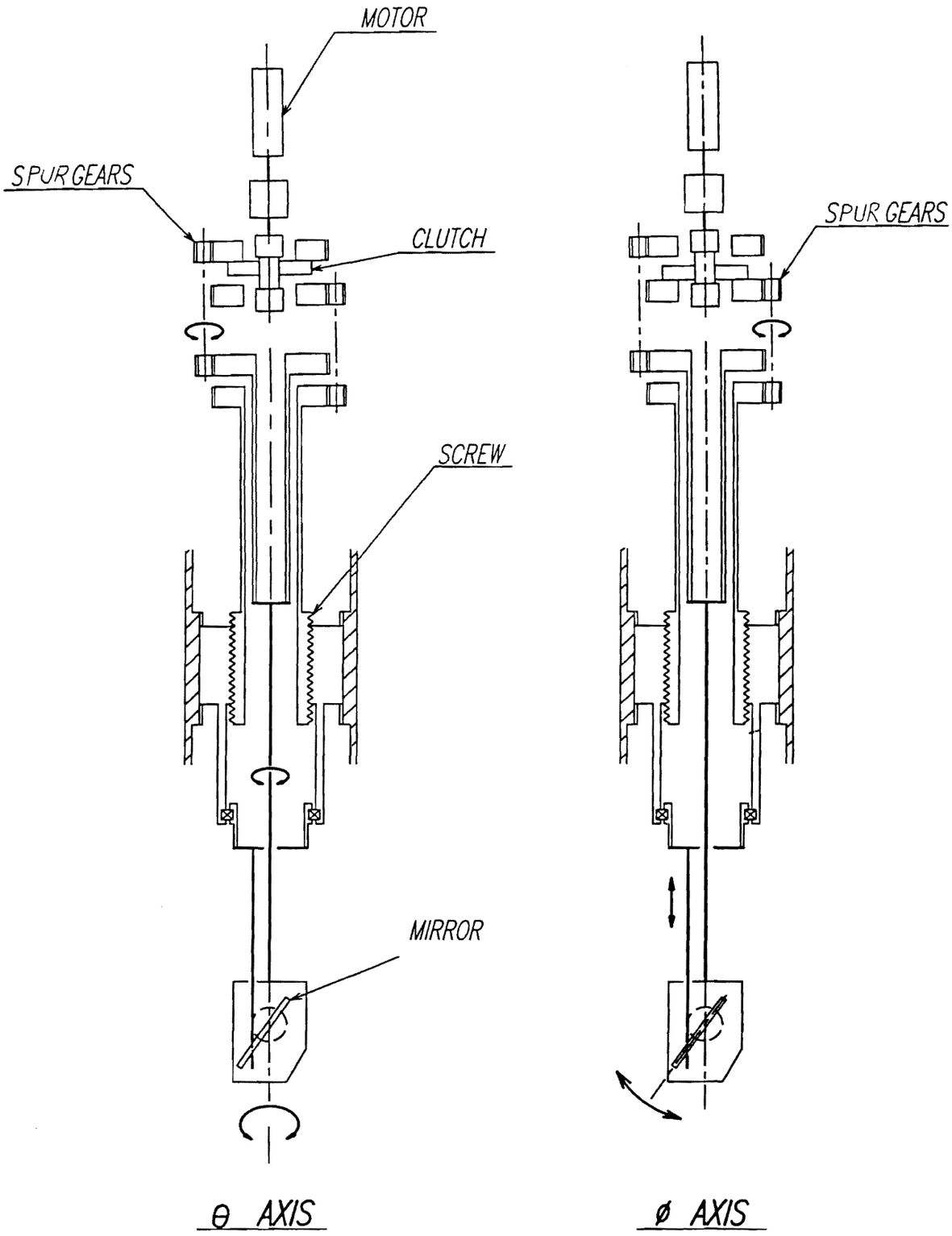

Fig. 11 Schemtic diagrams of mirror driving mechanism.

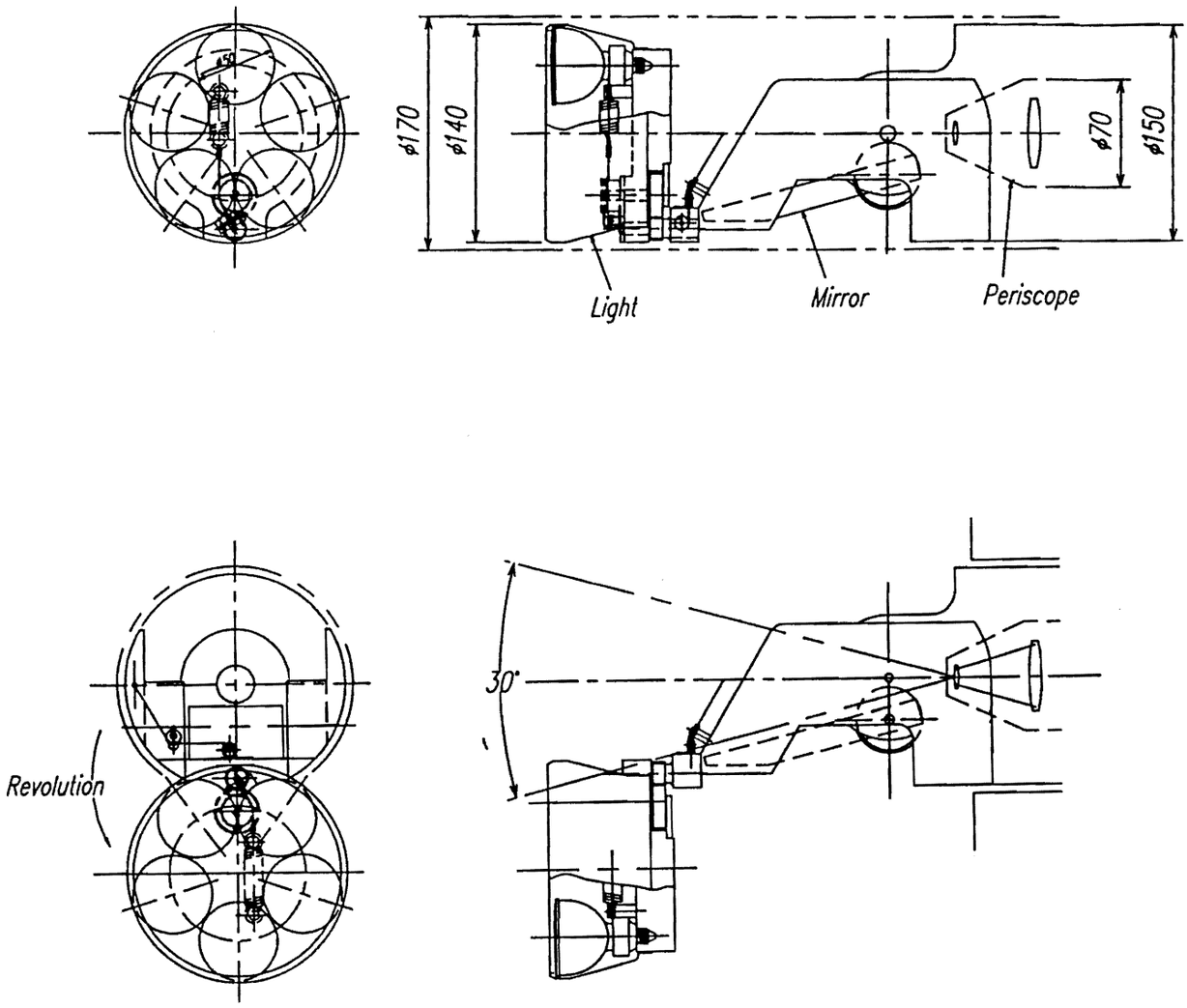

Fig. 12 Design concept of lighting device attached to tip of the periscope body.

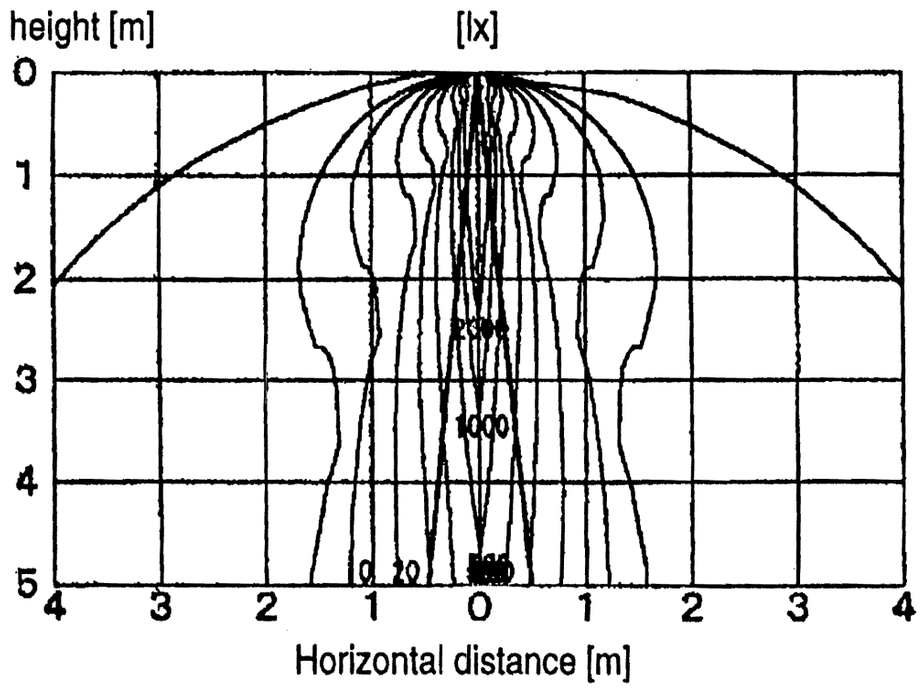

Fig. 13 Illuminance distribution of halogen lamp used the lighting device.

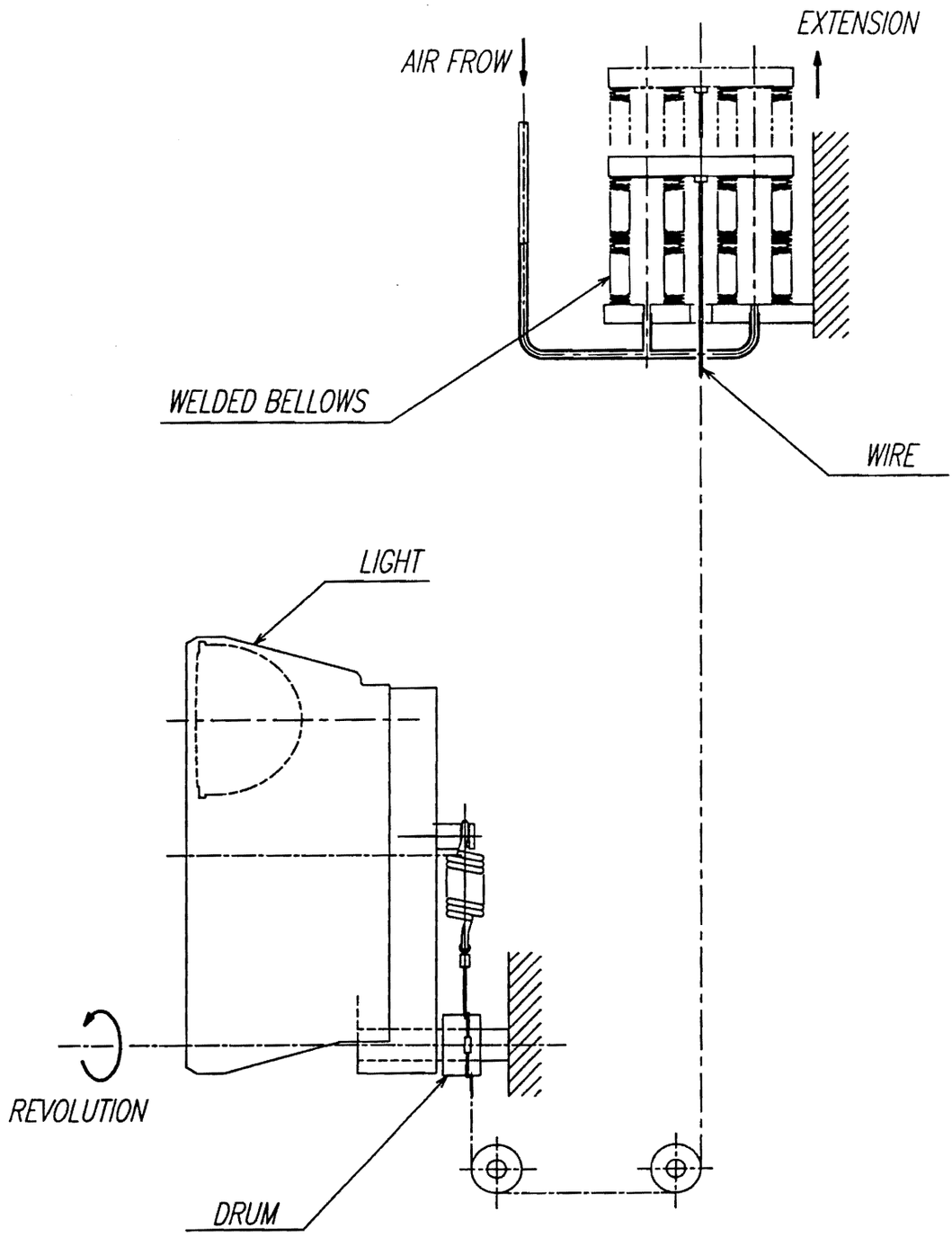

Fig. 14 Schematic diagram of off-centered driving mechanism for the lighting device.

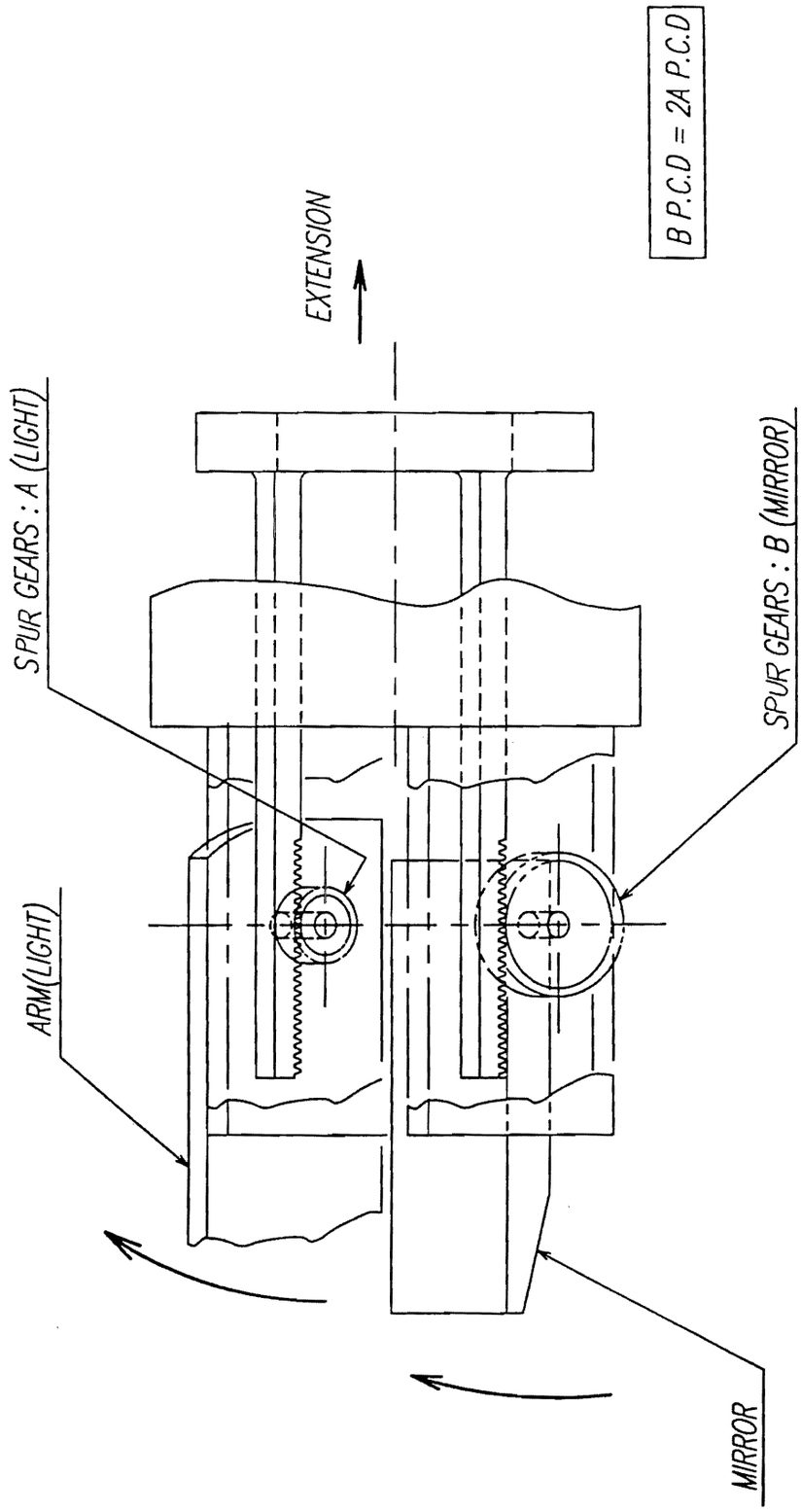

Fig. 15 Design concept of tilting mechanism for the lighting device.

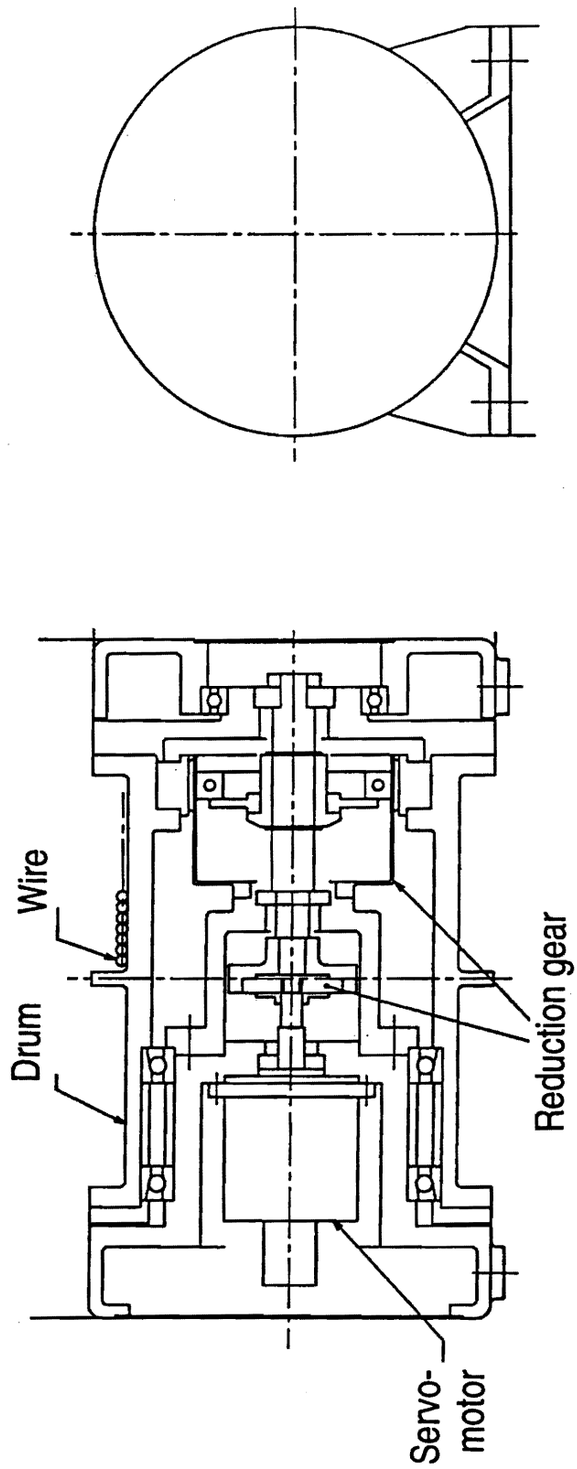

Fig. 16 Outline of winch for insertion/lifting equipment.

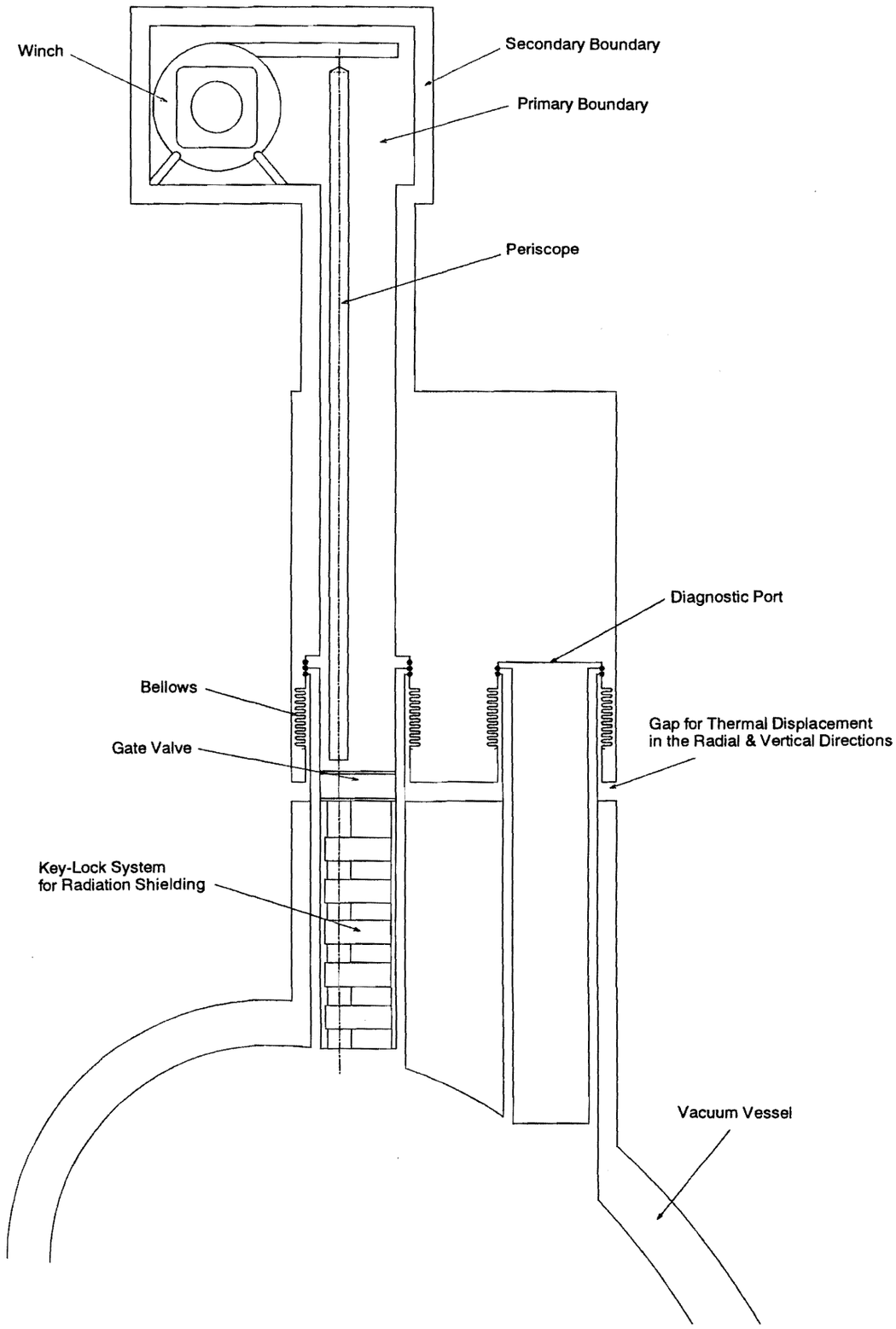

Fig. 17 Concept of upper port interface.

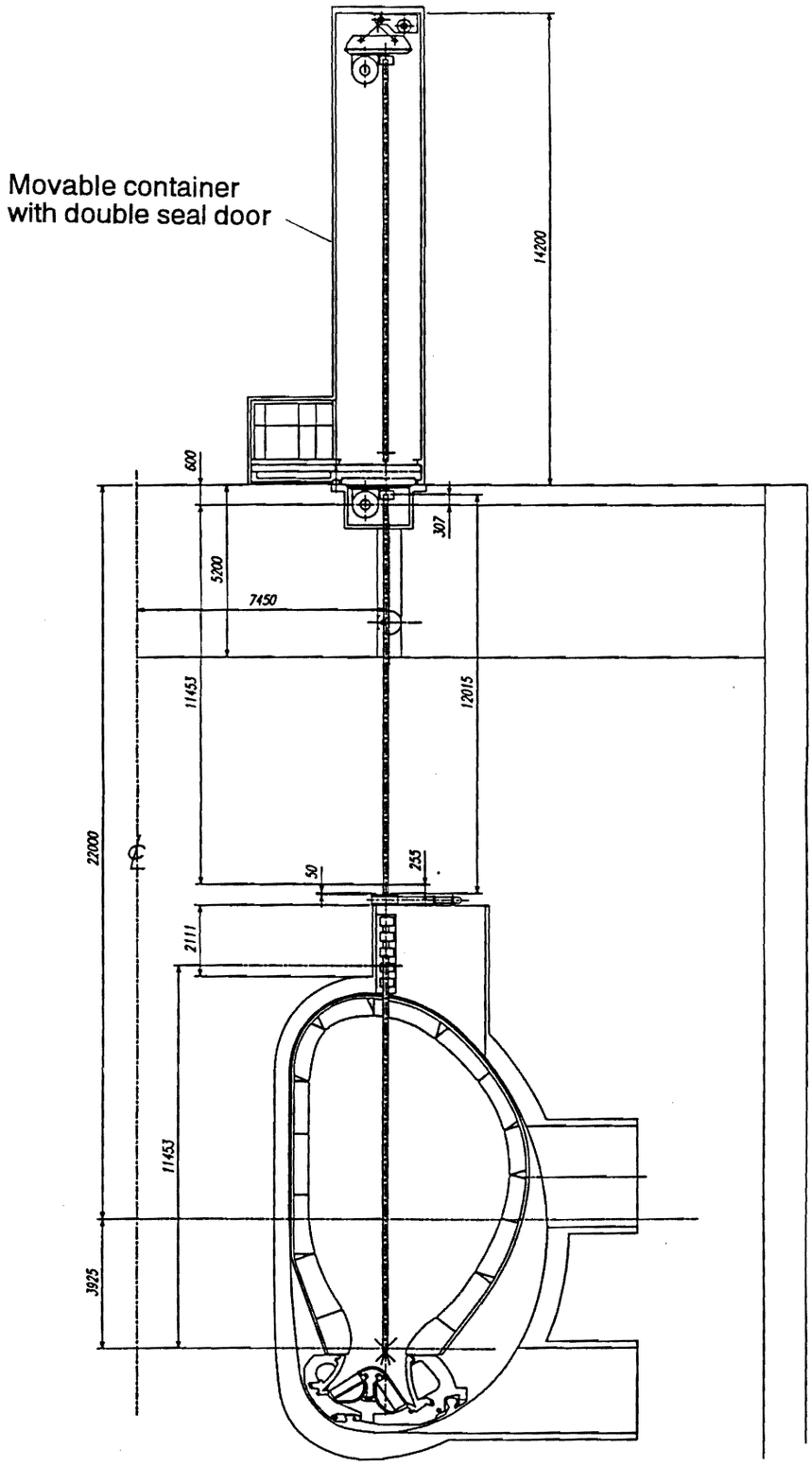

Fig. 18 Concept of movable container for maintenance of the periscope.

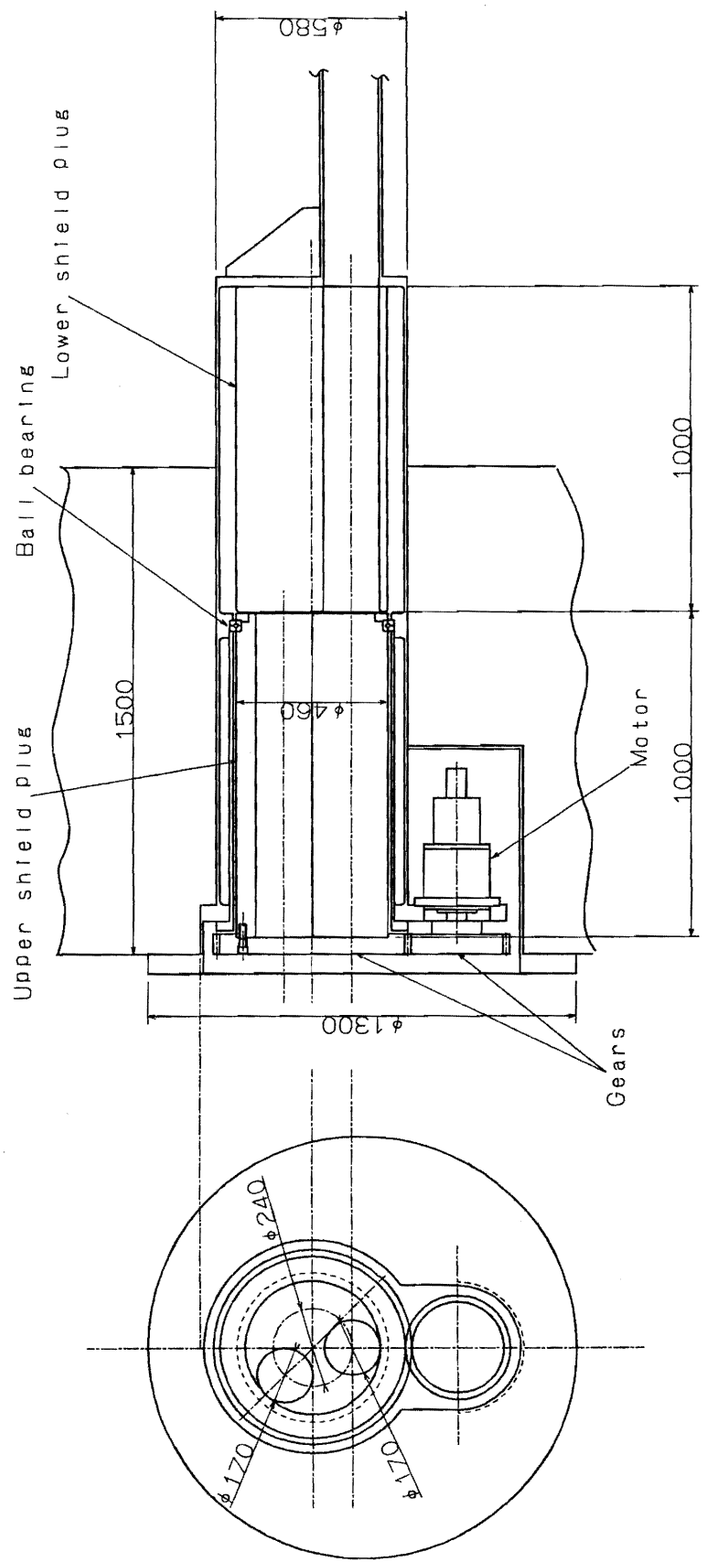

Fig. 19 Design concept of shielding plug.

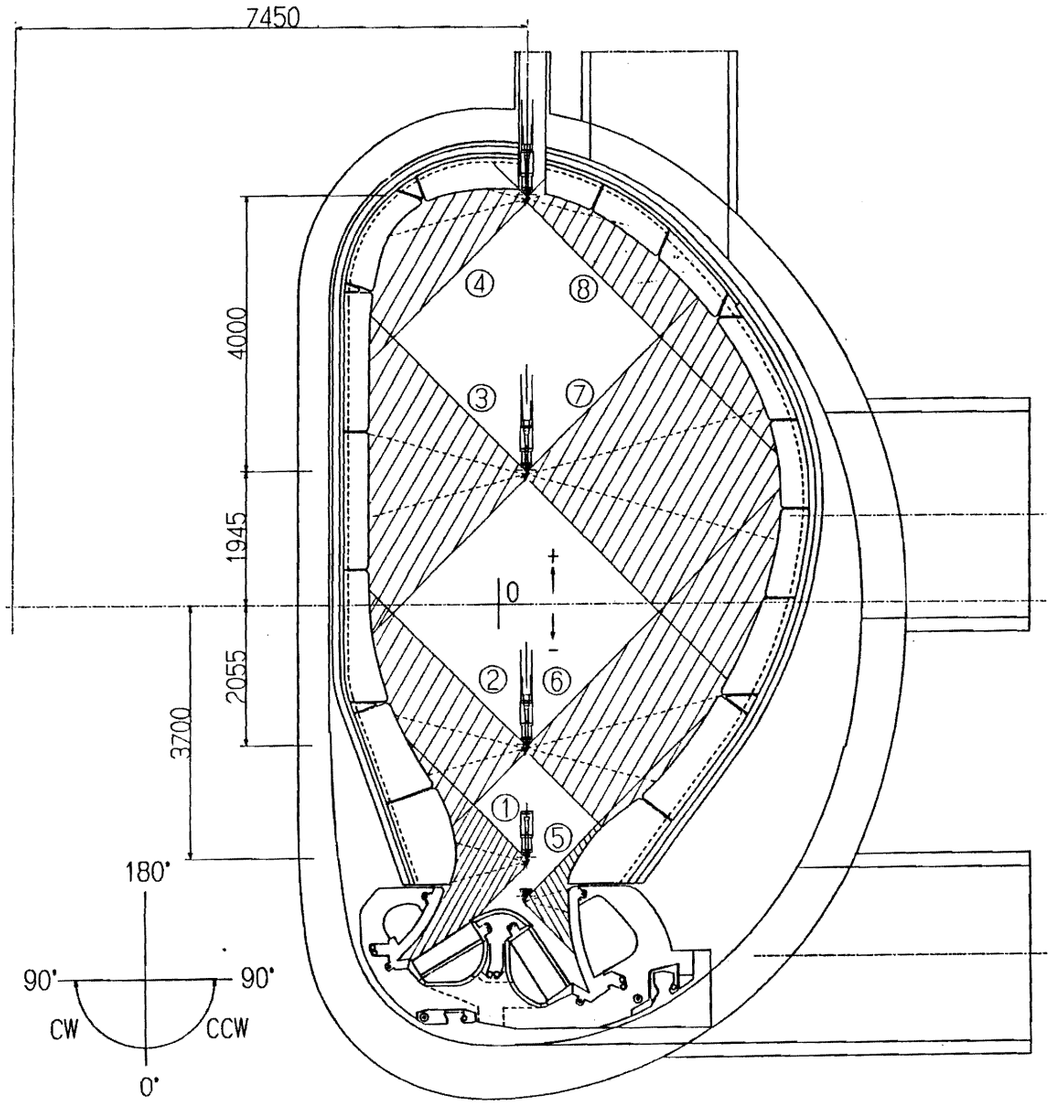

Area No.	1	2	3	4
Port position (mm)	7450	7450	7450	7450
Insertion depth (mm)	-3700	-2055	+1945	+5945
Mirror dimension (mm)	140 x 60	140 x 60	140 x 60	40 x 60
Mirror position (θ axis)	cw 90°	cw 90°	cw 90°	cw 90°
Mirror position (ϕ axis)	30° ~ 60°	30° ~ 60°	30° ~ 60°	30° ~ 60°

Area No.	5	6	7	8
Port position (mm)	7450	7450	7450	7450
Insertion depth (mm)	-4200	-2055	+1945	+5945
Mirror dimension (mm)	140 x 60	140 x 60	140 x 60	40 x 60
Mirror position (θ axis)	ccw 90°	ccw 90°	ccw 90°	ccw 90°
Mirror position (ϕ axis)	30° ~ 60°	30° ~ 60°	30° ~ 60°	30° ~ 60°

Fig. 20 Installation position and viewing range of in-vessel viewing periscope.

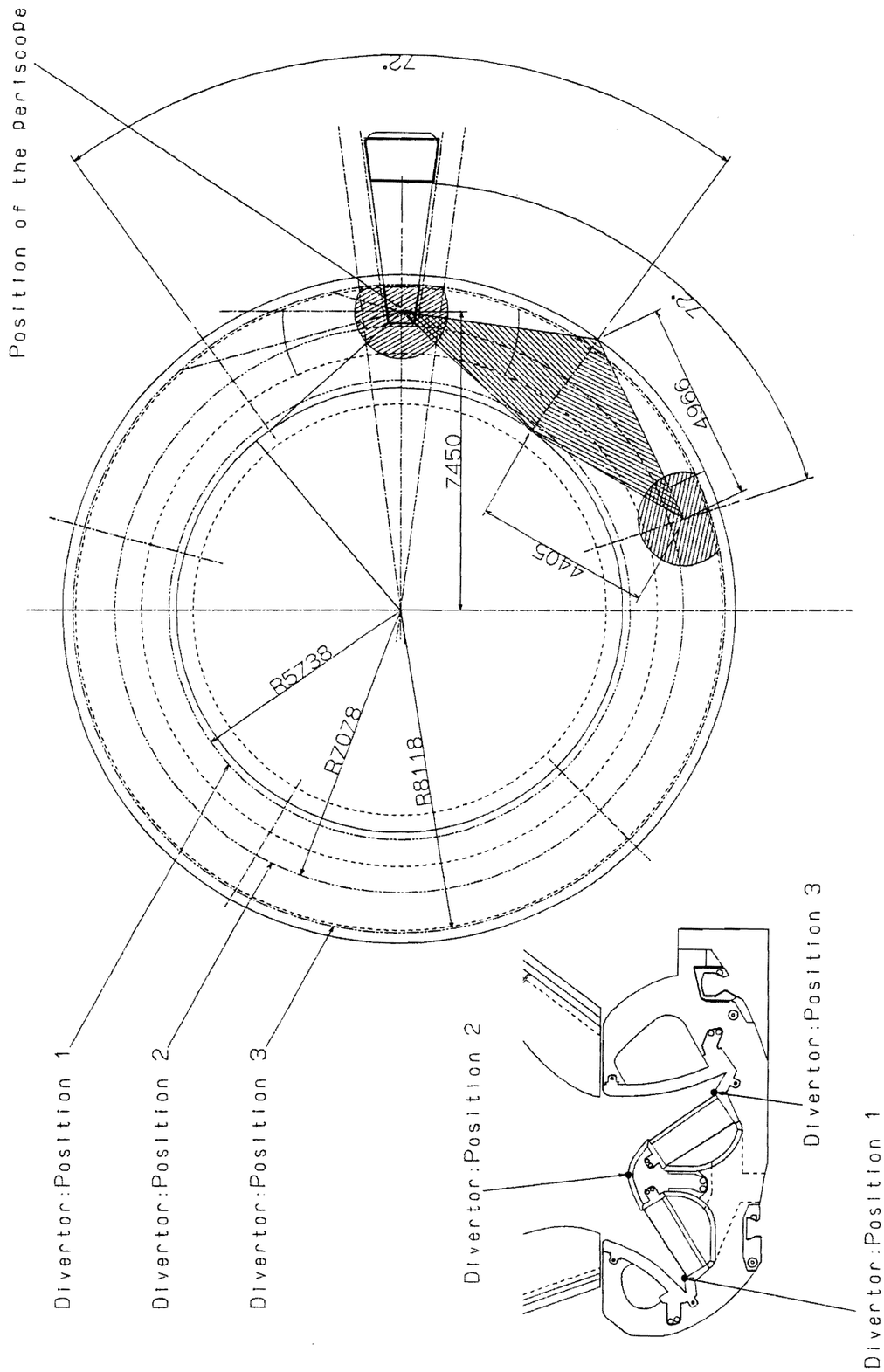

Fig. 21 Visible range of periscope in the toroidal direction.

Table 2 Calculation results of temperature rise of CFRP periscope body.

t (min)	$X = (\alpha \cdot t) / L^2$	Yo	Tn (°C)
10	28.359	0.55	146.0
20	56.719	0.325	209.0
30	85.078	0.185	248.2
40	113.437	0.115	267.8
50	141.797	0.063	282.36
60	170.156	0.037	289.64
70	198.515	0.021	294.12
80	226.875	0.012	296.64
90	255.234	0.0065	298.18
100	283.593	0.0037	298.96
110	311.953	0.0021	299.41
120	340.312	0.0012	299.66

Table 3 Calculation results of temperature rise of Al alloy periscope body.

t (min)	$X = (\alpha \cdot t) / L^2$	Yo	Tn (°C)
10	13.667	0.75	90.0
20	27.333	0.57	140.4
30	41.000	0.44	176.8
40	54.667	0.34	204.8
50	68.333	0.25	230.0
60	82.000	0.20	244.0
70	95.667	0.15	258.0
80	109.333	0.12	266.4
90	123.000	0.091	274.52
100	136.667	0.069	280.68
110	150.333	0.053	285.16
120	164.000	0.037	289.64
130	177.667	0.031	291.32
140	191.333	0.021	294.12
150	205.000	0.019	294.82
160	218.667	0.013	296.36
170	232.333	0.011	296.92
180	246.000	0.007	298.04

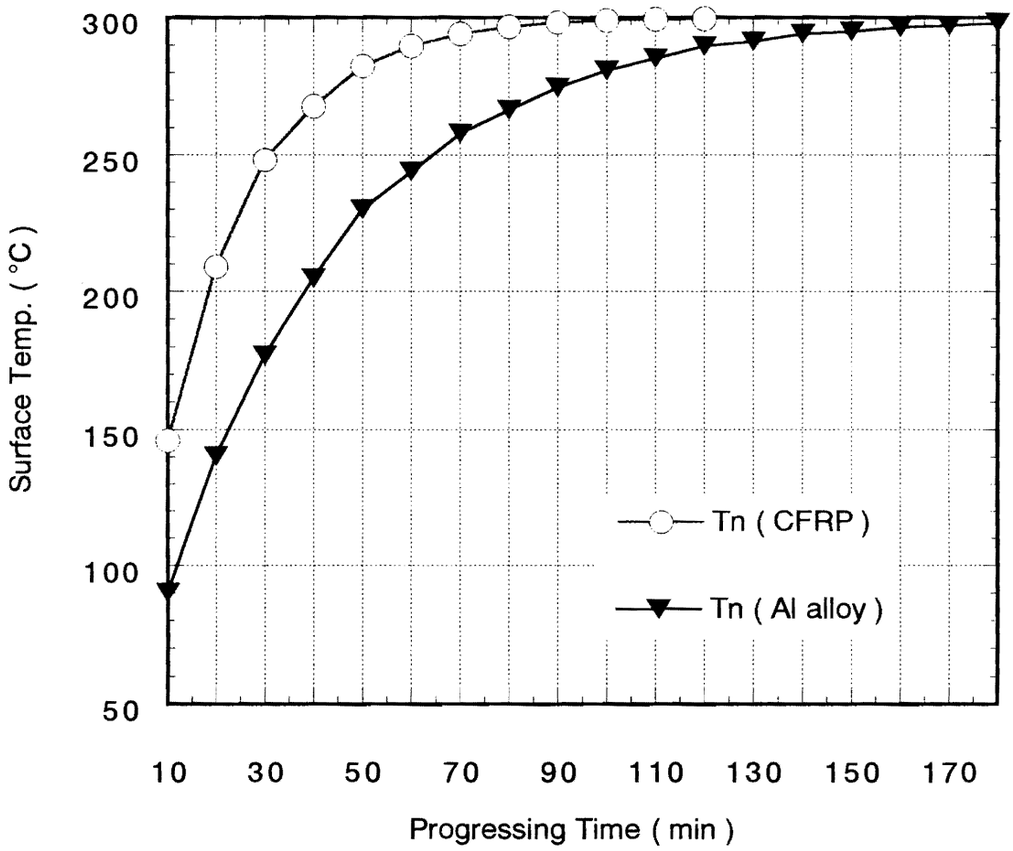

Fig. 22 Temperature rise of CFRP and Al alloy periscope bodies by thermal radiation heat from in-vessel wall.

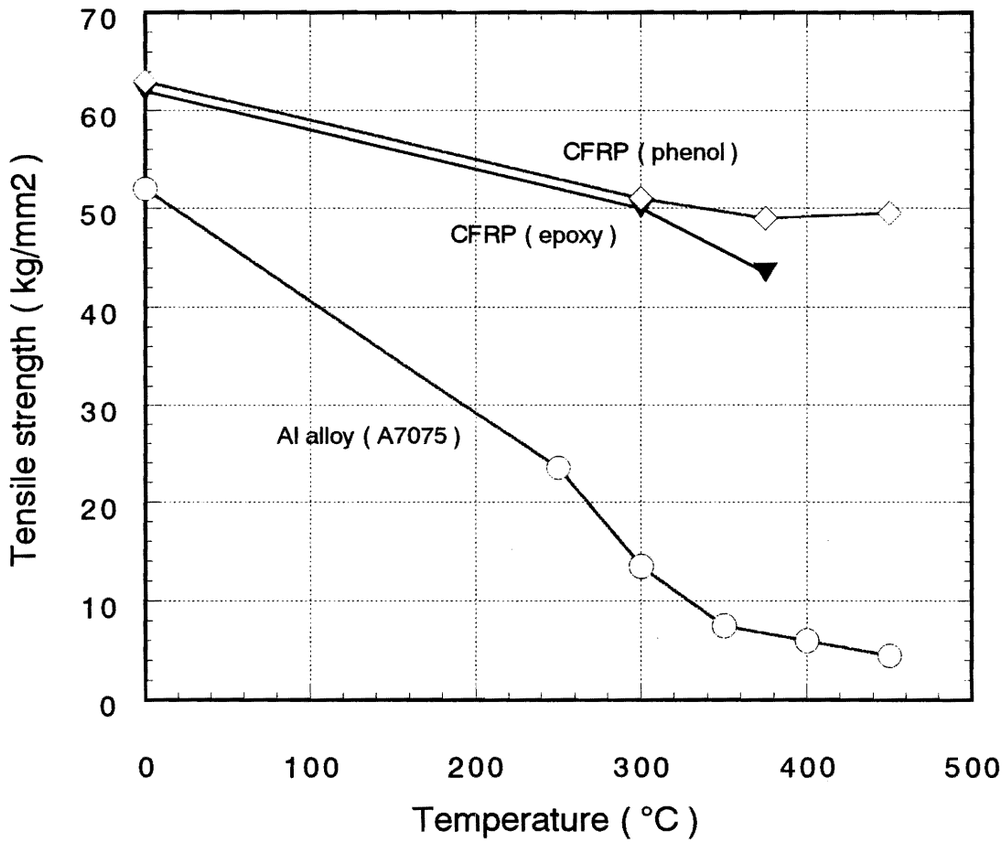

Fig. 23 Tensile strength change of CFRP and Al alloy as a function of temperature.

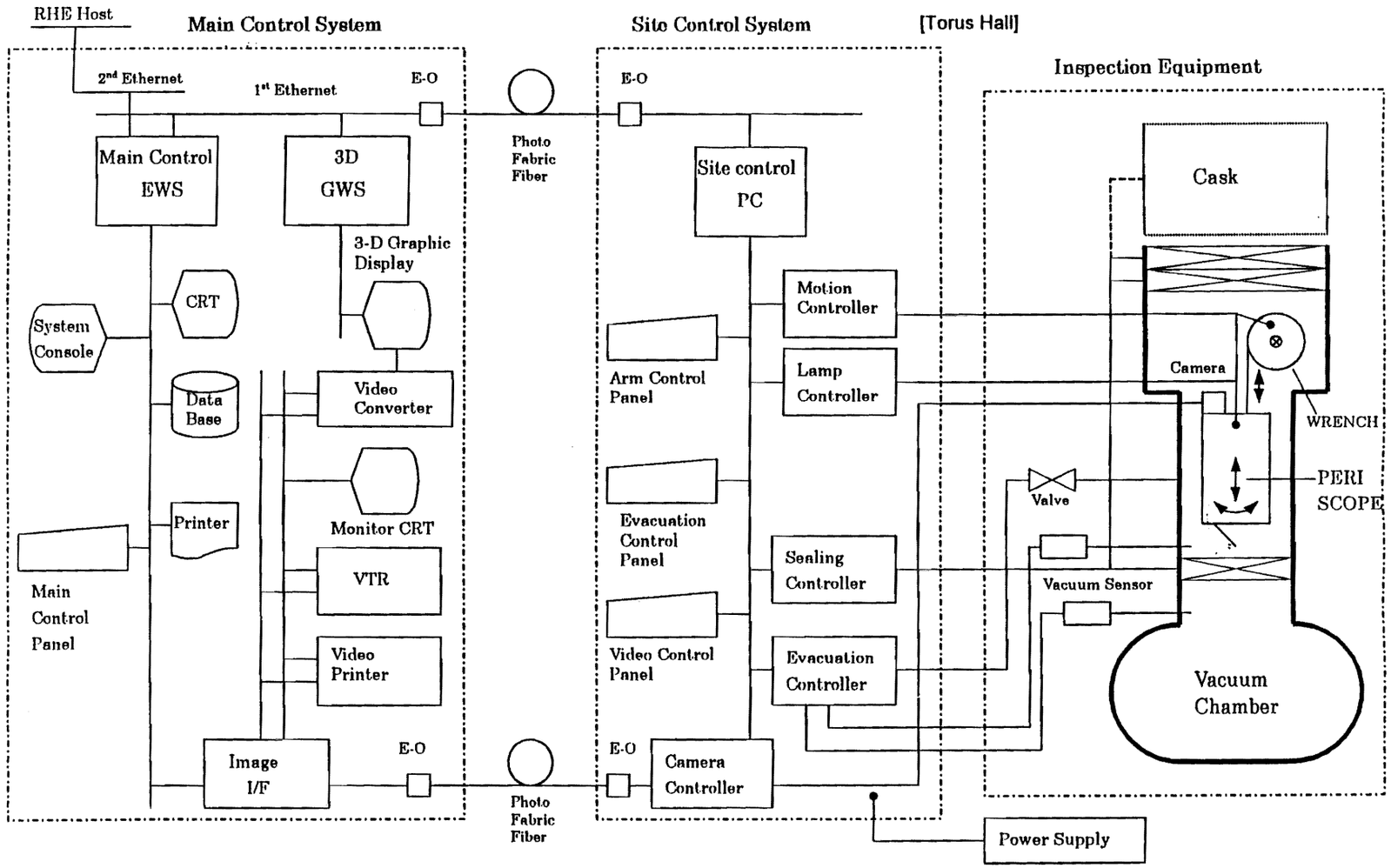

Fig. 24 Schematic diagram of control system for in-vessel viewing periscope system.

5. STATUS OF TECHNOLOGY DEVELOPMENT

5. 1 Background and scope

In parallel with the Design Task (a part of the D311), the R&D Task (T328) is conducting in order to develop an in-vessel viewing periscope, as mentioned previously. The main objective of this R&D Task is to provide the R&D to support the detail design of the in-vessel viewing system. The R&D Task consists of 3 phases. Phase 1 of development includes initial assessment of viewing resolution and quality through the long probe tube as a function of distance between target and sensor, and radiation hardness data and selection of components. In Phases 2 and 3, partial mock-up tests using a long periscope and a mirror driving mechanism are included as well as assessment on radiation hardness and optical adjustment mechanism.

This section summarizes the status of these technology development as a final report of the R&D Task.

5. 2 Refracting type optical periscope

Four types of refracting optical periscopes, which are major component of the in-vessel viewing periscope, have been fabricated and tested. As the 1st stage of development, two types of 6m-long periscopes: a standard type periscope composed of standard glass lenses and a radiation hard type periscope composed of radiation hard glass lenses were fabricated and irradiated using a gamma irradiation test facility with a maximum dose rate of 15 kGy/h. Each periscope includes four reflectors to change optical angles. The irradiation experiments show that the standard type periscope becomes invisible after 2 hr irradiation, while the radiation hard type periscope shows no degradation in viewing performance for more than 1000 hr irradiation.

Based on these results, as the 2nd stage of development, an advanced radiation hard type periscope with a zooming mechanism has been fabricated and irradiated. In this gamma irradiation test, the zooming mechanism was broken due to lubrication trouble at an accumulated dose of 1.2 MGy although the viewing performance is not changed over 40 MGy irradiation. However, four reflectors were replaced with new ones at an accumulated dose of 26.5 MGy due to erosin. From these results, it has been confirmed that the radiation hard periscope composed of radiation hard glass lenses can be used under intense gamma irradiation environment for sufficient length of time. Acceptance doses of this rad-hard periscope is estimated over 100 MGy and the irradiation test has been continued up to an integrated dose of 200 MGy.

As the 3rd stage of development, a 15m-long periscope composed of radiation hard lenses without reflectors, which is a full-scale ITER in-vessel viewing periscope, has been fabricated to verify scalability of the optical performance and to investigate the effects of high temperature conditions on viewing capability. In this test, the periscope is heated up to 250°C using electrical heaters attached on the periscope body and it is found that the thermal expansion of the periscope body in the longitudinal and radial directions are 85 mm and 0.5 mm, respectively. In addition, it has been demonstrated that an optical focal adjustment mechanism equipped to the periscope can focus to view a 8-mm wide black line located at 5 m distance from the objective lens of the 15-m long periscope even if the periscope is heated to 250°C.

(1) Radiation hard type 6m-long periscope

a) Outline

Figure 22 shows a general layout of the radiation hard type 6m-long periscope with a zooming mechanism fabricated as the 2nd stage of development. The 6m-long periscope has four

bends in order to install it in the gamma irradiation test facility. A reflector is equipped at each bend to align optical angles. The visual images through an objective lens, four relay lenses and reflectors is directly focused on the CCD area image sensors. Each picture in Fig. 23 shows parts of the 6m-long periscope installed inside/outside the gamma irradiation test facility. The zooming mechanism and CCD camera head are equipped to the tip and eyepiece of the periscope, respectively. The followings are main specifications of the periscope.

Optical system
- Objective zoom lens : 1 (10 lenses combined)
- Relay lens : 4 (2 lenses combined)
- Reflector : 4
- Eyepiece : CCD area image sensor
- Magnification of zooming : 3
- Auto focusing mechanism

Materials of lens and reflector
- Lenses : Alkaline barium glass and lead glass containing CeO_2, OH doped synthetic quartz
- Reflector : Aluminum coated on synthetic quartz

Dimensions and periscope body material
- Dimensions : 80-mm diameter, 6-m length
- Periscope body material : Aluminum alloy (Alumite treated black body)

b) Gamma irradiation test

Figures 24. 1, 24. 2, 24. 3 show pictures of the images taken by the 2nd stage radiation hard type 6m-long periscope under the gamma irradiation of 8.5 ~ 13 kGy/h. Viewing distance from the objective lens to the test chart is 55 cm and illuminance on the test chart is 7500 lx. It is found that the viewing performance is not so changed up to doses of 19 MGy but it is drastically changed after 20 MGy irradiation and becomes invisible at doses of 26 MGy. At that time, therefore, the periscope was disassembled to inspect the optical elements.

The results showed that the surface of two relay lenses became dirty due to adhesion (see Fig. 25) and two reflectors were eroded by gamma irradiation and humidity in the irradiation cell (see Fig. 27). Due to this, reflectance was decreased by approximately 15 ~ 40 % (see Fig. 28) although tranmittance loss of the relay lenses were only 2% degradation in wavelength of 400 ~ 800 nm (see Fig. 26). In addition, discoloring of the periscope body from black to white was observed but it is no effect for the viewing performance. The irradiation tests have been restarted after surface cleaning of the relay lenses and exchange of the reflectors and periscope body with new ones.

(2) Radiation hard type 15m-long periscope

a) Outline

Based on the irradiation test results of the 6m-long periscope, a radiation hard type 15m-long periscope has been fabricated and tested. Figures 29 and 30 represent an external view of the 15m-long periscope fabricated. This periscope is a full-scale in-vessel viewing periscope for ITER and the main purposes are to verify scalability of optical performance using radiation hard lenses in a relatively long body and to clarify the effects of high temperature operation on

viewing performance. The major specifications of this 15m-long periscope are as follows. The length and diameter of this periscope is different from the latest design of 11m-long periscope but the basic performance is the same 11m-long periscope.

Optical system
- Objective lens : 1 (7 lenses combined)
- Relay lens : 6 (2 lenses combined)
- Reflector : no
- Eyepiece : CCD area image sensor
- Zooming mechanism : no
- Focusing adjuster for thermal expansion : Manual

Materials of lens and reflector
- Lenses : Cerium oxide (CeO_2) contained lead glass
  OH doped synthetic quartz

Heaters
- Number of heaters : 44
- Maximum temperature : 250°C

Dimensions and material of periscope body
- Dimensions : 100-mm diameter, 15-m length
- Periscope body material : Aluminum alloy (Alumite treated black body)

b) Thermal expansion test

Figure 31 shows the measured thermal expansion of the periscope body heated up to 250°C. The maximum thermal expansion of the periscope body in the axial and lateral directions are 85 mm and 0.5 mm at 250°C, respectively. Figure 32 shows pictures of the images taken by the 15m-long periscope before and after the focal adjustment during high temperature tests.

Due to thermal expansion of the periscope body, the clear images before heating gets blurred. However, using the focal adjuster which is equipped to the eyepiece to accommodate the radial thermal expansion, the blurred images become clear. The lateral thermal expansion causes also optical misalignment which is specifically originated by different thermal expansion coefficient between the lens and periscope body materials. In order to accommodate the lateral thermal expansion, each lens is fixed to the periscope body using a special lens holder which is a thermal expansion absorber and allows relative displacement between lens and periscope body so as to maintain the original optical axis.

5. 3 Mirror driving mechanism

A mirror driving mechanism to rotate and tilt a mirror is attached to the tip of periscope body so as to allow inspection of the whole in-vessel area. Accordingly, the mirror driving mechanism composed of many mechanical and electric components should be capable of operating under the severe environmental conditions as same as the periscope body. The design of this mirror driving mechanism is different from the latest design of 11m-long periscope but the results of gamma irradiation tests will be available for the design of 11m-long periscope.

(1) Outline

Figure 33 shows an elevation view of a prototypical mirror driving mechanism being fabricated to attach to the 15m-long periscope. In this design, eight halogen lamps are assembled around the driving mechanism. The prototypical mirror driving mechanism will be installed in a vacuum chamber as shown in Fig. 34 and irradiated under the gamma ray radiation of 10 kGy/h in order to verify total system performance including durability of mechanical and electrical components under intense of gamma radiation. Figure 35 shows typical kinematics of the mirror tilting /rotating mechanisms. The main specifications of the prototype mirror driving mechanism are as follows.

Tilting mechanism (ϕ axis)	
- Movable range	: 0 ~ 105°
- Driver	: AC servo motor
Rated power & voltage	: 30 V / 20W
Rated torque	: 2 kg-cm
Rated number of rotation	: 3000 rpm
Stator	: Ceramic insulator wire
Rotor	: Magnet (Sm / Co)
Lubricant of bearings	: Solid type or rad. hard grease
Position sensor	: Resolver (rad. hard type)
- Reduction gear	: Harmonic drive type
Lubricant	: Radiation hard grease
Retainer	: Thermosetting type polyimide or metal
Flame	: Aluminum
- Mirror	: Aluminum (surface polished by diamond)
Dimensions	: 130 mm x 125 mm x 19 mm(t)
Reflectance	: ca. 90%
Rotating mechanism (θ)	
- Movable range	: 0 ~ 360°
- Driver	: same as the ϕ axis
- Reduction gear	: same as the ϕ axis
- Driving mechanism	: Ball screw
Lighting system	
- Type of lamp	: Rod type halogen lamp x 8
- Rated power, voltage, flux	: 100 V / 1 kW, 26 klm
- Rated lifetime	: ca. 200 hr.
- Reflector	: Aluminum (surface treatment : Alumite)
- Slipring	: Ring (oxygen free copper) / Burush (Ag-C)
Common materials	
- Bearing	: SS440C, SS304, MoS2
- Limit switch	: SS, Pt, ceramic
- Wire	: Ni coated Cu, Inorganic polymer, Glass fiber

(2) Gamma irradiation tests

The prototypical mirror driving mechanism will be completed by the end of 1996 and thereafter, the gamma irradiation test will be started using the gamma irradiation facility in Takasaki Establishment of JAERI.

5. 4 CCD camera

A CCD camera as eyepiece of the periscope is always located in a top port outside the vacuum vessel, so that the impact of thermal load and gamma dose rate on viewing performance seems small compared with the lenses and mirror driving mechanism. However, heat resistance and radiation hardness of CCD camera, which is composed of many semiconductors and electronic elements, are generally quite low : typically the temperature and radiation dose limits are approximately 40°C and 400 Gy, respectively.

For this, qualification and improvements of heat resistant and radiation hardness of CCD cameras are essential to develop the detail design of periscope and ensure the viewing performance. As the 1st stage of development, gamma irradiation tests of commercial base CCD cameras (area image sensor and objective lens) was carried out for confirmation of the radiation dose limits. Based on the 1st stage results, a radiation hard type CCD camera system has been developed by replacing with a radiation hard objective lens and adopting an improved camera control unit with new electric circuits to correct the electric degradation [6].

(1) Gamma irradiation tests for standard type CCD camera

a) Specifications and experimental setup

Figure 36 shows a setup of CCD cameras for the gamma irradiation test. Camera control units (CCU) are set outside the irradiation cell. The followings are major specifications of the CCD cameras tested.

- CCD camera
  - · Area image sensor : 400,000 pixel, 1/2 inch, Color (IK-C40 / Toshiba)
  - · Objective lens : focal length 12 mm (JK-L12 / Toshiba)
  - · Camera control unit : for IK-C40 (Toshiba)

- Observation recording system
  - · Quadrant picture unit : JK-S44CS (Toshiba)
  - · Wave form monitor : LBO-5865 (LEADER)
  - · Time lapse video recorder : KV-6220 (Toshiba)
  - · Color monitor : P21CS04 (Toshiba)

b) Irradiation test results

Three CCD camera heads of C1, C2 and C3 were placed under different dose rates of 100 Gy/h, 11 Gy/h, 1 Gy/h in the gamma irradiation cell, respectively. These dose rates correspond to the estimated dose rate outside the vacuum vessel in ITER. Each camera head includes area image sensor and objective lens. During the gamma irradiation, the images taken by the cameras were continuously monitored and recorded to the color monitor and video recording system.

Figure 37 shows the images taken by the C1 camera under exposure dose rate of 100 Gy/h. The images are rapidly deteriorated at doses of 2 kGy and it becomes invisible at doses of 3 kGy. The other two cameras showed a similar tendency. As a result, allowable doses of the present CCD camera is specified to be 2 kGy regardless of the dose rates ranging from 1 to 100 Gy/h. On the other hand, electrical characteristics such as dark current and white pattern noise have shown the dose rate dependency : large dark current and white pattern noise are observed in case of low dose rate irradiation comparing with high dose rate irradiation. Figures 38 and 39 show the measured dark current and white pattern noise as a function of doses and exposure dose rates, respectively. Figure 40 shows the measured transmittance changes of the objective lenses. The transmittance at wavelength of 450 ~ 620 nm is decreased by 10 ~ 50 % after 3.2

kGy irradiation. In case of the in-vessel viewing periscope, an image is directly focused on the area image sensor, so that the objective lens is not necessary. Further improvement of the radiation dose limits is under planned, including modification do electrical circuit of CCU.

(2) Gamma irradiation tests for radiation hard type CCD camera

a) Functions of rad-hard type CCD camera system

In order to improve the radiation hardness of the CCD camera, a rad-hard lens and new electric circuits to correct the electric degradation have been adopted to the objective lens and the CCU, respectively. Figures 41 and 42 show the external view of the modified CCD camera and the block diagram of the modified CCU, respectively.

The new correction circuits were attached to the standard CCU for correcting sensitivity, shading and optical black level (OB level) degraded by irradiation. The OB level means an output signal level of shaded CCD sensor. The sensitivity correction circuit is designed to increase the CCD output gain over a factor of five. The OB level correction circuit can adjust off-set of the level from ± 60 % to the original level of ± 7.5 %. The shading correction circuit is to correct the OB wave profile deviated by irradiation into the original straight profile.
To improve radiation hardness, a radiation hard lens developed for the in-vessel viewing periscope has been adopted to the objective lens of the CCD camera. This lens is basically composed of hydroxyl group (OH) doped synthetic quartz and CeO2 contained lead glasses. Focal length and diameter of the lens are specified to be 12.5 mm and 32 mm, respectively.

b) Specifications and experimental setup

Three standard CCD camera heads with standard objective lenses (C11, C21, C31) and one standard CCD camera head with rad-hard type objective lens (C41) as following were irradiated at the dose rates of 10 and 100 Gy/h. The modified CCU is equipped for all tested CCD cameras. Figure 43 shows a schematic experimental setup of the rad-hard CCD camera systems and layout of the CCD camera heads with objective lenses inthe radiation cell. Electric signals from the CCD camera heads irradiated are obtained through each modified CCU (CCU1 ~ CCU4). A test-chart was set at a distance of 475 mm from the CCD camera heads for monitoring the viewing performance during irradiation. The image taken from the test-chart was continuously recorded by a quadrant picture unit and time lapse video recorder. After the iradiation, electric characteristics of each rad-hard CCD camera system were measured and the degrded signals such as sensitivity, OB level and shading wave form were corrected corresponding to the degree of deterioration by the modified CCU.

- CCD camera

C11, C21, C31

· Area image sensor	: 400,000 pixel, 1/2 inch, Color (IK-C40 / Toshiba)
· Objective lens	: focal length 12 mm (JK-L12 / Toshiba)
· Camera control unit	: modified CCU

C41

· Area image sensor	: 400,000 pixel, 1/2 inch, Color (IK-C40 / Toshiba)
· Rad-hard type objective lens	: focal length 12.5 mm (newly-developed, MINOLTA)
· Camera control unit	: modified CCU

- Observation recording system

· Quadrant picture unit	: JK-S44CS (Toshiba)
· Wave form monitor	: LBO-5865 (LEADER)
· Time lapse video recorder	: KV-6220 (Toshiba)

· Color monitor : P21CS04 (Toshiba)

- Iradiation conditions
  · Dose rate : C11 (100 Gy/h), C21 (106 Gy/h)
  : C31 (11.5 Gy/h), C41 (11.5 Gy/h)
  · Atmosphere : air / room temperature

c) Irradiation test results

- Sensitivity changes

Figure 44 shows the CCD camera video output measured by the video tape recorder (VTR) as a function of accumulation doses. The video outputs of the C11 and C21 cameras irradiated at a higher dose rate of 100 Gy/h show large degradation compared with the C31 camera irradiated at a dose rate of 11.5 Gy/h. The C41 camera with radiation hard lens shows the lowest degradation and almost no effect up to 1 kGy. From this, it can be conducted that degradation of the video output is caused by coloring of the objective lens in the region of lower accumulation doses. On the other hand, in the region of higher accumulation doses, the slope of the degradation is almost similar for all cameras, so that the sensitivity reduction of the CCD camera head will become dominant.

Figure 45 shows the effect of sensitivity correction circuit on the video output of the C41 camera measured as a function of the accumulation doses. Although the video output signal is decreased down to 10 % at the accumulation doses of 3 kGy, it is recovered up to 80 % after correction. In this experiment, the gain of sensitivity correction is limited to be a factor of eight since the noise level is increased in proportion to amplification. As to the effect of sensitivity correction circuit on the gray-scale chart, the gray-scale wave forms are decreased down to 25 % at the accumulation doses of 2.64 kGy and are recovered up to 85 % after correction.

- Shading and optical black level changes

A shading level is increased in proportion to the accumulation doses and can be decreased by correcting the sensitivity of the CCD camera head. On the other hand, the OB level shifts with a large deviation from the original level of + 7.5 % by increasing of the accumulation doses. In addition, the wave form was also deviated from the original straight profile to inclined or uneven profile but these are recovered to the original level and wave profile by the correction circuit.

- Combined effect of correction circuits

Total effect of a combination of the correction circuits for sensitivity, OB level and shading was verified by the gray-scale and color-bar measurment. Figure 46 shows the images measured from the C41 camera system before and after irradiation. The images become invisible after the accumulation doses of 3 kGy and are recovered visible similar to the original images after correction.

- Transmittance changes of objective lens

Figure 47 shows the transmittance changes of the objective lens equipped to each CCD camera at a wave length of 540 nm which corresponds to green color. The vertical axis indicates the relative value to the original transmittance before irradiation. In case of the standard type lenses (C11, C21 and C31), the transmittance is rapidly decreased with increasing the accumulated dose. On the other hand, the rad-hard type lens (C41) shows almost no degradation up to 3 kGy.

5. 5 Cooling system for CCD camera

For the quick inspection of the in-vessel component surfaces just after plasma disruption, the environmental temperature of the CCD camera is assumed to be as high as 100°C since the CCD camera located at about 8 m distance from the plasma center where the maximum temperature is about 200°C. As the CCD camera is required to be operated at around 40°C, the cooling system is needed to keep the operating temperature below 40°C in such environmental conditions. Figure 48 shows a cooling chamber fabricated to cover the CCD camera head and focal adjustment mechanism. Figure 49 represents the measured temperature profile of the CCD camera when the external wall of the chamber is heated up to 100°C by heaters. It is shown that the CCD camera temperature can be maintained around 20°C by the cooling air circulation. The followings are major specifications of the cooling system for CCD camera.

- Dimensions of chamber	: 115 mm in diameter, 600 mm in length
- Materials	: SS304, ceramics (SiO_2), Al alloy (A5056)
- Heater	: rubber heater
- Baking temperature	: 100 °C
- Cooling system	: air compressor
- Air flow rate	: ~ 103 l / min (intake air temperature 25°C)
- Cooling capability	: to keep a temperature of under 40°C on the CCD camera head
- Focus adjusting	: adjusting distance / 100 mm (max.)
	: adjusting speed / 0.5 mm / sec

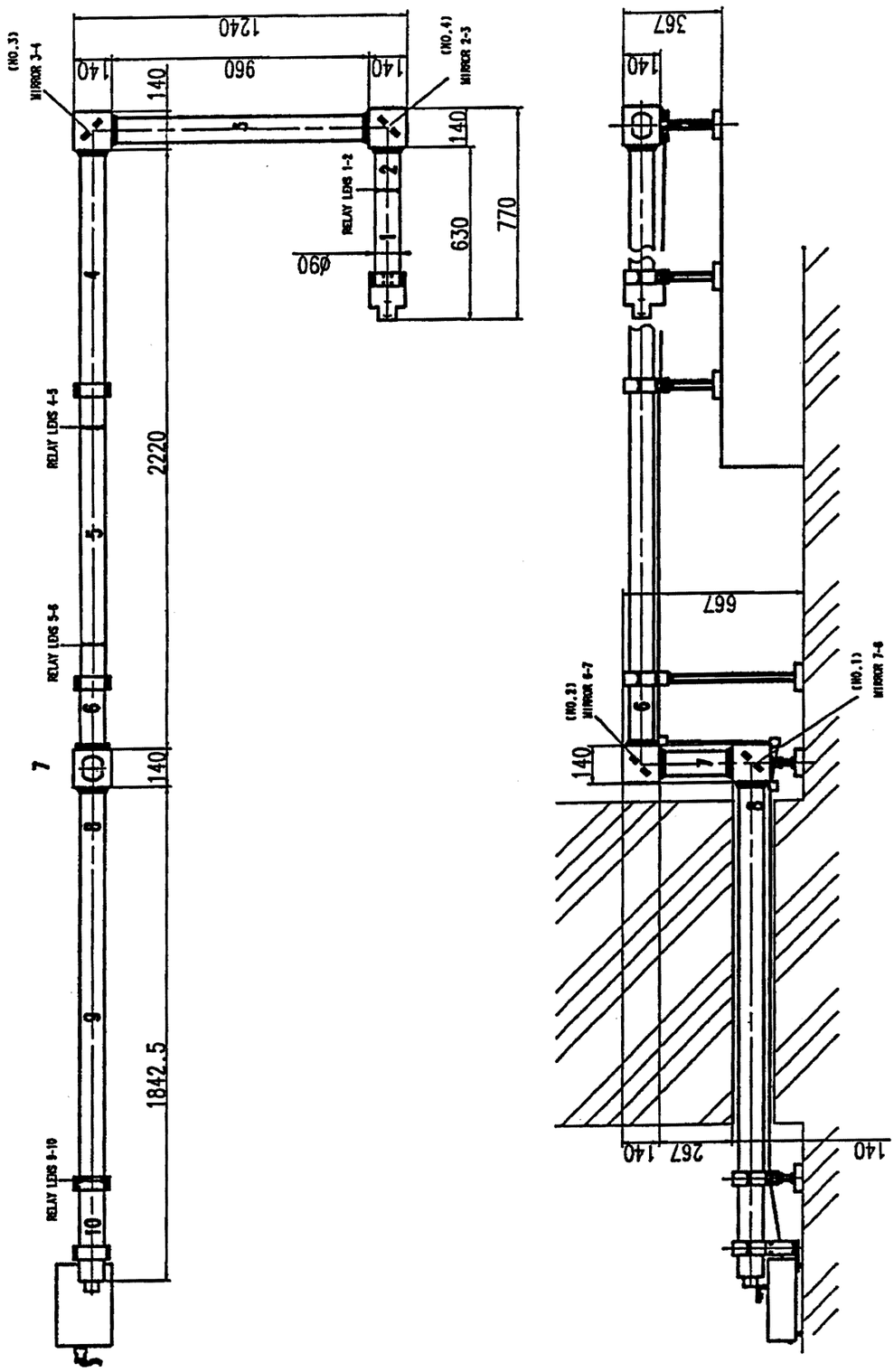

Fig. 25 Layout of rad-hard type 6m-long periscope with a zooming mechanism in gamma irradiation cell.

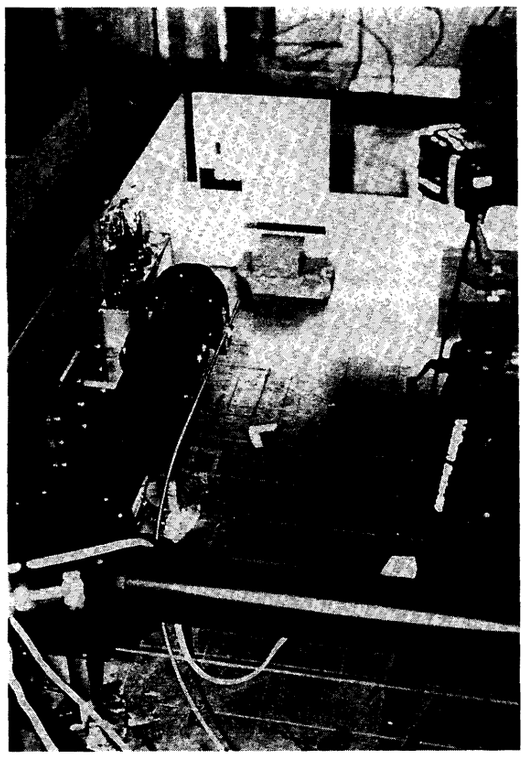

a) Tip of the periscope

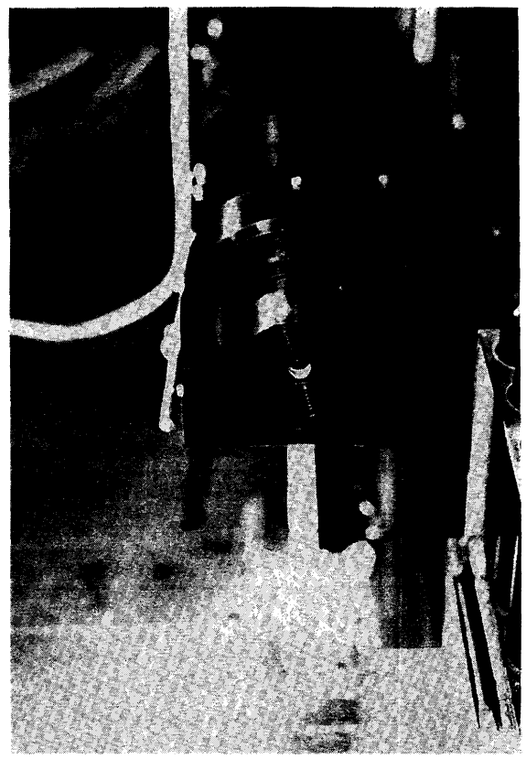

b) Objective lens with zooming mechanism

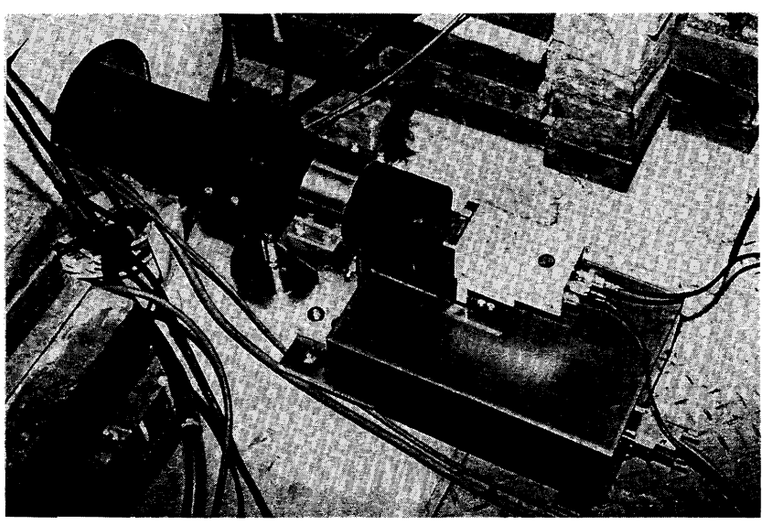

c) Eyepiece, attached CCD camera
with auto focusing mechanism

Fig. 26 Appearance of rad-hard type 6m-long periscope in gamma irradiation cell.

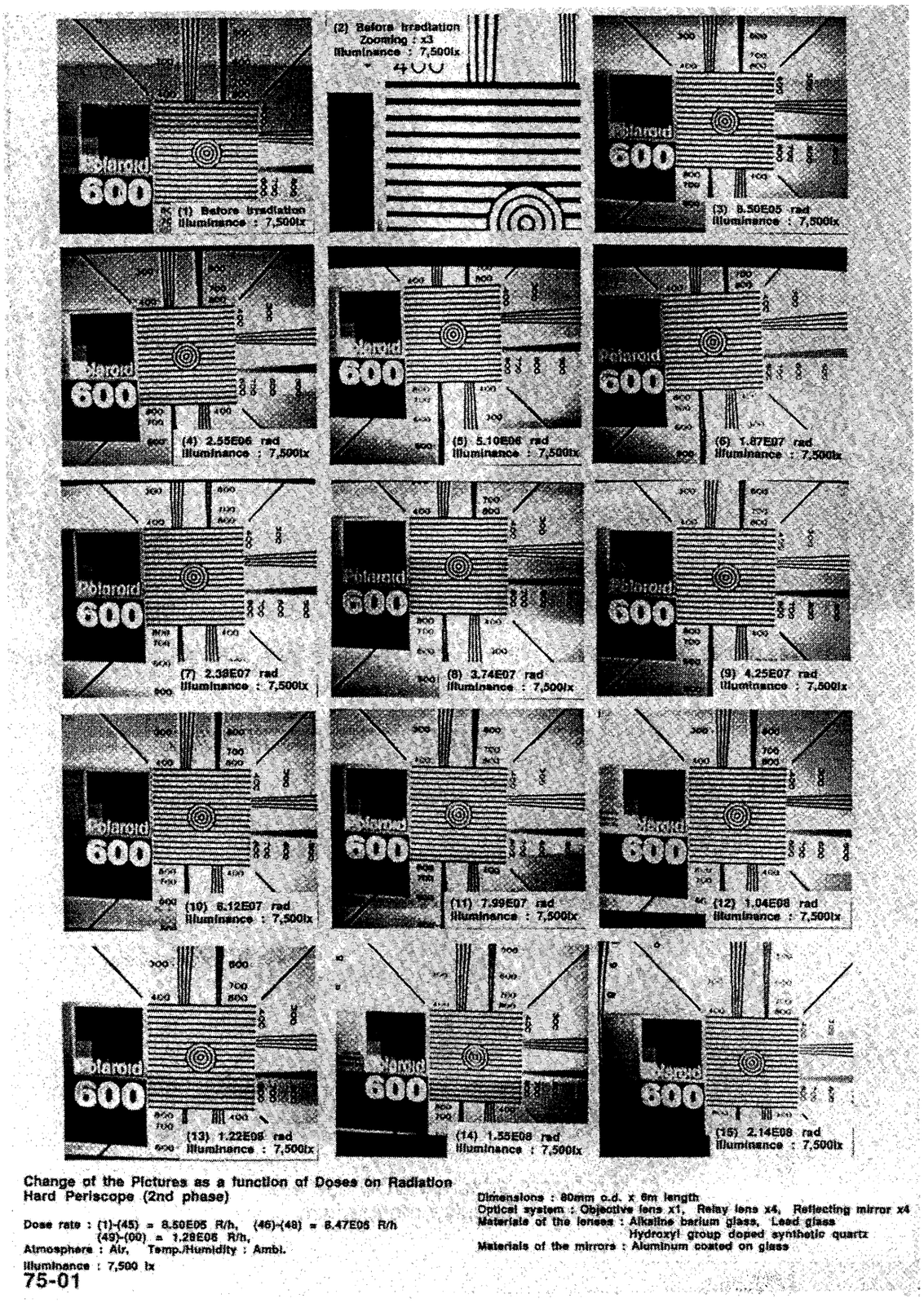

Fig. 27. 1 Measured images by rad-hard type 6m-long periscope as a function of doses.

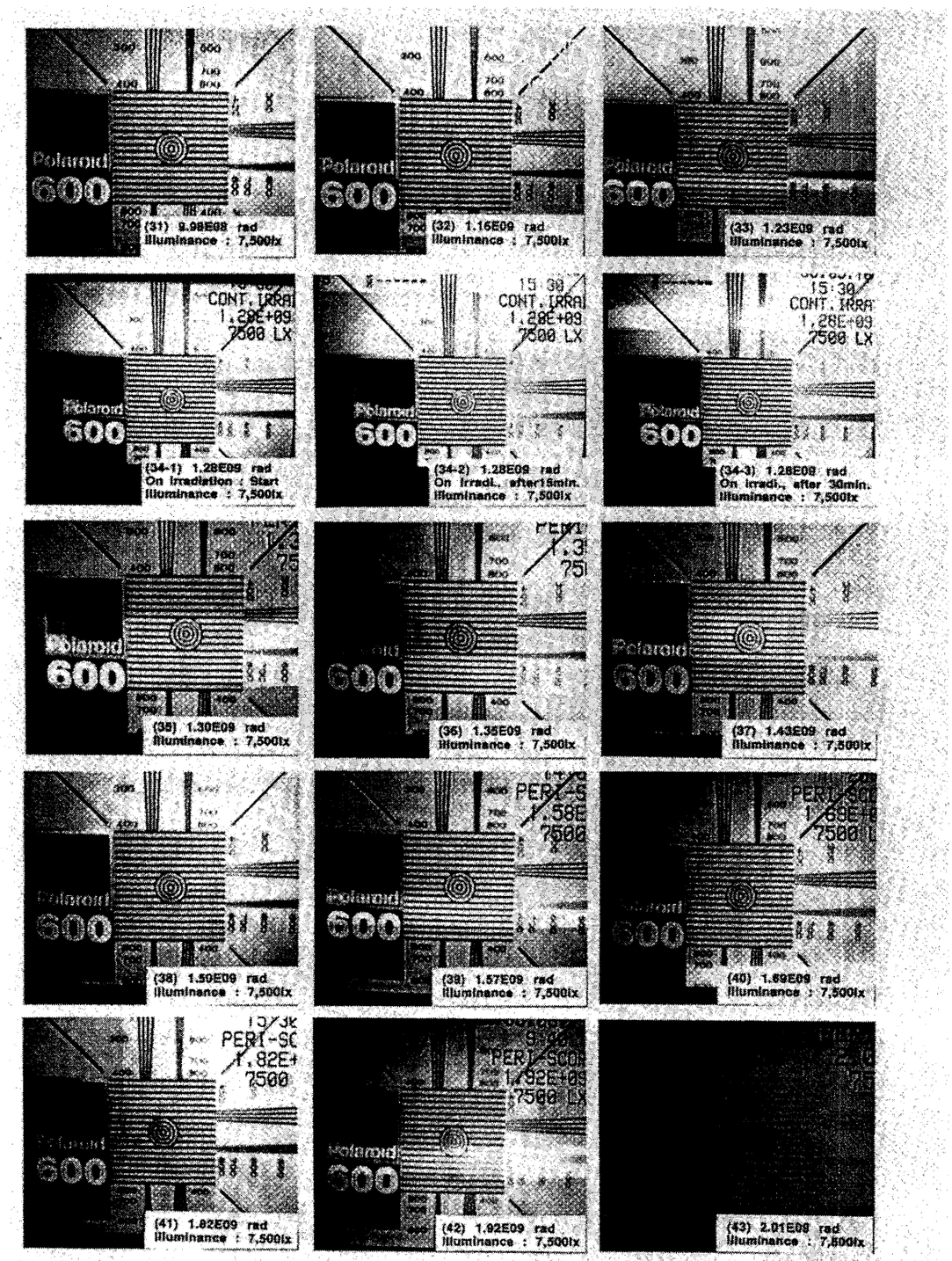

Change of the Pictures as a function of Doses on Radiation Hard Periscope (2nd phase)

Dose rate : (1)-(45) = 8.50E05 R/h, (46)-(48) = 8.47E05 R/h
(49)-(00) = 1.28E06 R/h,
Atmosphere : Air, Temp./Humidity : Ambi.
Illuminance : 7,500 lx
75-03

Dimensions : 80mm o.d. x 6m length
Optical system : Objective lens x1, Relay lens x4, Reflecting mirror x4
Materials of the lenses : Alkaline barium glass, Lead glass
Hydroxyl group doped synthetic quartz
Materials of the mirrors : Aluminum coated on glass

Fig. 27. 2 Measured images by rad-hard type 6m-long periscope as a function of doses.

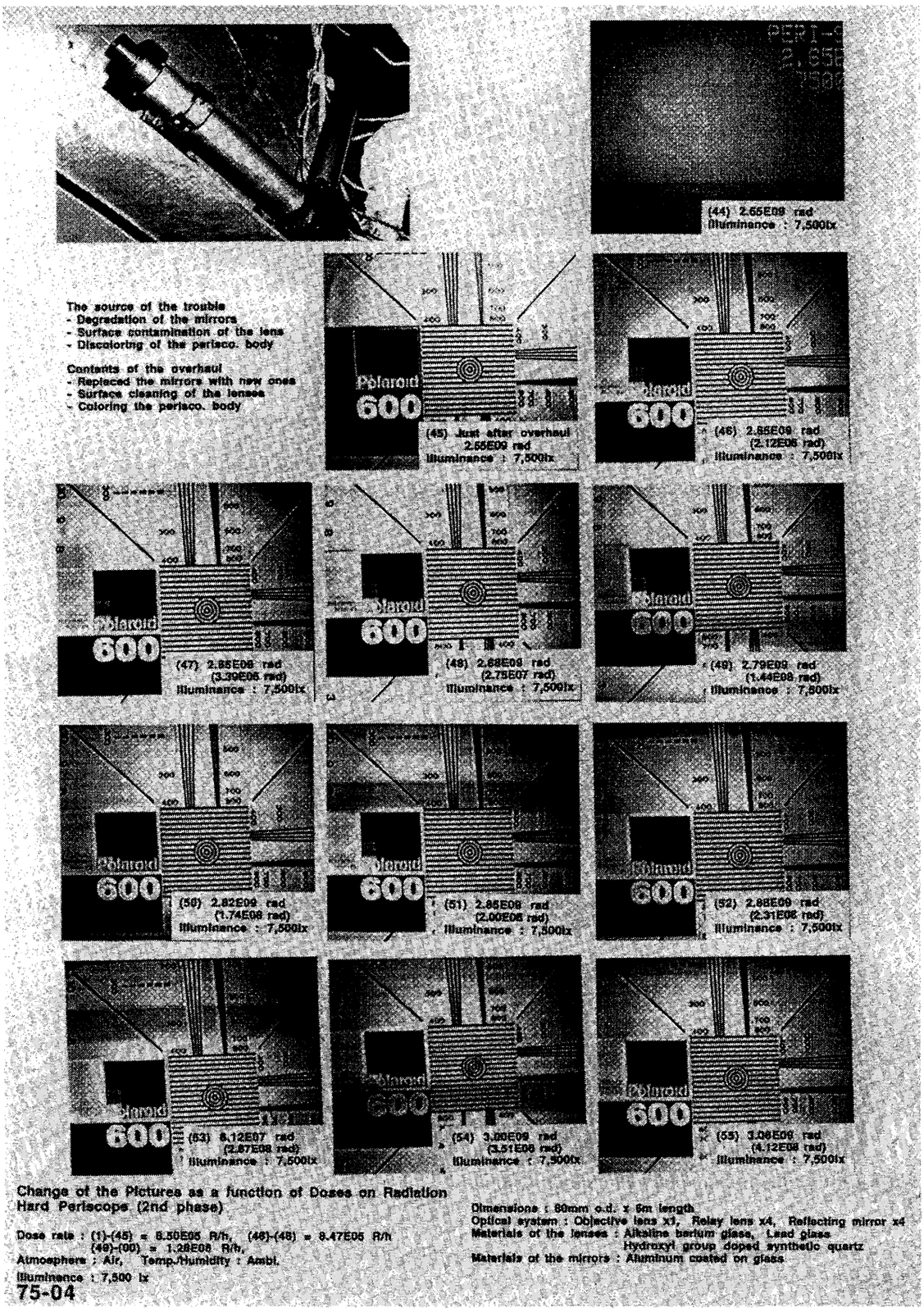

Fig. 27. 3 Measured images by rad-hard type 6m-long periscope as a function of doses.

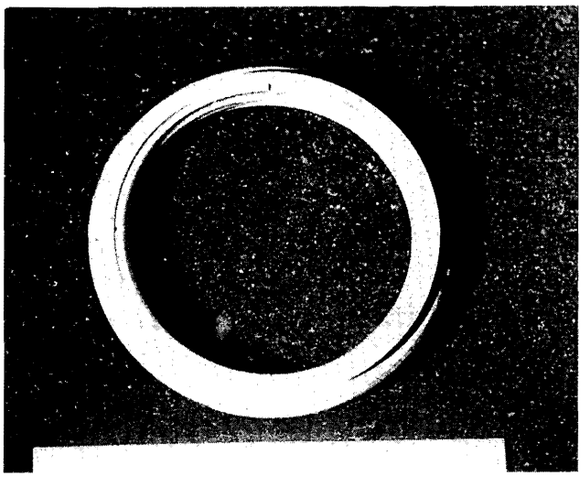

a) No. 1-2

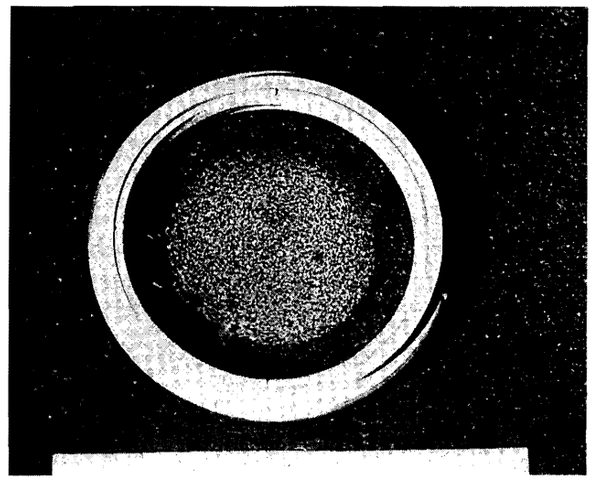

b) No. 4-5
Foreign substances are attached on the surface

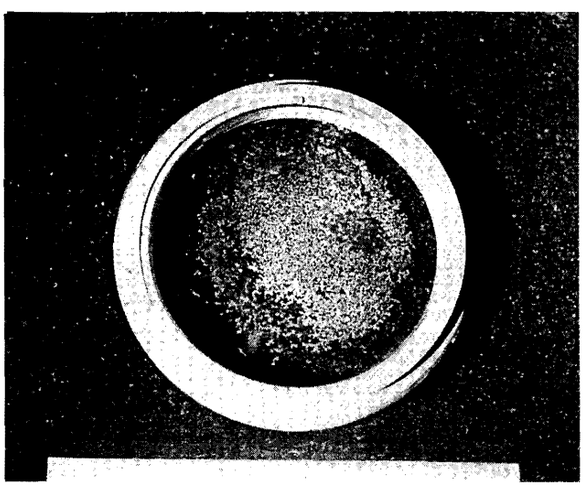

c) No. 5-6
Foreign substances are attached on the surface

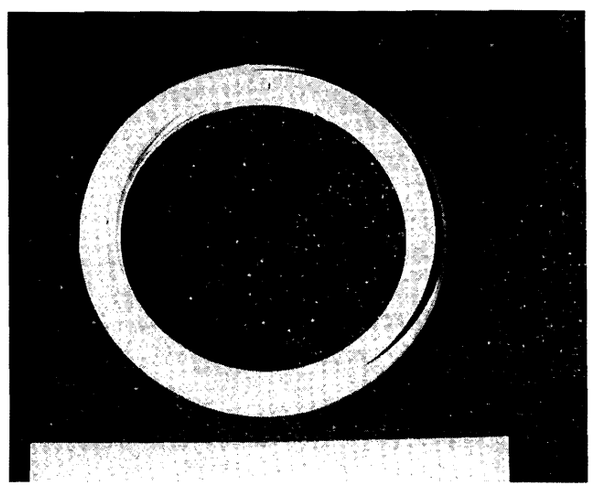

d) No. 9-10

Fig. 28 Appearance of relay lenses for 6m-long periscope after irradiation of 26.5 MGy.

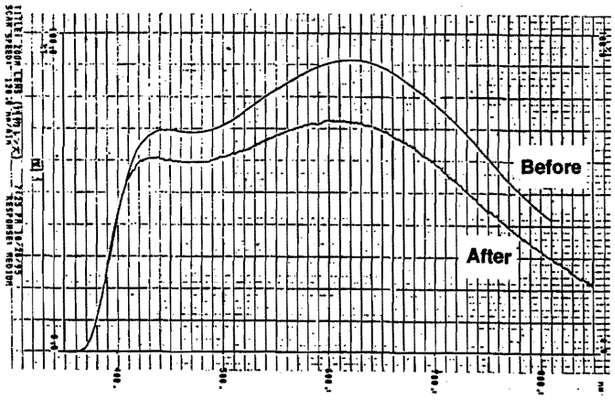

a) Objective lens

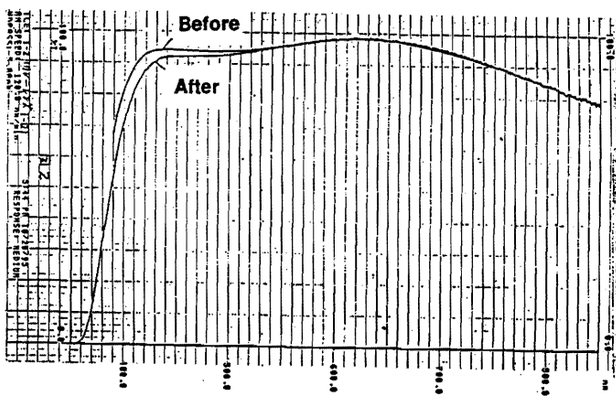

b) Relay lens : No. 1-2

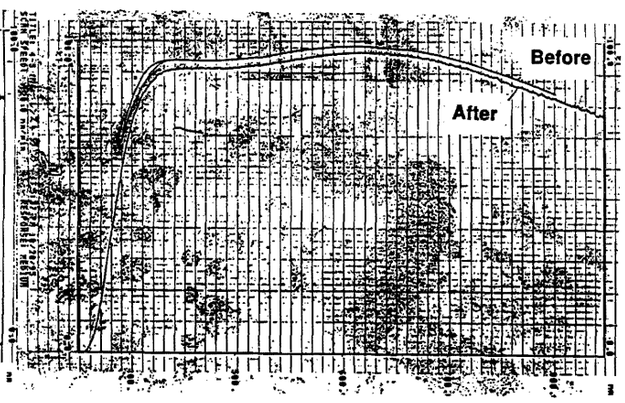

c) Relay lens : No. 4-5

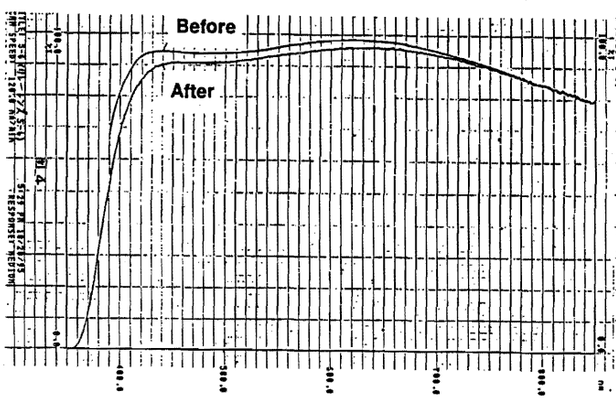

d) Relay lens : No. 5-6

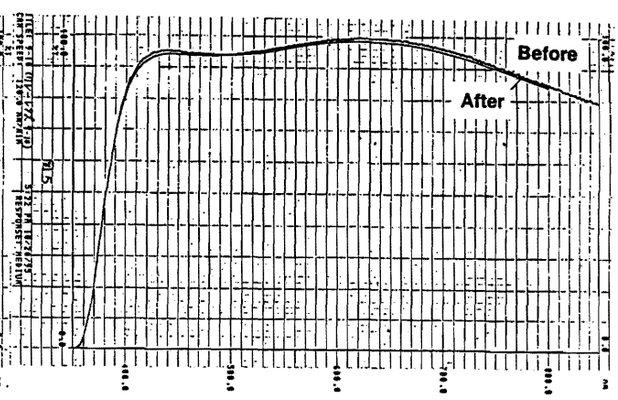

e) Relay lens : No. 9-10

Fig. 29 Transmittance changes of relay lenses for 6m-long periscope after irradiation of 26.5 MGy (horozontal line : wavelength (400-800nm), vertical line : transmittance (%)).

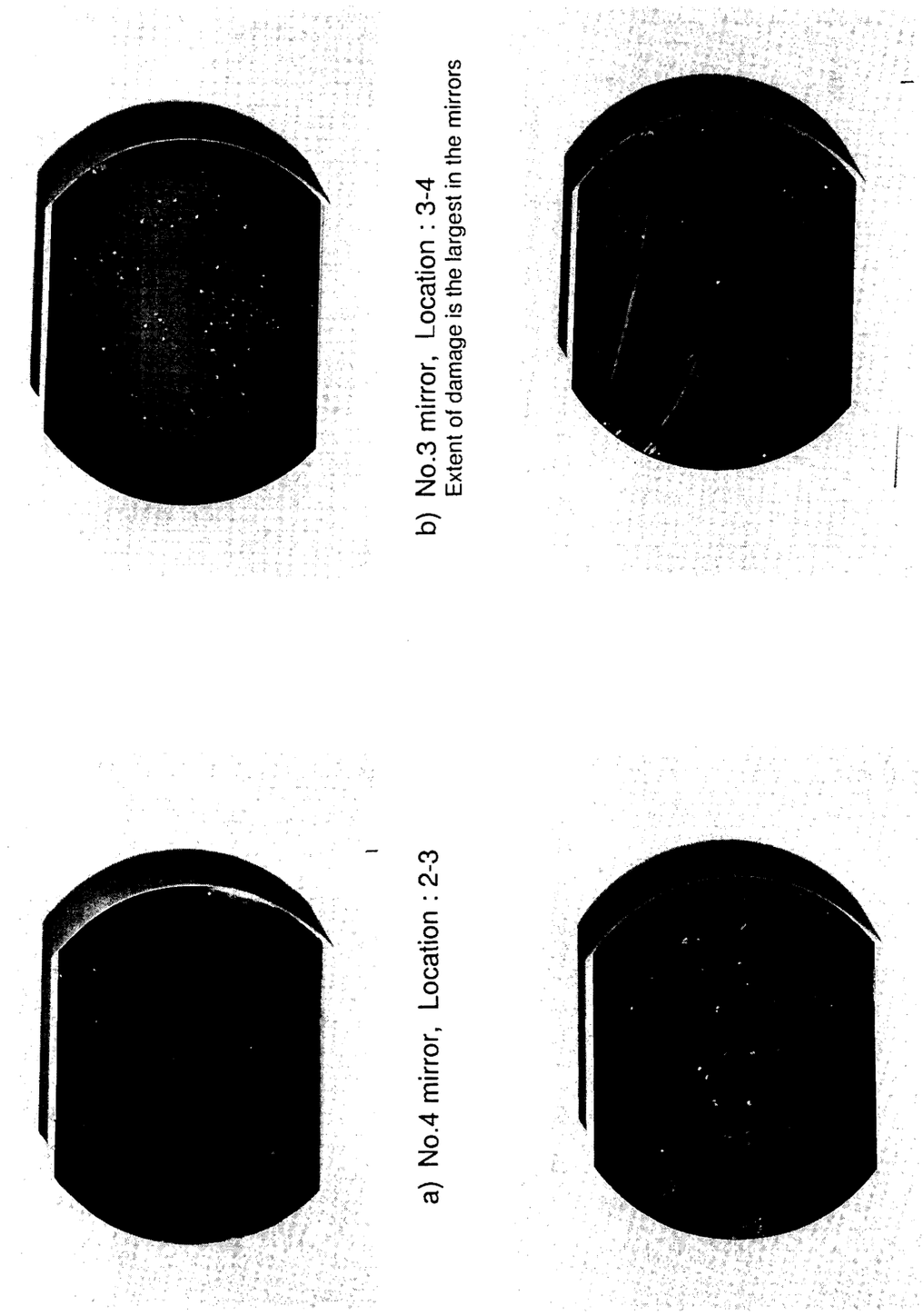

Fig. 30 Appearance of reflecting mirrors for 6m-long periscope after irradiation of 26.5 MGy (specification of the mirror : aluminum coating on synthetic quartz)).

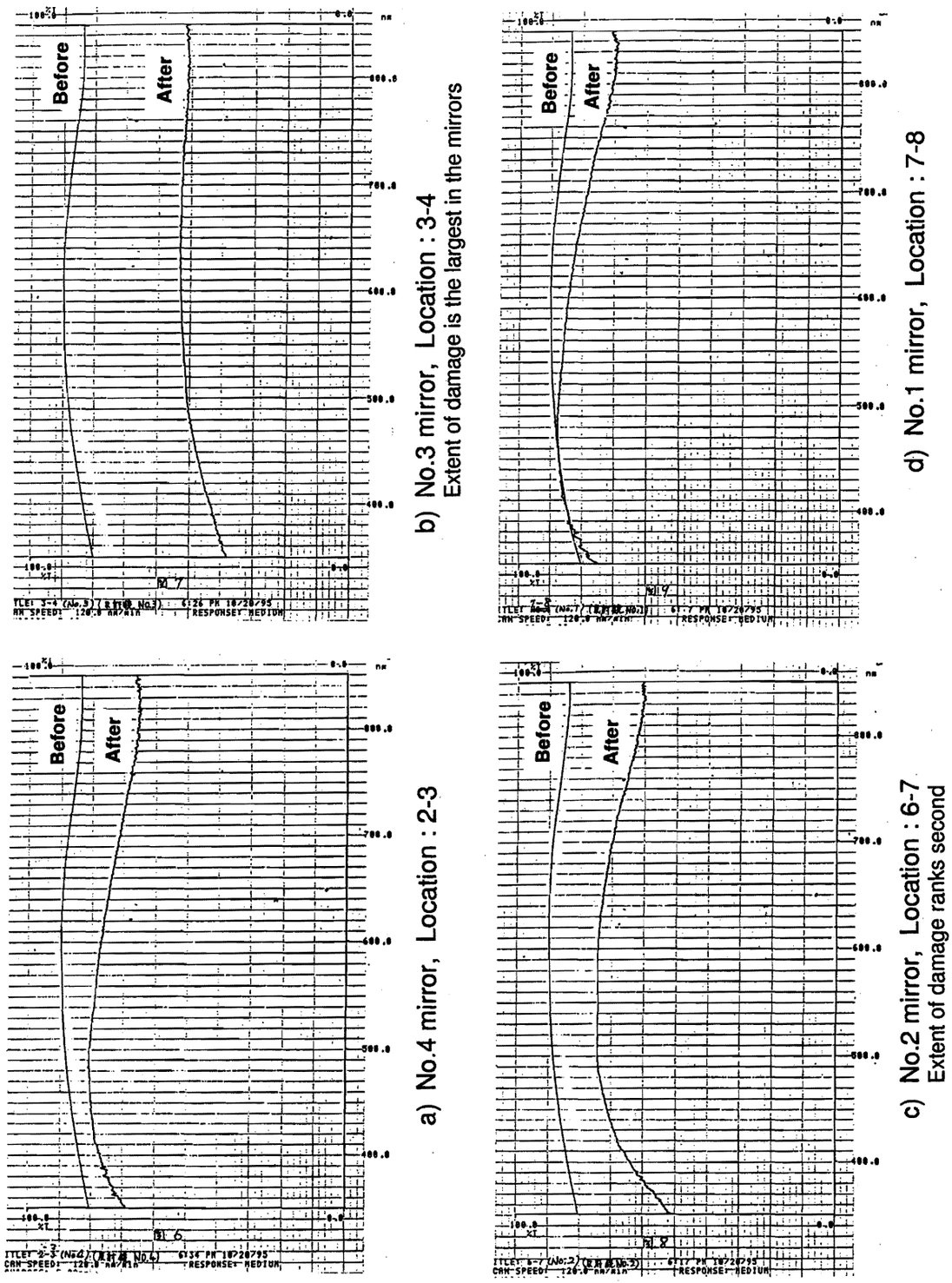

Fig. 31 Reflectance changes of mirror for 6m-long periscope after irradiation of 26.5 MGy (horozontal line : wavelength (400-800nm), vertical line : reflectance (%)).

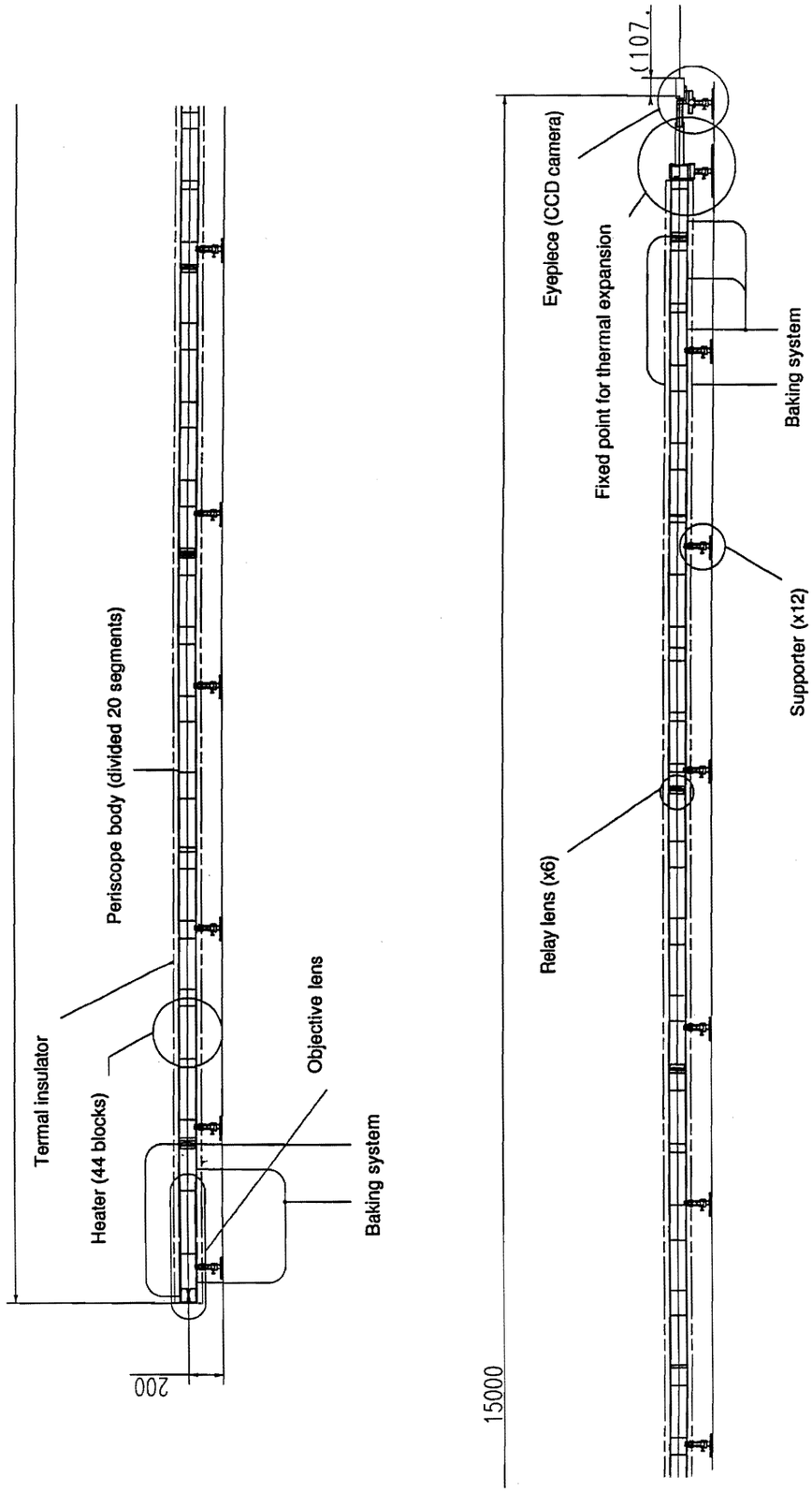

Fig. 32 Outline of full-scale rad-hard type 15m-long periscope for ITER iv-vessel viewing.

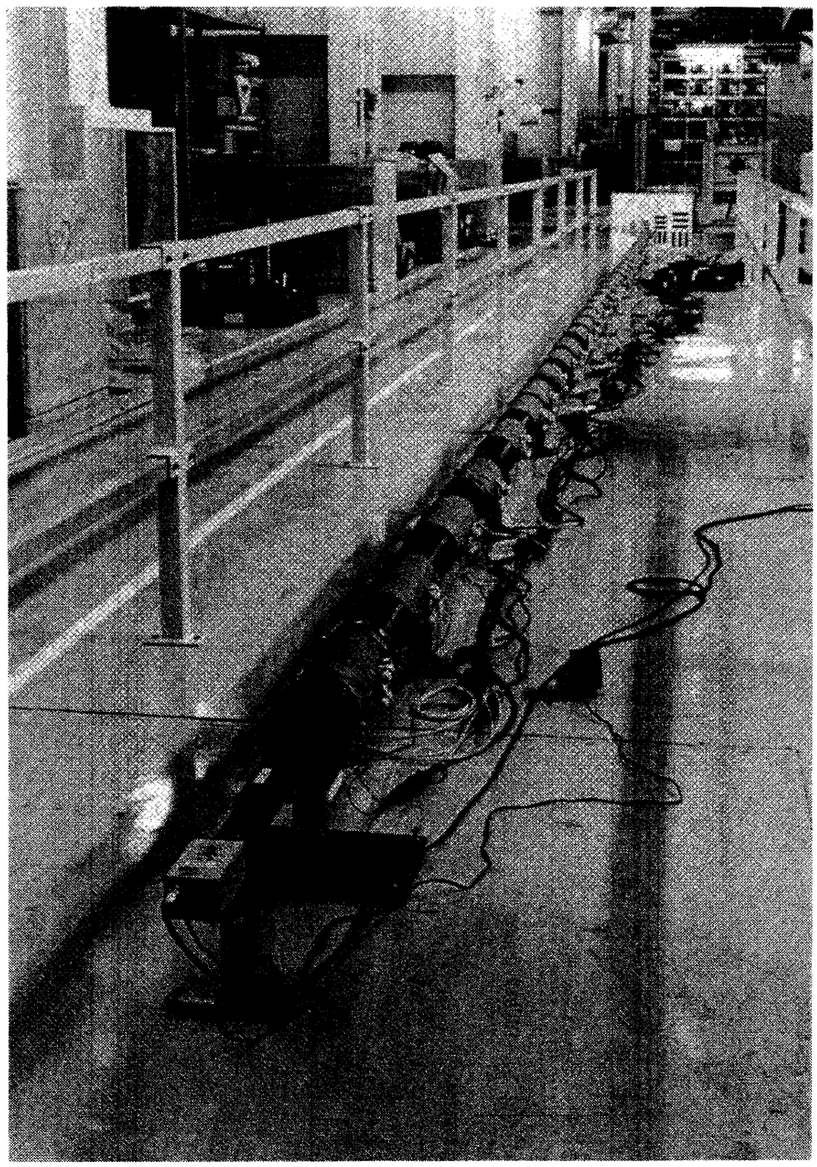

Fig. 33 Appearance of full-scale rad-hard type 15m-long periscope for ITER.

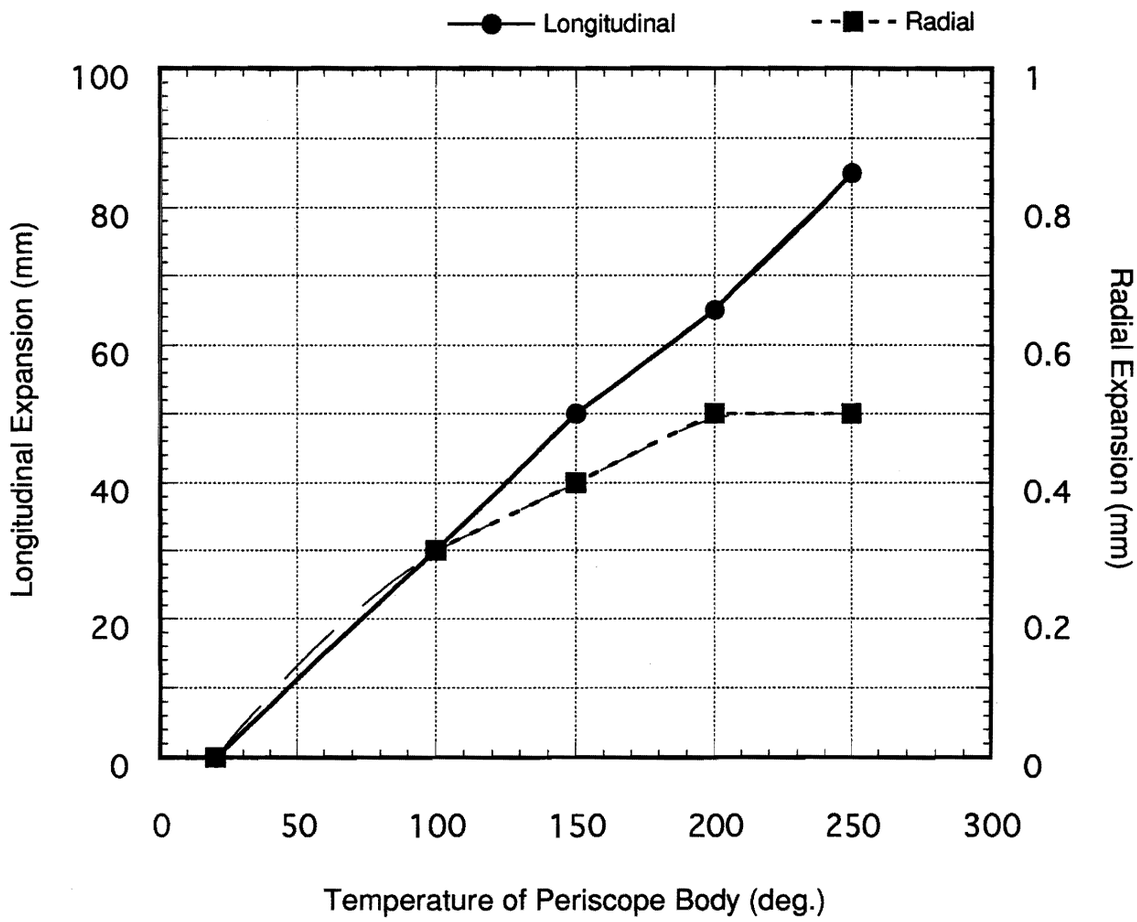

Fig. 34 Thermal expansion test results of 15m-long periscope (original length and diameter are 14,835 mm and 100 mm, respectively).

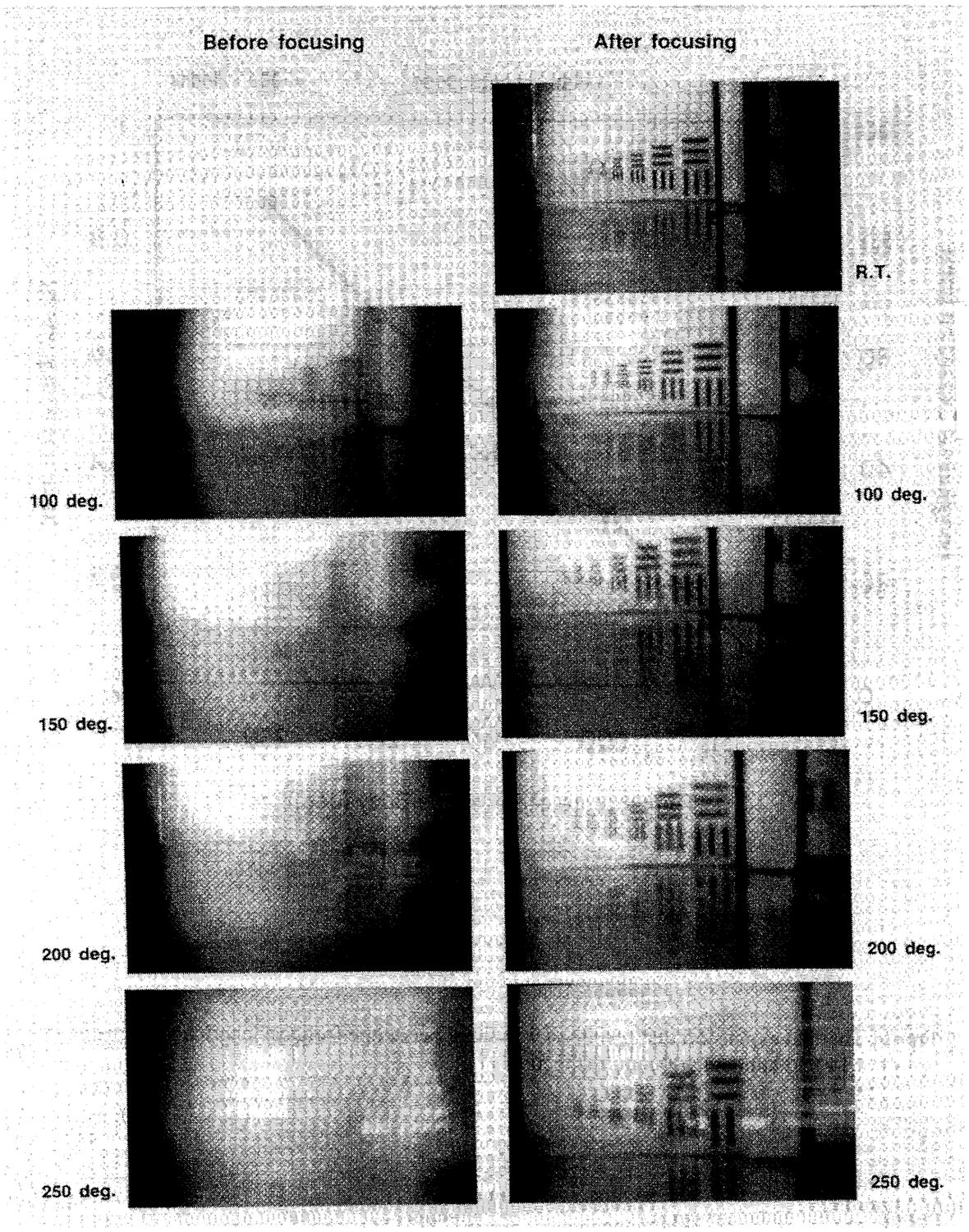

Fig. 35 Measured images taked by 15m-long periscope as a function of baking temperature (distance from the objective lens to the bar chart : 5 m, width of black lines on the bar chart : 32, 25, 16, 12, 8, 6 mm from right side, illuminance : 3,500 lx).

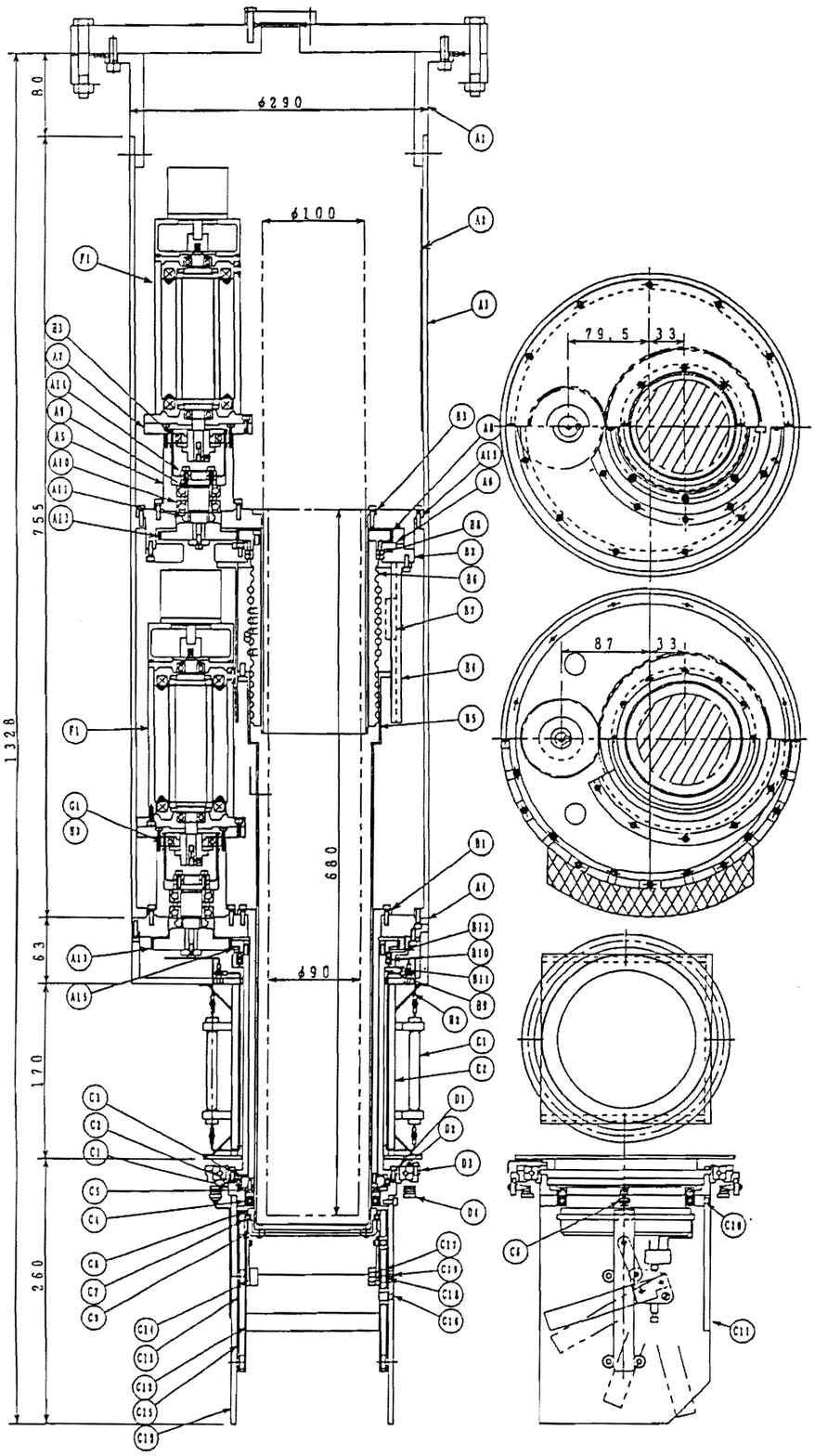

Fig. 36 Fabricated mirror driving mechanism for 15m-long periscope.

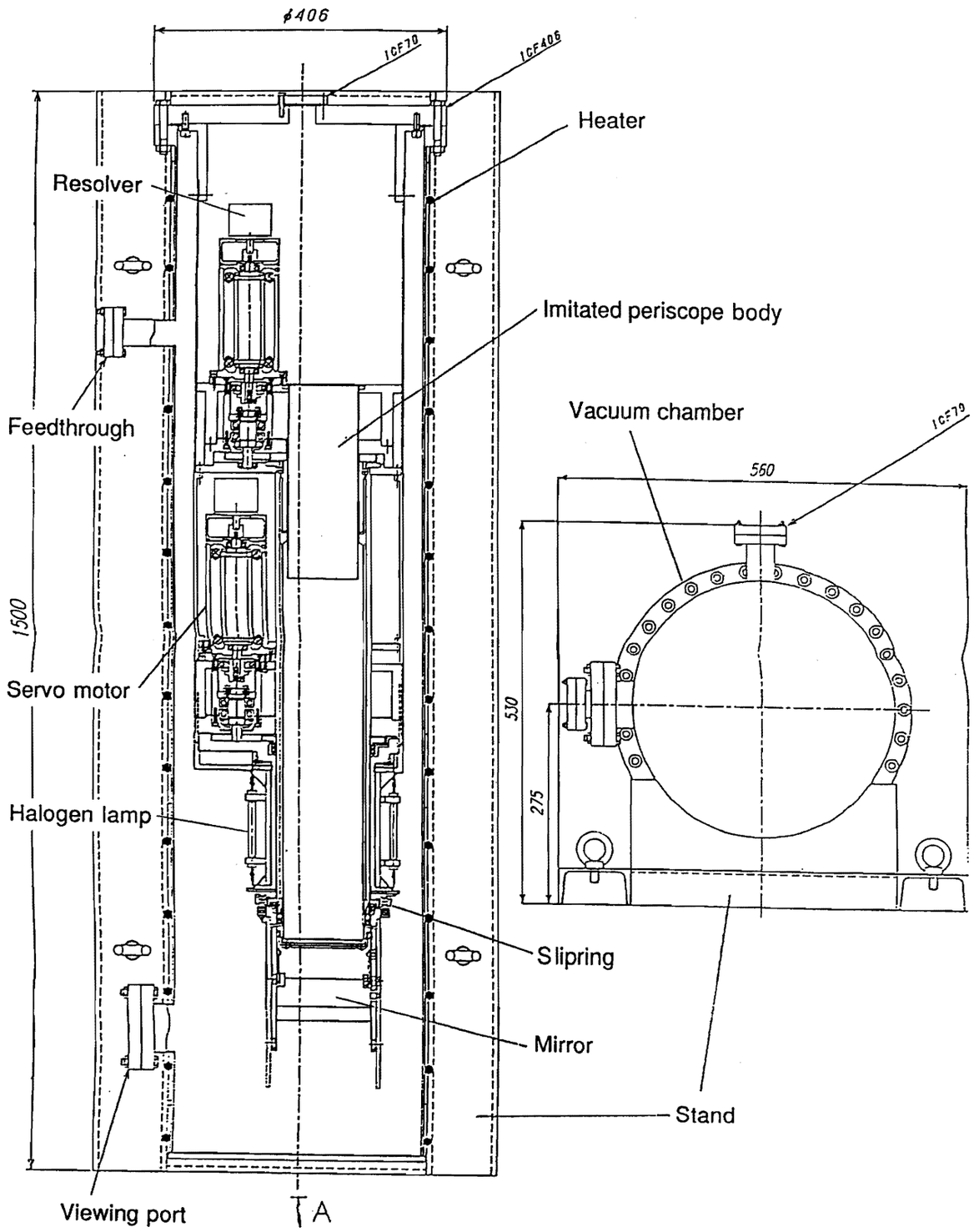

Fig. 37 Mirror driving mechanism installed in a vacuum chamber for irradiation test.

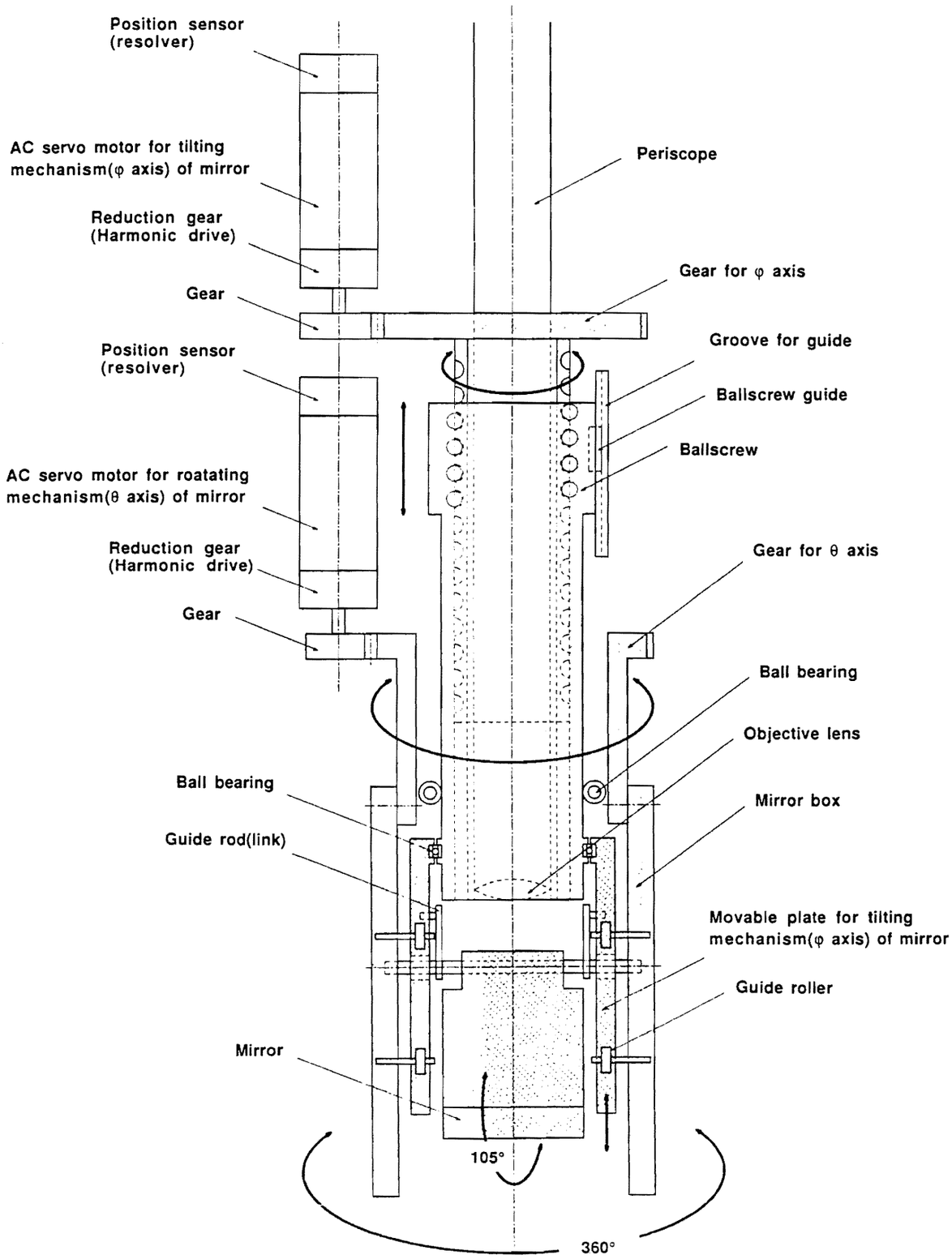

Fig. 38 Kinematics of mirror tilting/rotating mechanism for 15m-long periscope.

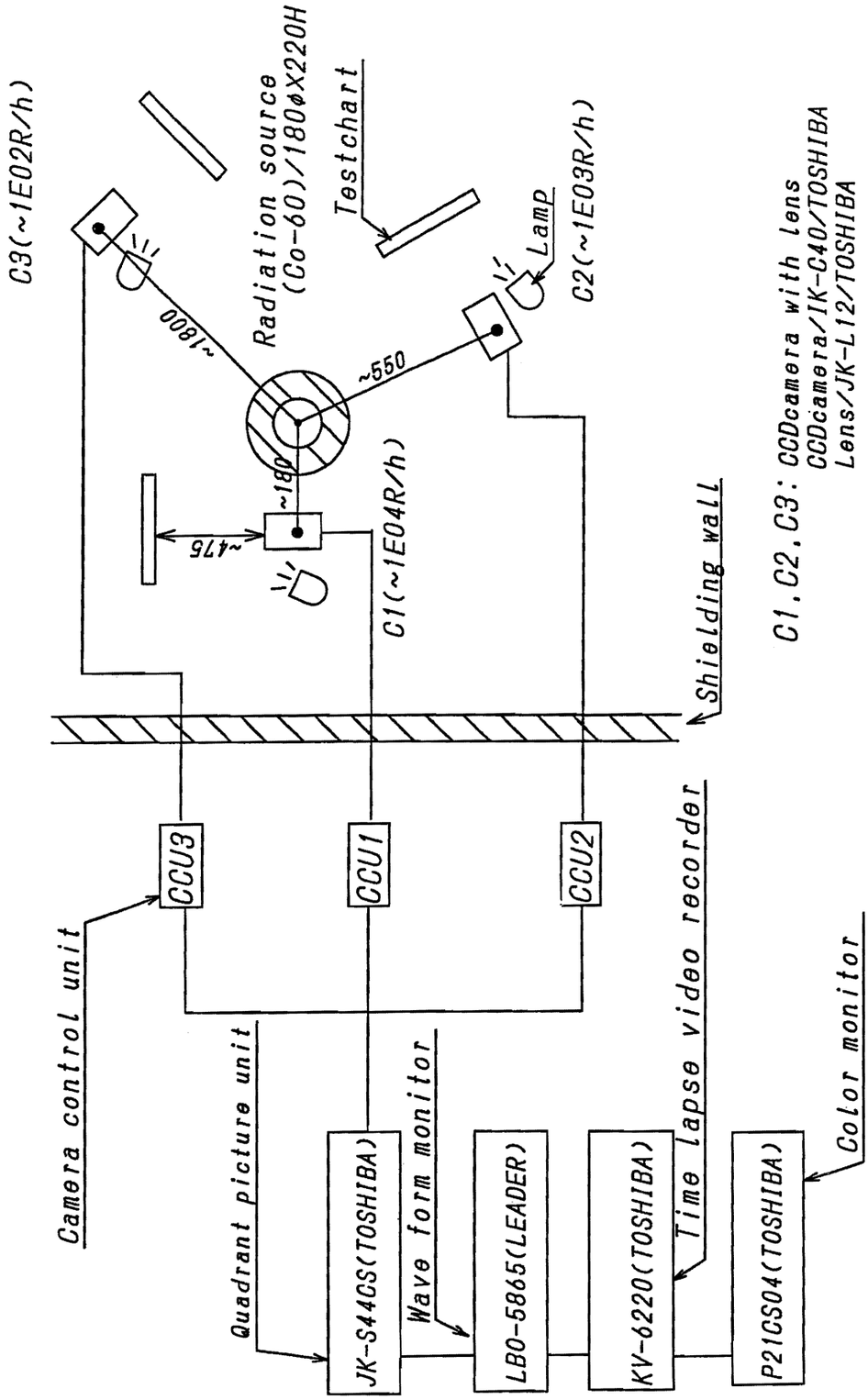

Fig. 39 Experimental setup of standard type CCD cameras for irradiation test in gamma irradiation cell.

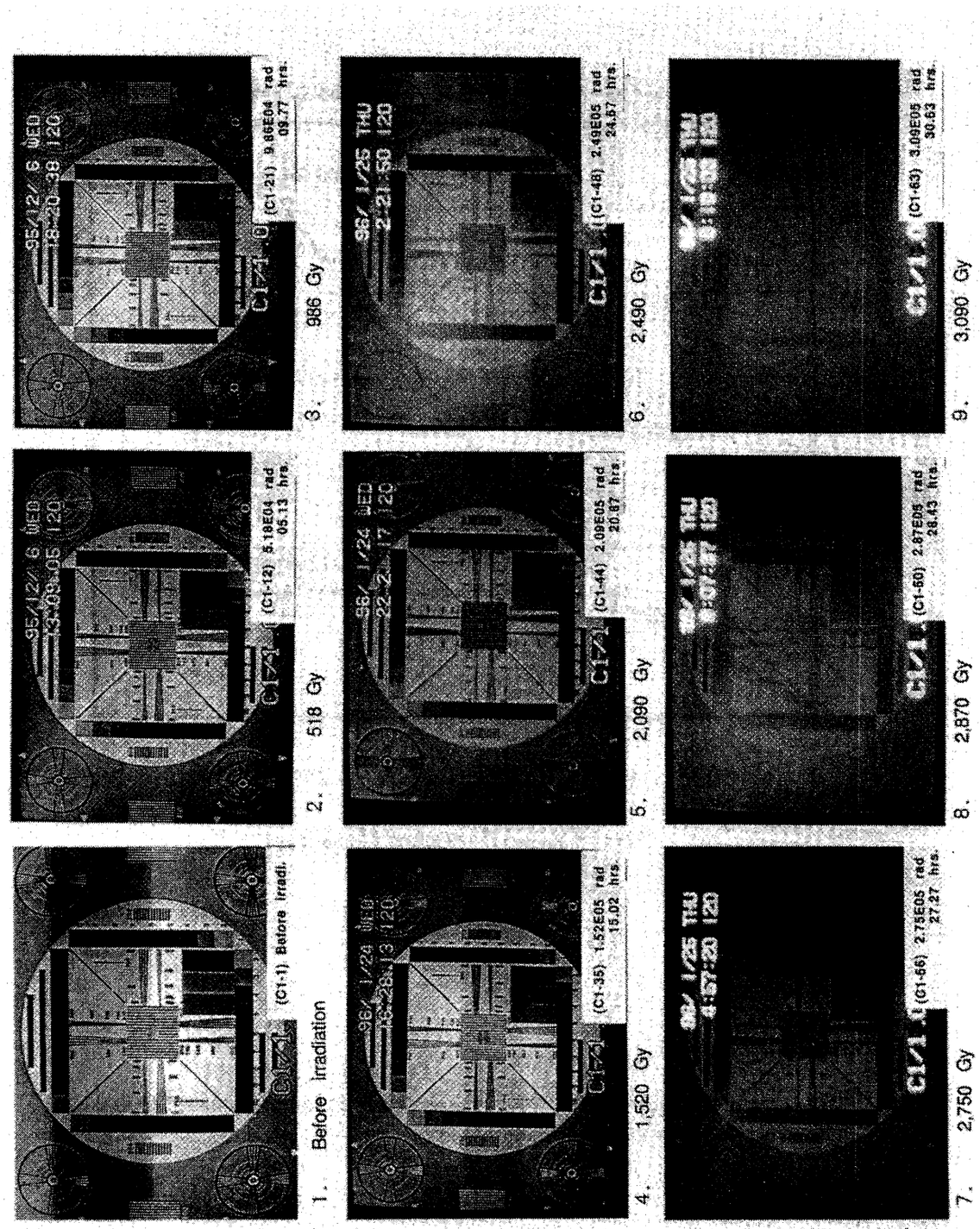

Fig. 40 Measured images taken by No. 1 CCD camera as a function of doses under dose rate of 1 kGy (the brownish lens was replaced a new one after irradaition of 1 kGy).

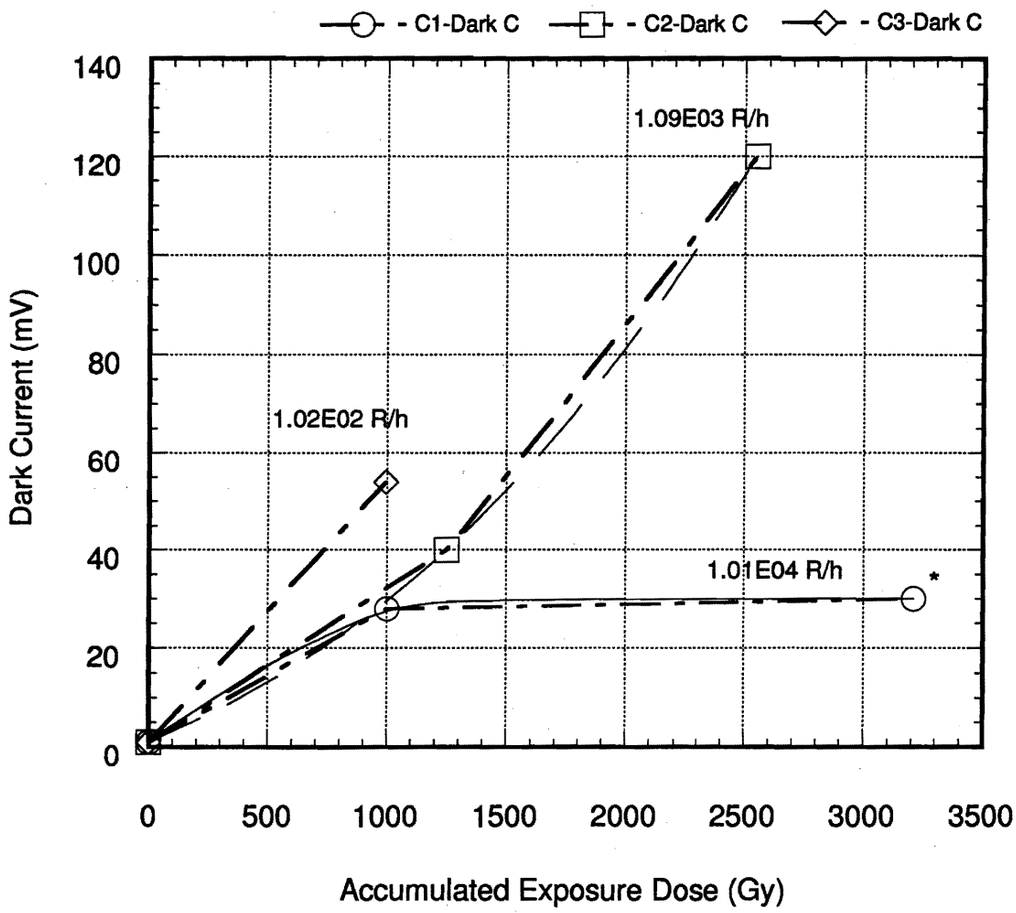

Fig. 41 Dark current changes of std. CCD cameras as a function of doses (* to make an allowance for deterioration of amplifier).

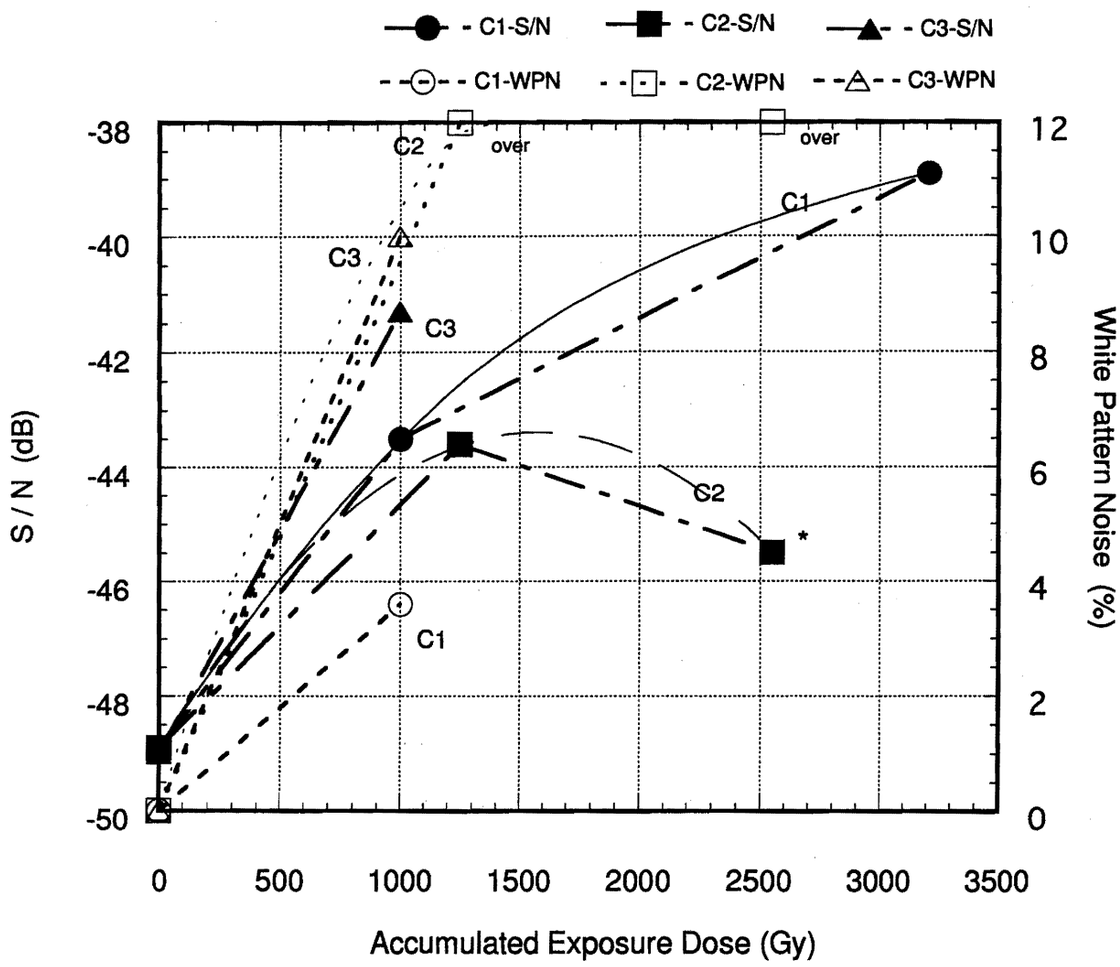

Fig. 42 Change of S/N and white pattern noise of std. CCD cameras as a function of doses
(* the S/N seems good in appearance caused by increasing the white pattern noise).

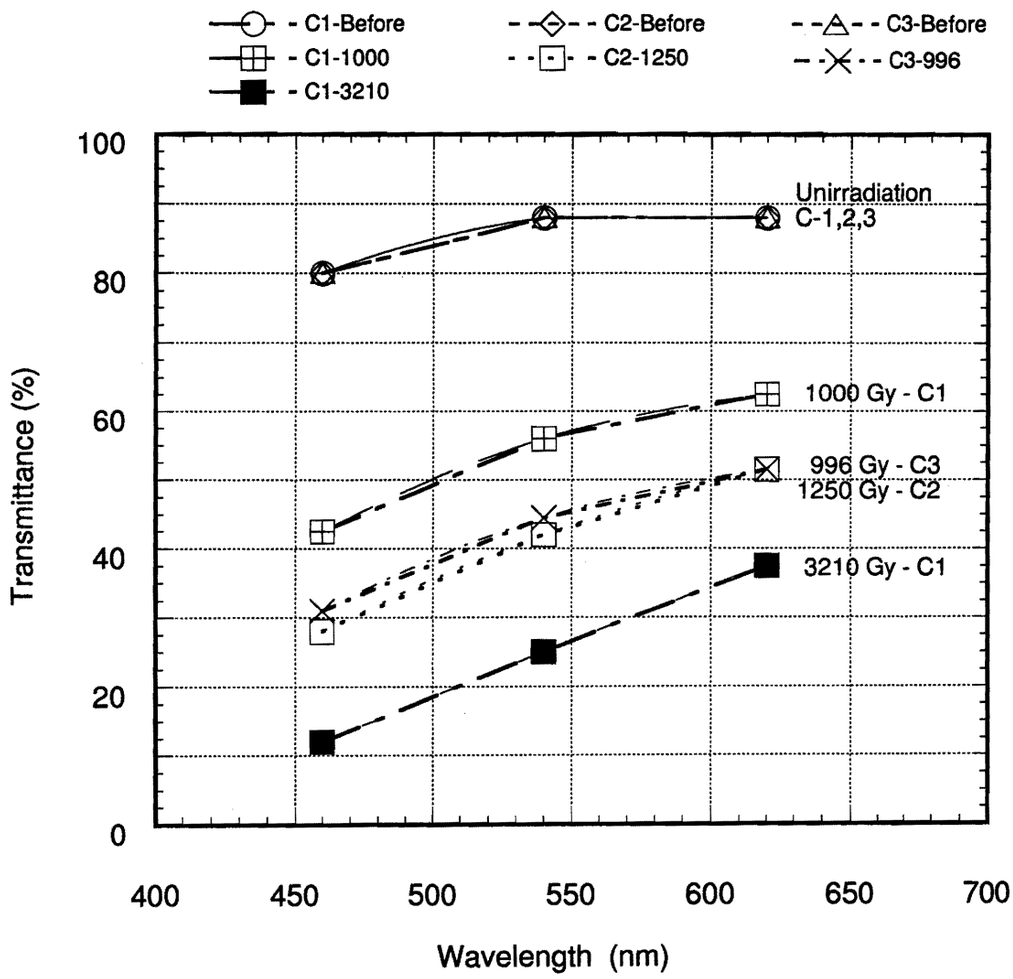

Fig. 43 Transmittance changes of objective lenses for No. 1, 2, 3 CCD cameras irradiated under 1.01E04, 1.09E03 and 1.02E02 R/h, respectively.

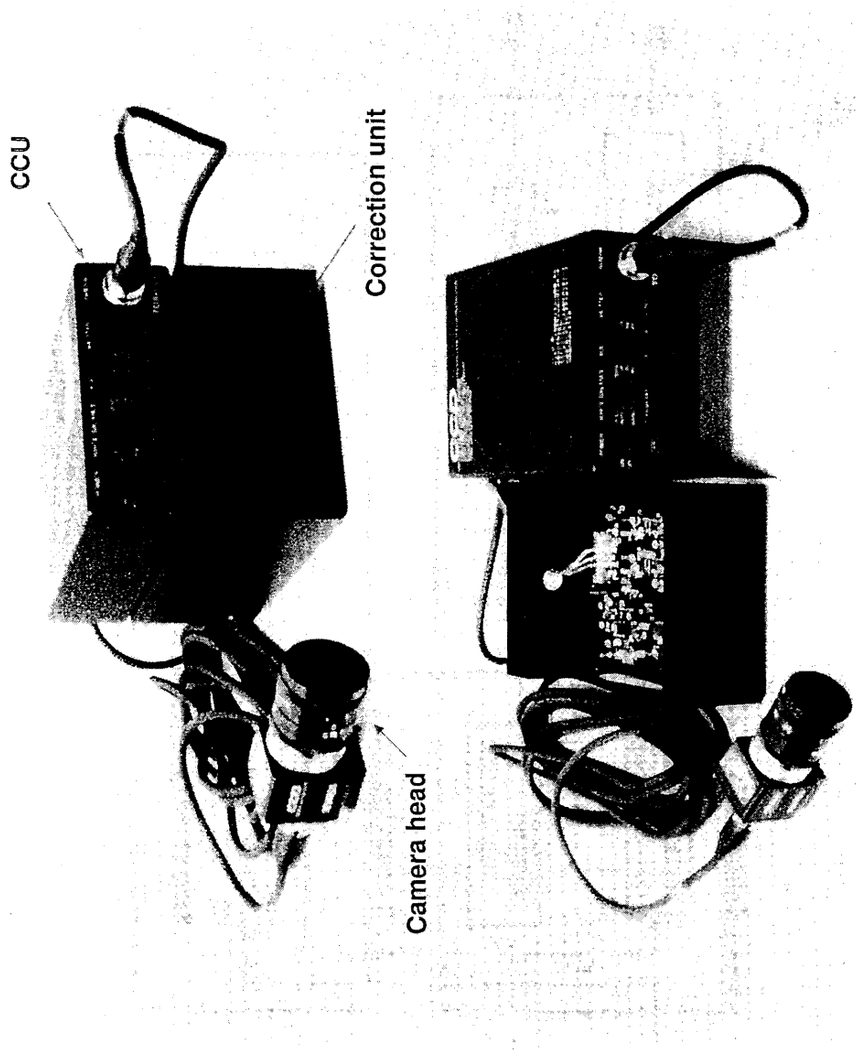

Fig. 44 External view of modified CCD camera, new correction circuits (left) was equipped to the standard CCU (right).

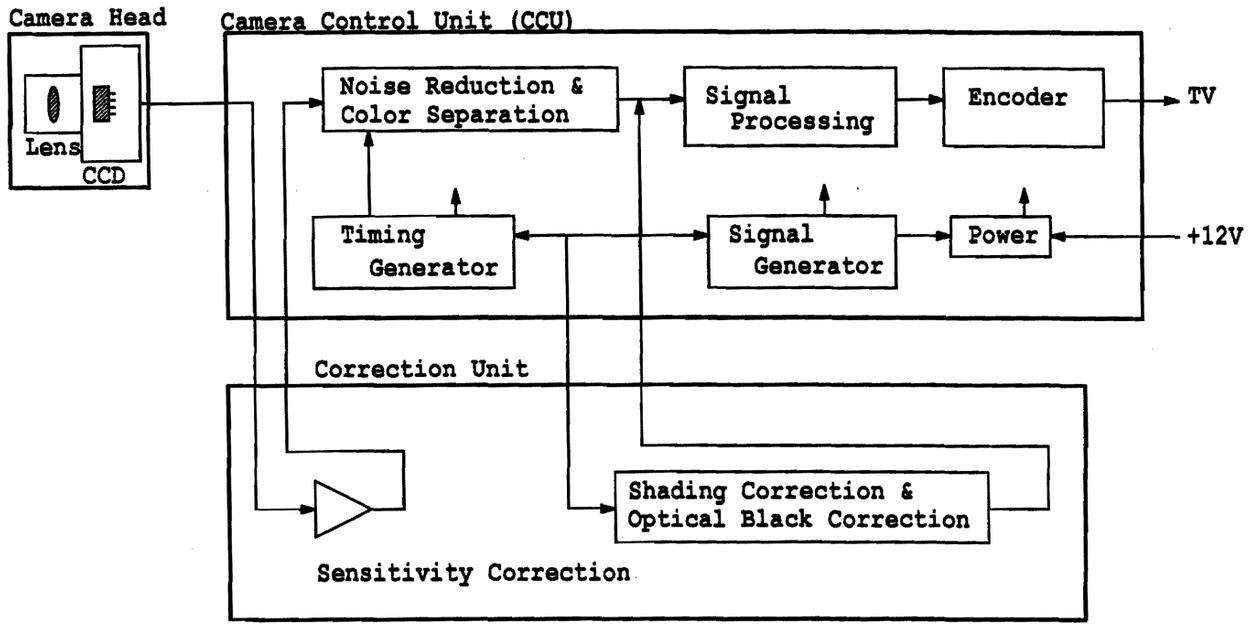

Fig. 45 Block diagram of modified CCU.

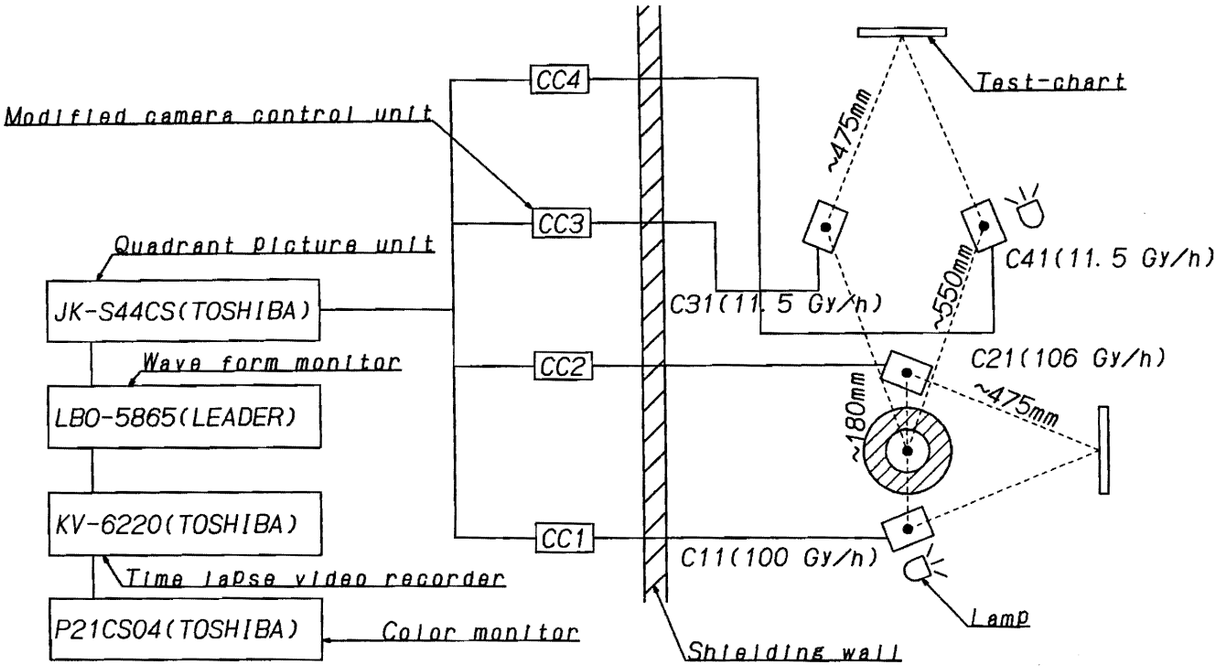

C11, C21, C31 : Std. type CCD camera head with objective lens
C41 : Std. type CCD camera head with rad-hard objective lens

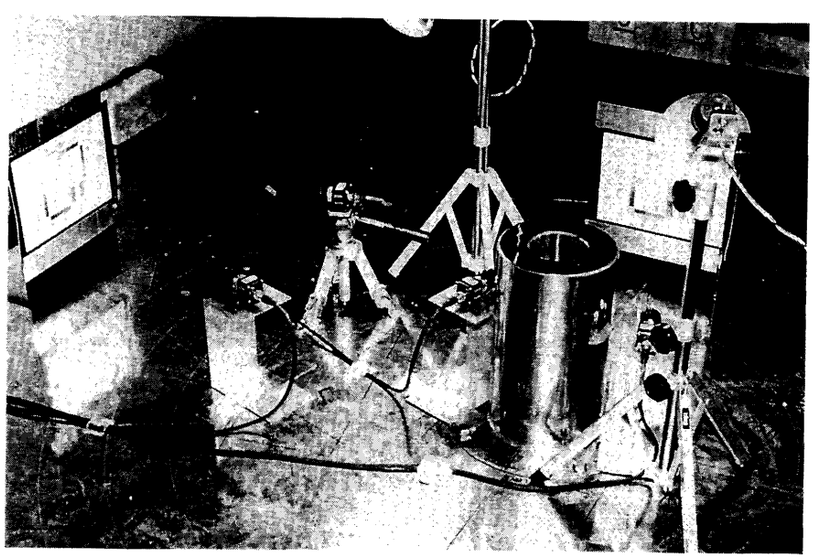

Fig. 46 Experimental setup of the radiation hard CCD camera systems in gamma irradiation cell.

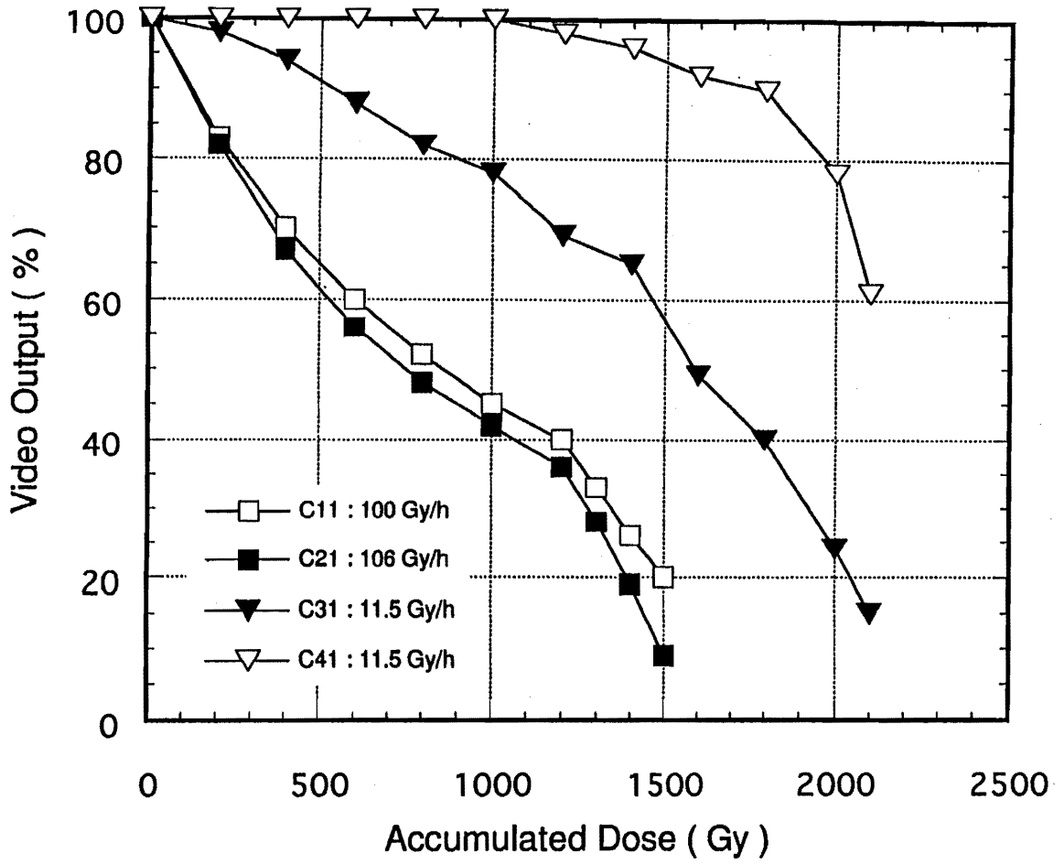

Fig. 47 Changes of video output signals measured by the video tape recorder (VTR) as a functin of accumulation doses.

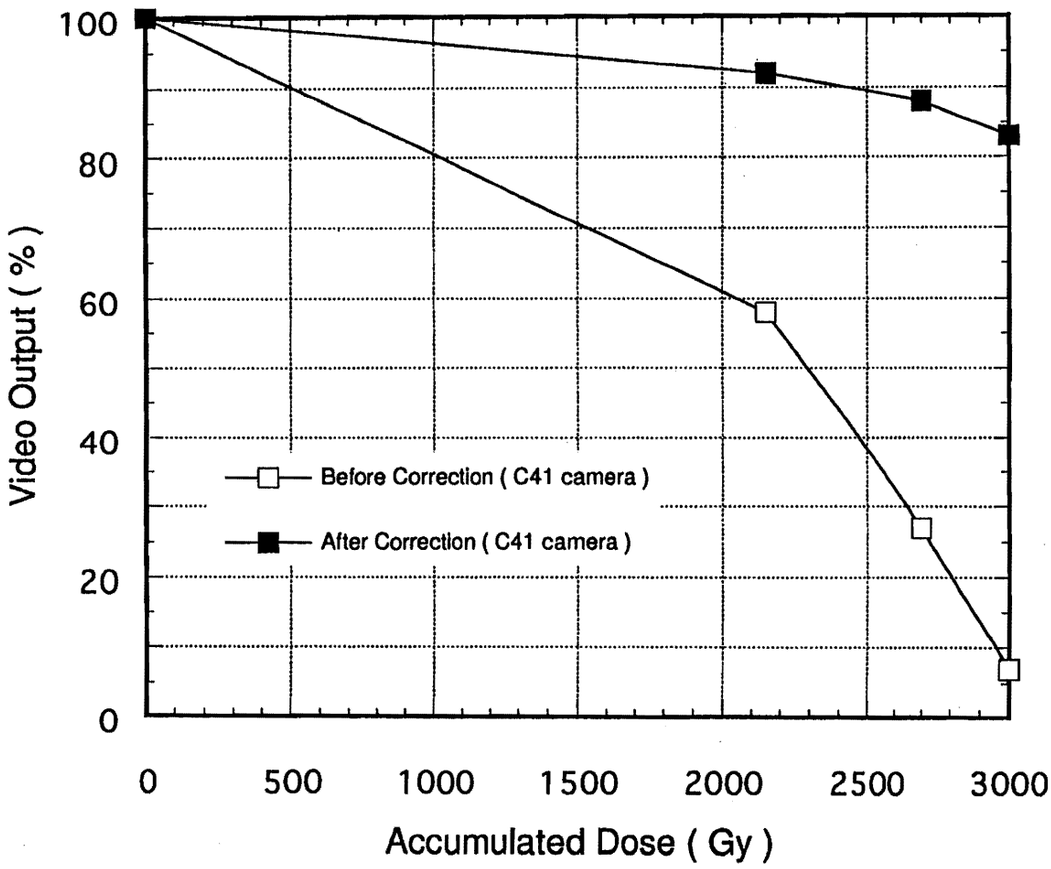

Fig. 48 Effect of sensitivity correction circuit on the video output signals of the C41 camera irradiated under 1.15 kR/h.

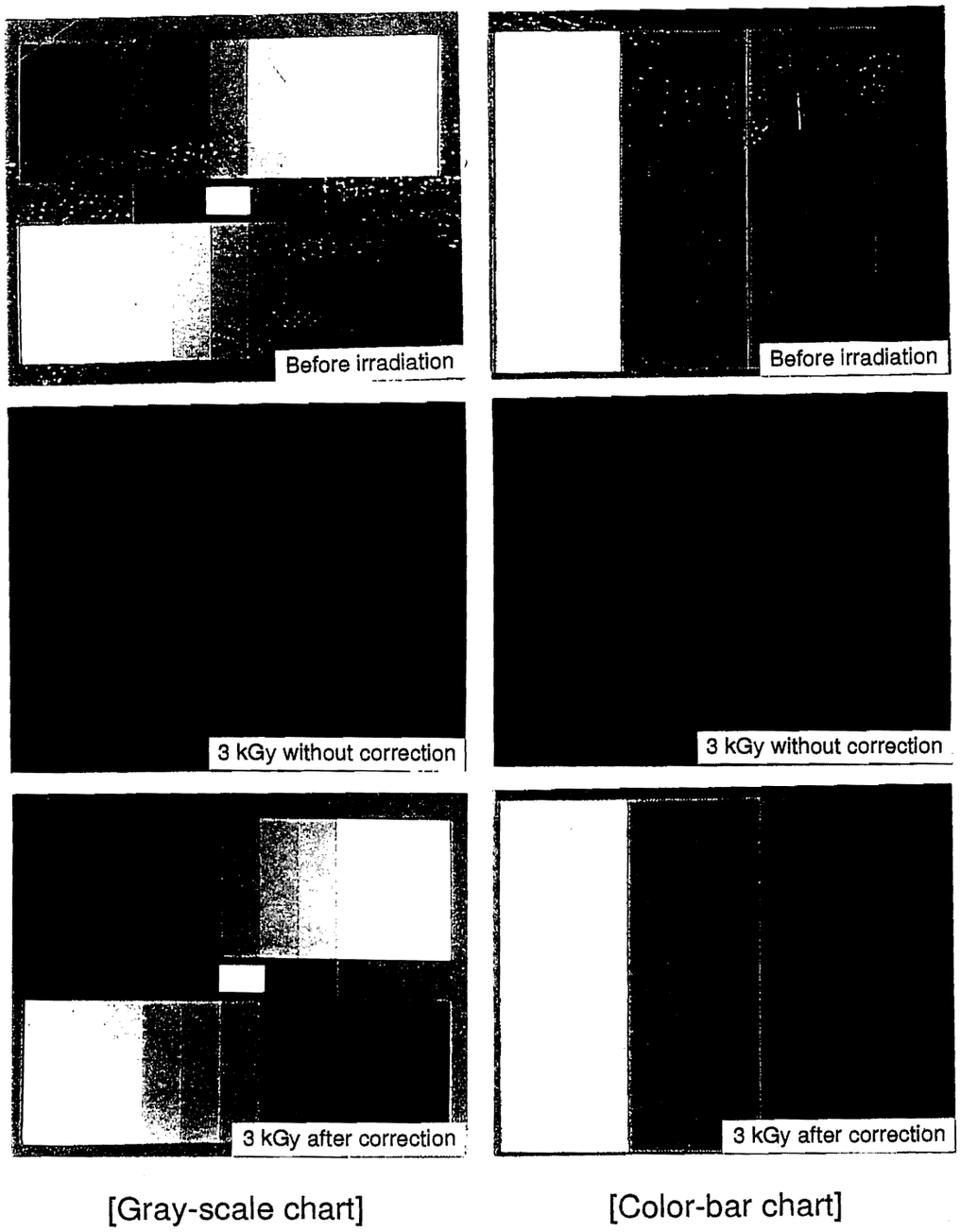

Fig. 49 Total effect of a combination of the correction circuits for sensitivity, OB level and shading on the gray-scale and color-bar charts of the C41 camera irradiated after 3 kGy.

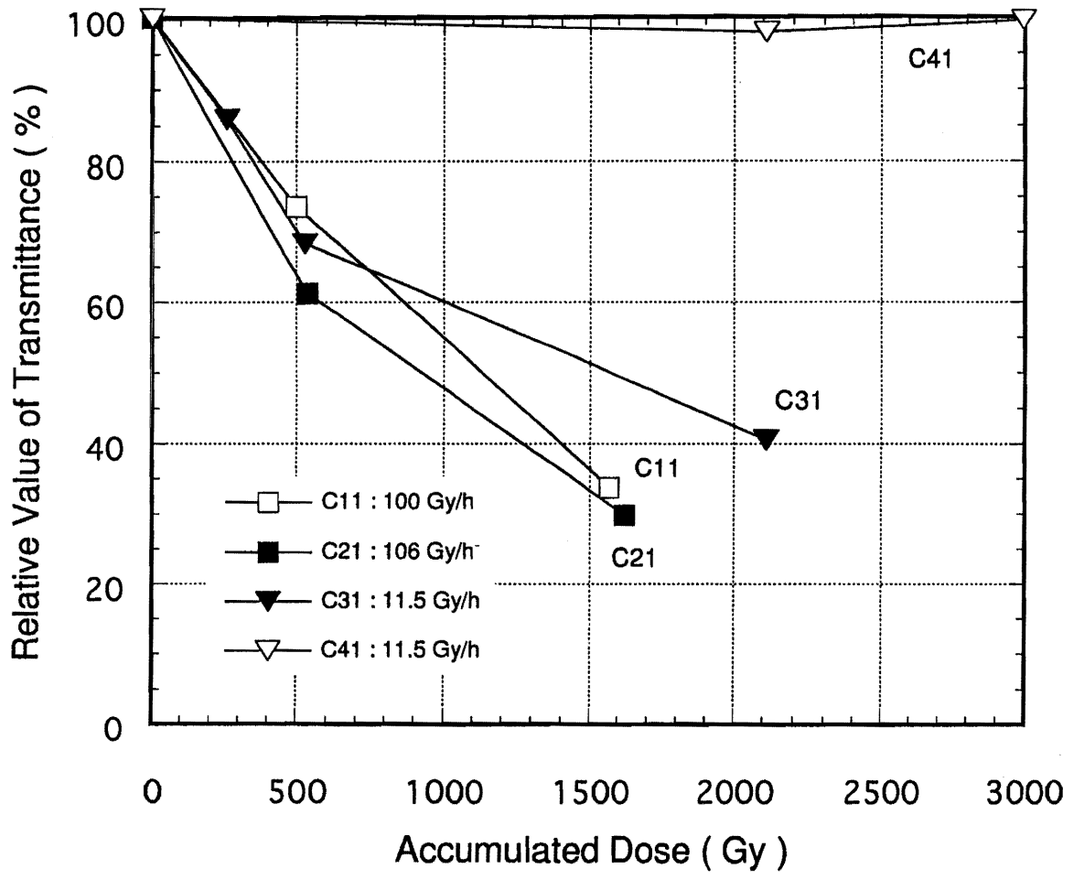

Fig. 50 Transmittance changes of the objective lenses equipped to each CCD camera at a wave length of 540 nm.

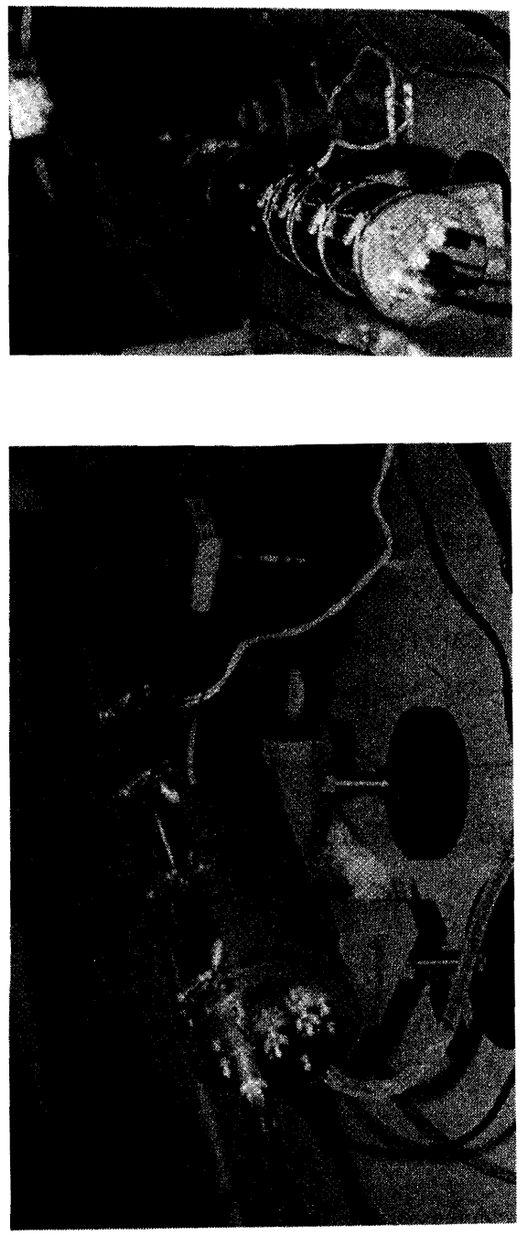

Fig. 51 Cooling chamber including a CCD camera and an focal adjusting mechanism attached to the eyepiece of 15m-long periscope.

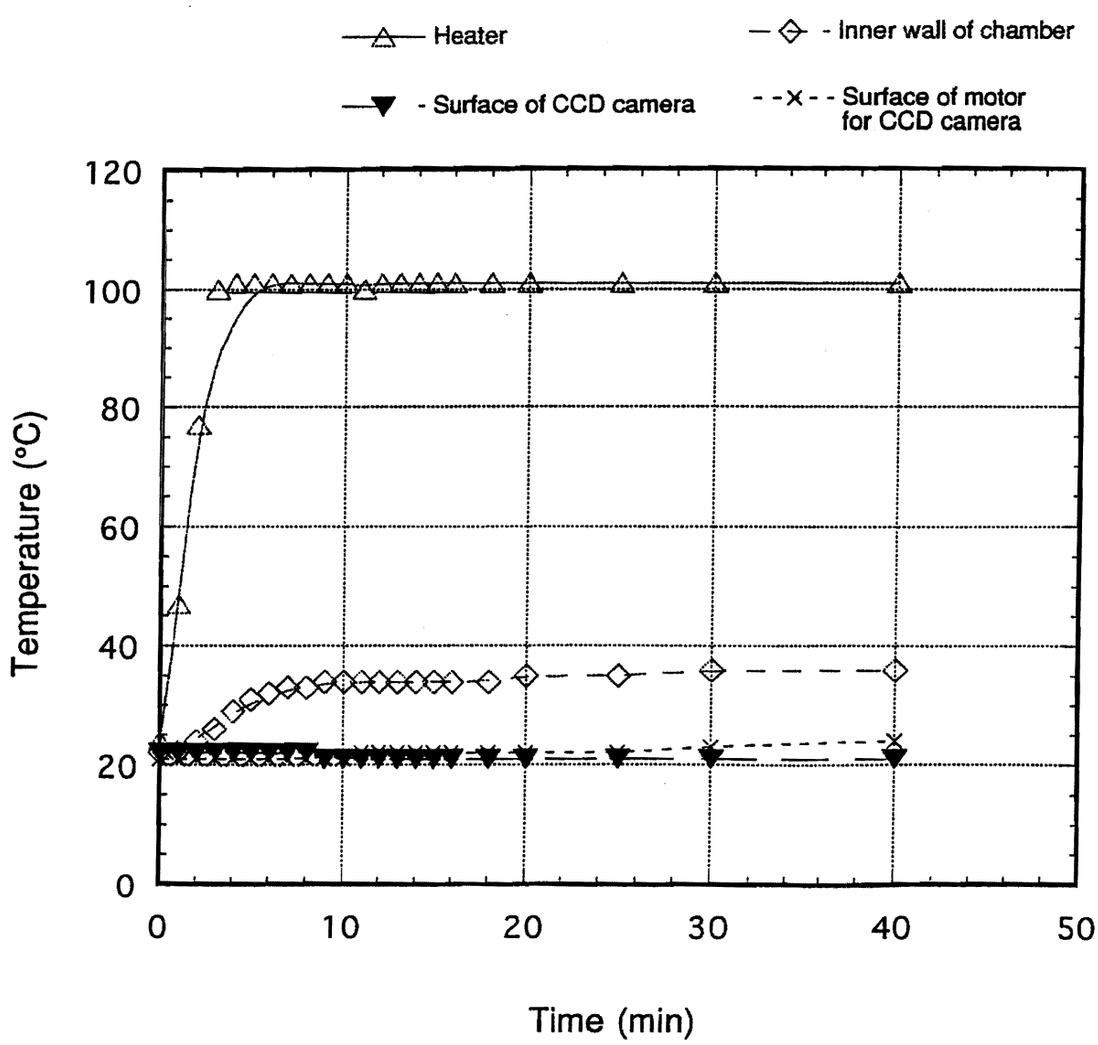

Fig. 52 Measured temperature profile of CCD camera in the cooling chamber heated up to 100 °C.

6. REMAINING ISSUES

The following items are to be involved in further design and technology development.
(1) Investigation of a zooming mechanism to be equipped to the 11m-long periscope.
(2) Performance test of the mirror driving mechanism including the actuator under high temperature (max. 200°C) and gamma radiation of 30 kGy/h (max.) in a vacuum (10^{-5}Pa).
(3) Improvement of radiation hardness and investigation of cooling system for CCD camera.
(4) Development of detail design of the structure to prevent the vibration, movable container for maintenance, cable management and control systems.
(5) As to the operation under high magnetic field, material must be chosen with care and/or new concept with pneumatic driving mechanism must be developed.

7. CONCLUSION

In accordance with the design requirements on the ITER remote maintenance scenario, a design concept of an in-vessel viewing periscope has been outlined and its basic feasibility and applicability to the ITER environmental conditions have been assessed on the basis of the current status of technology development such as radiation hard components and prototypical testing of 6 ~ 15 m long periscopes. The results have shown the credibility of radiation hard 11m-long periscope developed for the ITER in-vessel viewing.

Further studies including detail analyses and assessment on structural and thermal loads are to be continued to develop the detail design and to ensure the viewing performance for the ITER in-vessel operation. In addition, extensive technology development including radiation hardness and performance tests of the periscope assembly is to be continued to verify the adequacy of the periscope design and to qualify the viewing performance for a sufficient length of time under intense of gamma radiation.

ACKNOWLEDGMENTS

The authors would like to express their sincere appreciation to Drs. S. Matsuda, T. Seguchi, Y. Seki and Y. Morita for their continuous guidance and encouragement. They also would like to acknowledge all of members who supported this work.

REFERENCES

[1] K. Obara et al., " Conceptual Design Studies of In-Vessel Viewing Equipment for ITER", JAERI-Tech 96-010, March (1996)
[2] K. Obara et al., " Development of 15m-long radiation hard periscope for ITER in-vessel viewing", Fusion Engineering and Design 42 (1998) 501-509.
[3] K. Obara et al., " Irradiation Test of Critical Components for Remote Handling in Gamma Radiation Environment", JAERI-Tech 94-003, August (1994)
[4] K. Obara et al., " Irradiation Test of Critical Components for Reemote Handling System in Gamma Radiation Environment", JAERI-Tech 96-011, March (1996)
[5] S. Seki et al., " Influence of Magnetic Field to Experimental Equipments ", Technical Symposium at KEK, (1994), (in Japanese)

[6] K. Obara et al., " Development of Radiation Hard CCD Camera and Camera Control Unit", RADECS 97 Conference (Cannes, 1997), Workshop Record (1998) 69-74.